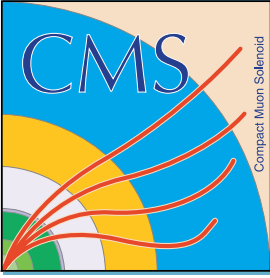


UNIVERSITY
of
VIRGINIA

A Search in the Two-Photon Final State for Evidence of New Particle Production in pp Collisions at $\sqrt{s} = 7 \text{ TeV}$

Rachel Yohay
University of Virginia
Thesis defense
Advisor: Brad Cox
July 11, 2012



Outline



- The Standard Model
- Supersymmetry
- The Large Hadron Collider
- The Compact Muon Solenoid
- Event selection
- Analysis
- Interpretation
- Conclusion

The Standard Model

- All matter is built up of elementary particles
- Interactions between matter particles involve exchange of force carrier particles \Rightarrow quantum theory of fundamental forces
- Field theoretic description of particles respecting translation and gauge symmetry

Three Generations of Matter (Fermions)				
	I	II	III	
mass \rightarrow	2.4 MeV/c ²	1.27 GeV/c ²	171.2 GeV/c ²	0
charge \rightarrow	2/3	2/3	2/3	0
spin \rightarrow	1/2	1/2	1/2	0
name \rightarrow	u	c	t	γ
	up	charm	top	photon
Quarks				
mass \rightarrow	4.8 MeV/c ²	104 MeV/c ²	4.2 GeV/c ²	0
charge \rightarrow	-1/3	-1/3	-1/3	0
spin \rightarrow	1/2	1/2	1/2	1
name \rightarrow	d	s	b	g
	down	strange	bottom	gluon
Leptons				
mass \rightarrow	<2.2 eV/c ²	<0.17 MeV/c ²	<15.5 MeV/c ²	91.2 GeV/c ²
charge \rightarrow	0	0	0	0
spin \rightarrow	1/2	1/2	1/2	1
name \rightarrow	e _ν	μ _ν	τ _ν	Z boson
	electron neutrino	muon neutrino	tau neutrino	Z boson
Gauge Bosons				
mass \rightarrow	0.511 MeV/c ²	105.7 MeV/c ²	1.777 GeV/c ²	80.4 GeV/c ²
charge \rightarrow	-1	-1	-1	± 1
spin \rightarrow	1/2	1/2	1/2	1
name \rightarrow	e	μ	τ	W boson
	electron	muon	tau	W boson

The Standard Model

- Fermions (matter particles)
 - Spin 1/2
 - Charged and neutral leptons
 - Charged quarks
 - Antiparticles

Three Generations of Matter (Fermions)				
	I	II	III	
mass	2.4 MeV/c ²	1.27 GeV/c ²	171.2 GeV/c ²	
charge	2/3	2/3	2/3	0
spin	1/2	1/2	1/2	0
name	u	c	t	γ
	up	charm	top	photon
Quarks				
mass	4.8 MeV/c ²	104 MeV/c ²	4.2 GeV/c ²	
charge	-1/3	-1/3	-1/3	0
spin	1/2	1/2	1/2	0
name	d	s	b	g
	down	strange	bottom	gluon
Leptons				
mass	<2.2 eV/c ²	<0.17 MeV/c ²	<15.5 MeV/c ²	
charge	0	0	0	1
spin	1/2	1/2	1/2	1
name	e	μ	τ	Z ⁰
	electron neutrino	muon neutrino	tau neutrino	Z boson
mass	0.511 MeV/c ²	105.7 MeV/c ²	1.777 GeV/c ²	
charge	-1	-1	-1	±1
spin	1/2	1/2	1/2	1
name	e	μ	τ	W [±]
	electron	muon	tau	W boson
Gauge Bosons				

The Standard Model

- Fermions (matter particles)
 - Spin 1/2
 - Charged and neutral leptons
 - Charged quarks
 - Antiparticles
 - Three generations
 - Mathematical description of generations is identical
 - Only difference is mass

Three Generations of Matter (Fermions)				Gauge Bosons
	I	II	III	
mass	2.4 MeV/c ²	1.27 GeV/c ²	171.2 GeV/c ²	
charge	2/3	2/3	2/3	
spin	1/2	1/2	1/2	
name	u up	c charm	t top	Y photon
	d down	s strange	b bottom	g gluon
Quarks				
Leptons				
mass	<2.2 eV/c ²	<0.17 MeV/c ²	<15.5 MeV/c ²	
charge	0	0	0	
spin	1/2	1/2	1/2	
name	e electron neutrino	ν_μ muon neutrino	ν_τ tau neutrino	Z^0 Z boson
	e electron	μ muon	τ tau	W^\pm W boson

The Standard Model



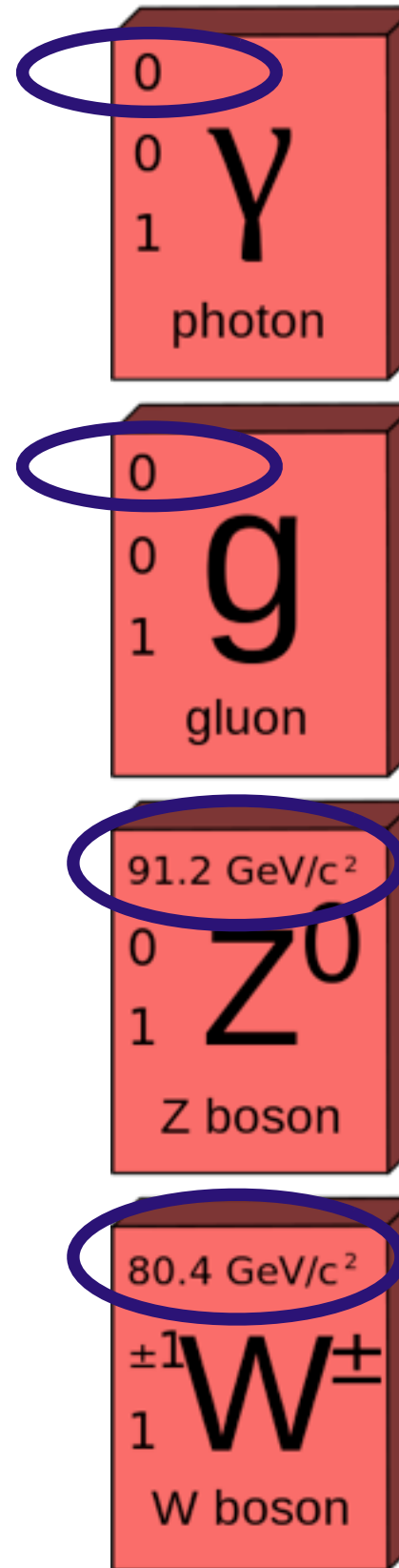
UNIVERSITY
of VIRGINIA

- Bosons (force carriers)
 - Spin 1 or 0
 - Photon (γ): mediates electromagnetic force
 - Gluon (g): mediates strong force between quarks in hadrons
 - Z^0 and W^\pm : mediate weak force (e.g. radioactive β decay)

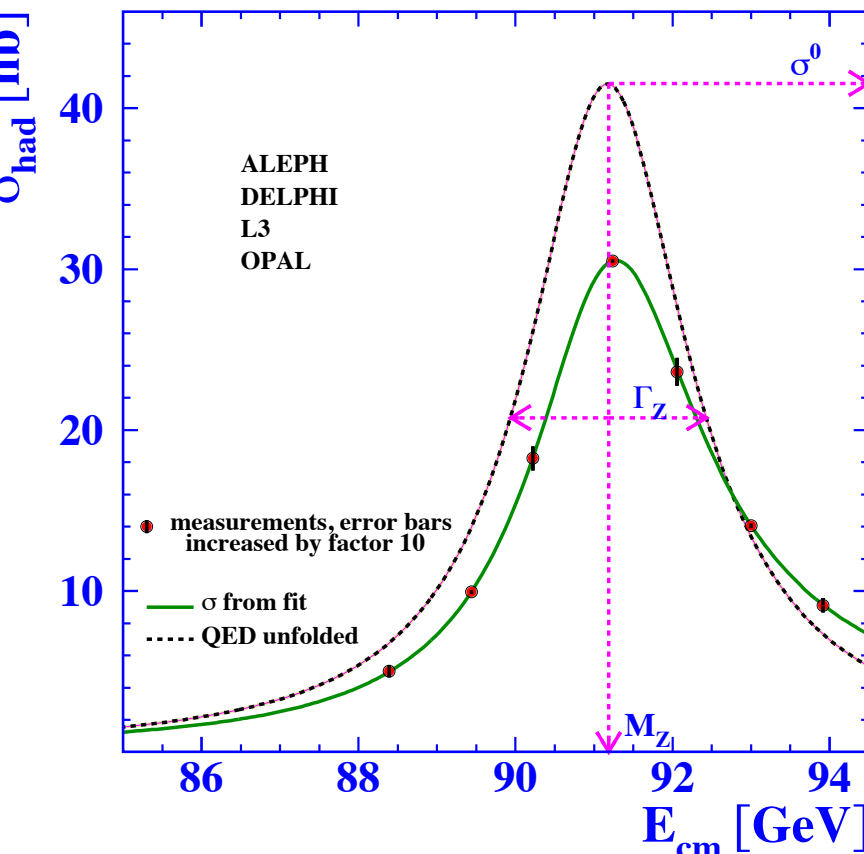
Three Generations of Matter (Fermions)				
	I	II	III	
mass →	2.4 MeV/c ²	1.27 GeV/c ²	171.2 GeV/c ²	
charge →	2/3	2/3	2/3	0
spin →	1/2	1/2	1/2	0
name →	u	c	t	γ
	up	charm	top	photon
Quarks				
mass →	4.8 MeV/c ²	104 MeV/c ²	4.2 GeV/c ²	
charge →	-1/3	-1/3	-1/3	0
spin →	1/2	1/2	1/2	0
name →	d	s	b	g
	down	strange	bottom	gluon
Leptons				
mass →	<2.2 eV/c ²	<0.17 MeV/c ²	<15.5 MeV/c ²	
charge →	0	0	0	1
spin →	1/2	1/2	1/2	1
name →	e	ν_μ	ν_τ	Z^0
	electron neutrino	muon neutrino	tau neutrino	Z boson
Gauge Bosons				
mass →	0.511 MeV/c ²	105.7 MeV/c ²	1.777 GeV/c ²	
charge →	-1	-1	-1	± 1
spin →	1/2	1/2	1/2	1
name →	e	μ	τ	W^\pm
	electron	muon	tau	W boson

The Standard Model

- Bosons (force carriers)
 - Spin 1 or 0
 - Photon (γ): mediates electromagnetic force
 - Gluon (g): mediates strong force between quarks in hadrons
 - Z^0 and W^\pm : mediate weak force (e.g. radioactive β decay)
 - **Photon and gluon are massless, Z^0 and W^\pm are heavy**
 - **Higgs boson gives W and Z mass (observation of Standard Model-like Higgs on July 4)**



Successes of the Standard Model

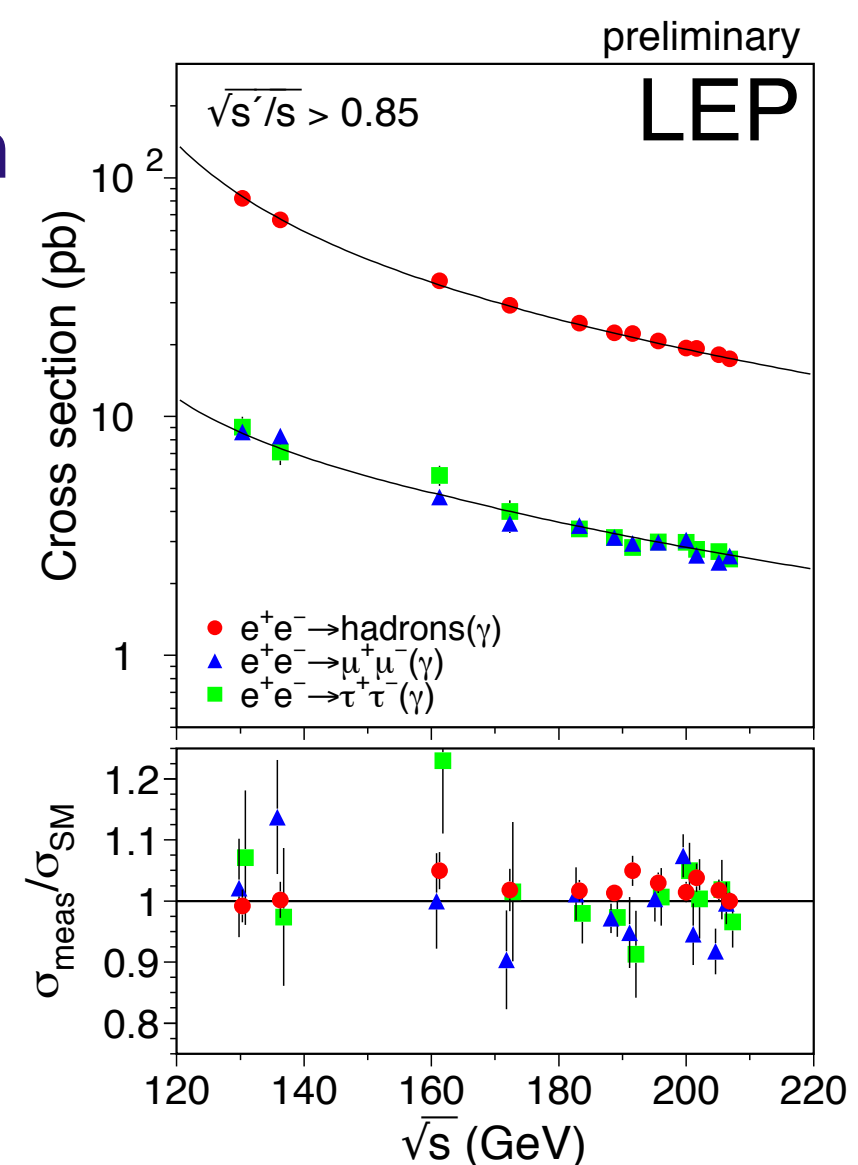


- ✓ Decay modes of the hadrons, heavy fermions, and heavy gauge bosons
- ✓ Lepton universality
- ✓ Flavor conservation

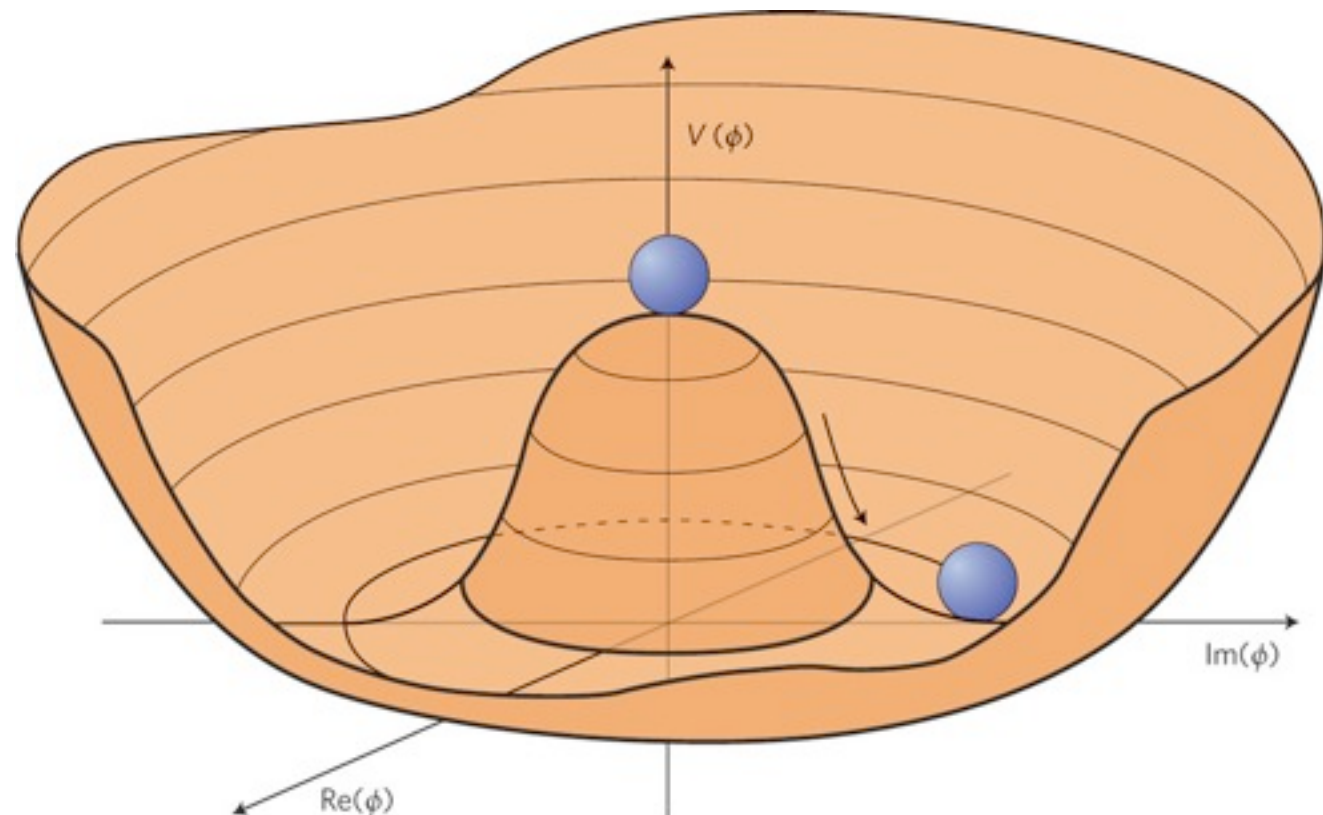
✓ Only three generations

✓ Quark content of hadrons

- Standard Model (SM) has passed all experimental tests to date

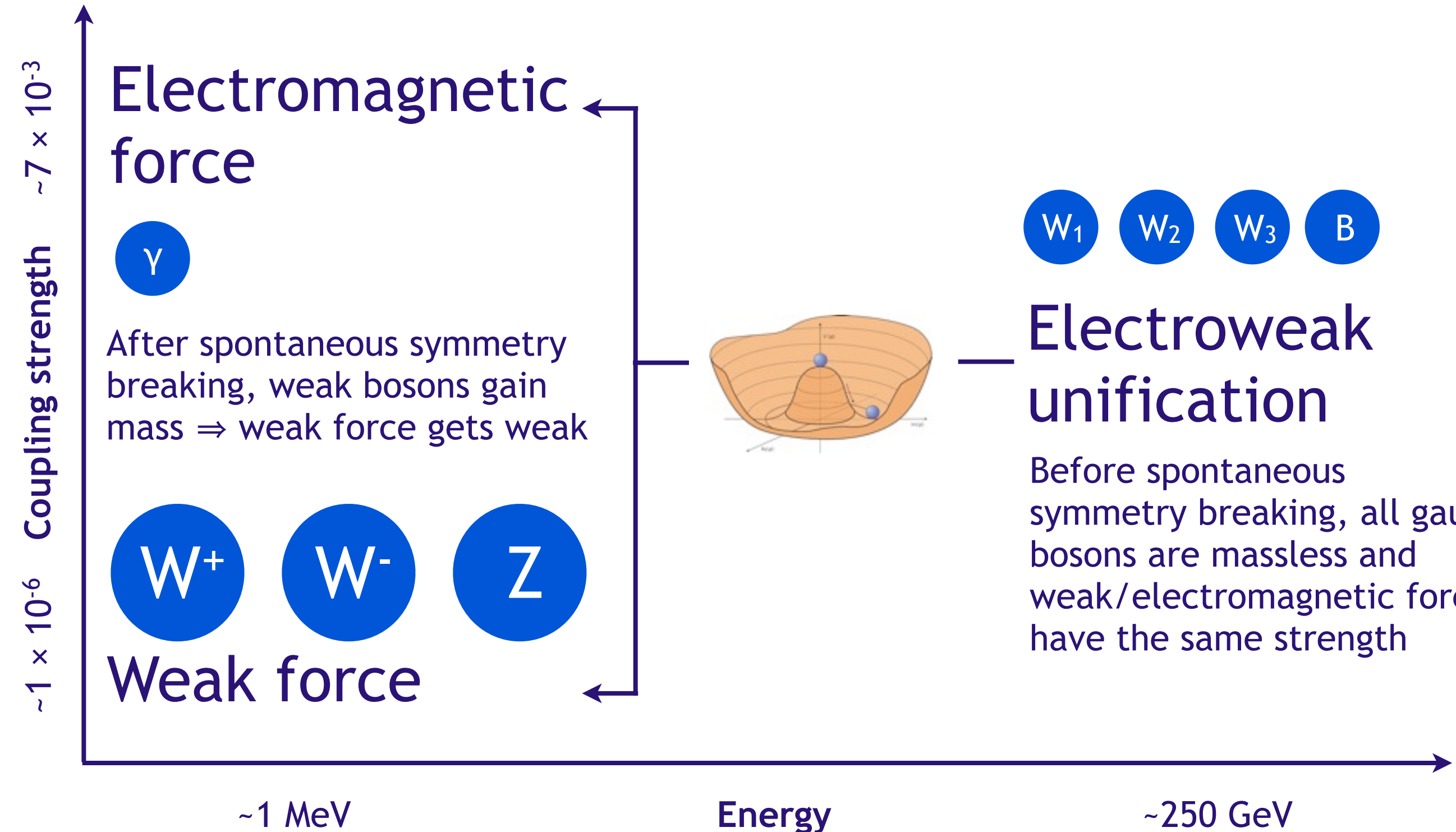


The Higgs mechanism



- Explicit Lagrangian mass term for the W and Z breaks gauge invariance
- Introduce a doublet of complex scalar fields ϕ that has a potential $\mu^2\phi^\dagger\phi + |\lambda|(\phi^\dagger\phi)^2$ with $\mu^2 < 0$
 - Minimum of the potential > 0
 - Spontaneous choice of vacuum state
- Expanding ϕ about its vacuum expectation value (VEV) in the Lagrangian generates one massive Higgs scalar and mass terms for the W and Z

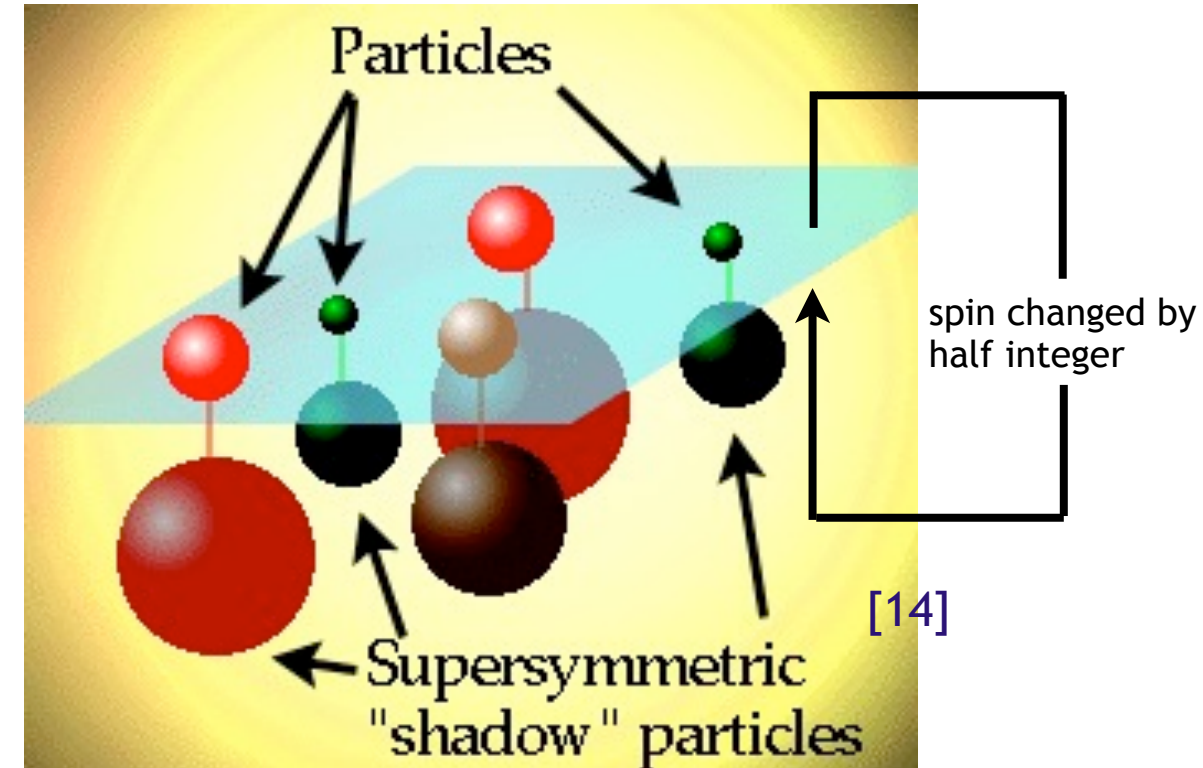
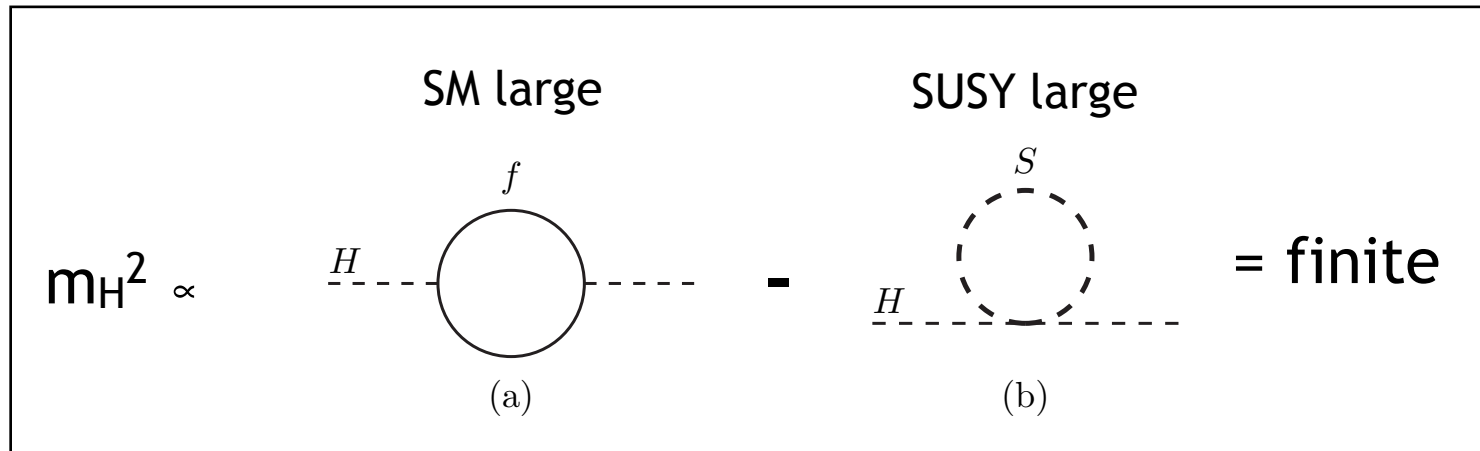
Electroweak symmetry breaking



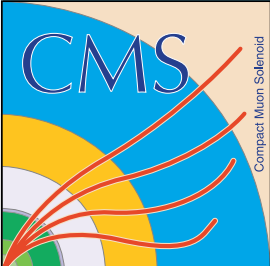
Implications

1. μ^2 must be less than 0 for electroweak symmetry breaking (EWSB)—why?
2. Higgs is a scalar particle \Rightarrow **hierarchy problem**
 - One-loop correction to Higgs self-energy diagram proportional to Λ_{UV}^{-2}
 - If $\Lambda_{\text{UV}} = M_{\text{Planck}}$, extremely finely tuned counterterm to bare m_H^2 needed to keep $m_H \sim$ few hundred GeV
3. No prediction of dark matter
4. No fermion mass terms in the Lagrangian without $-\zeta_f f_R^\dagger \phi^\dagger f_L + \text{h.c.}$ Yukawa couplings to the Higgs (ζ_f proportional to m_f/v where v is the Higgs VEV)

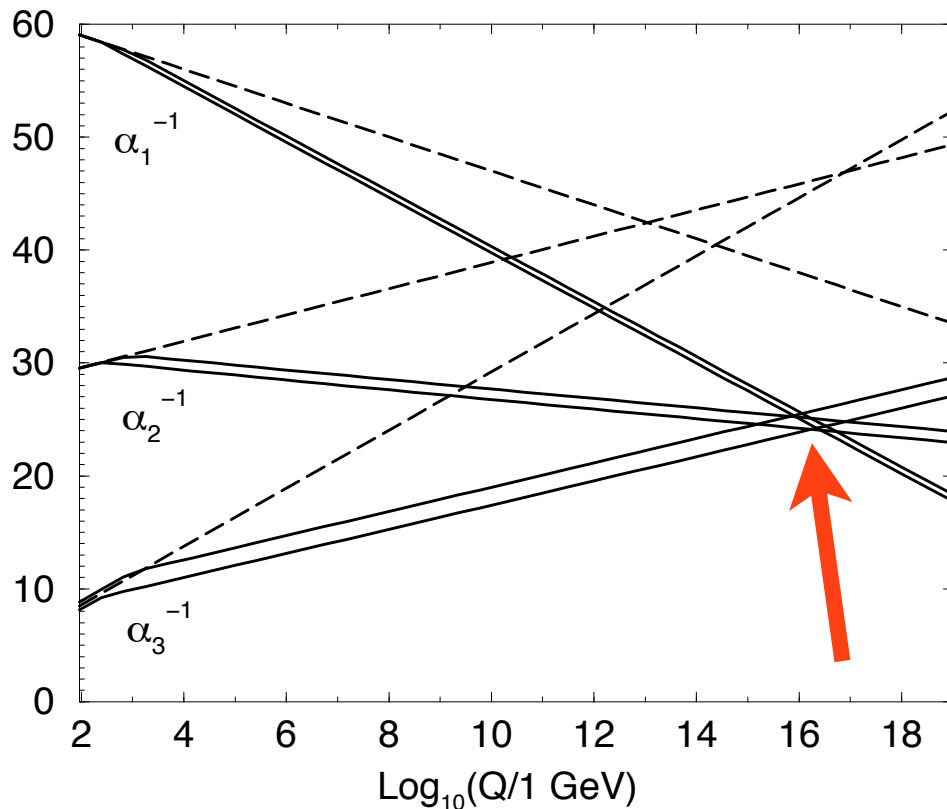
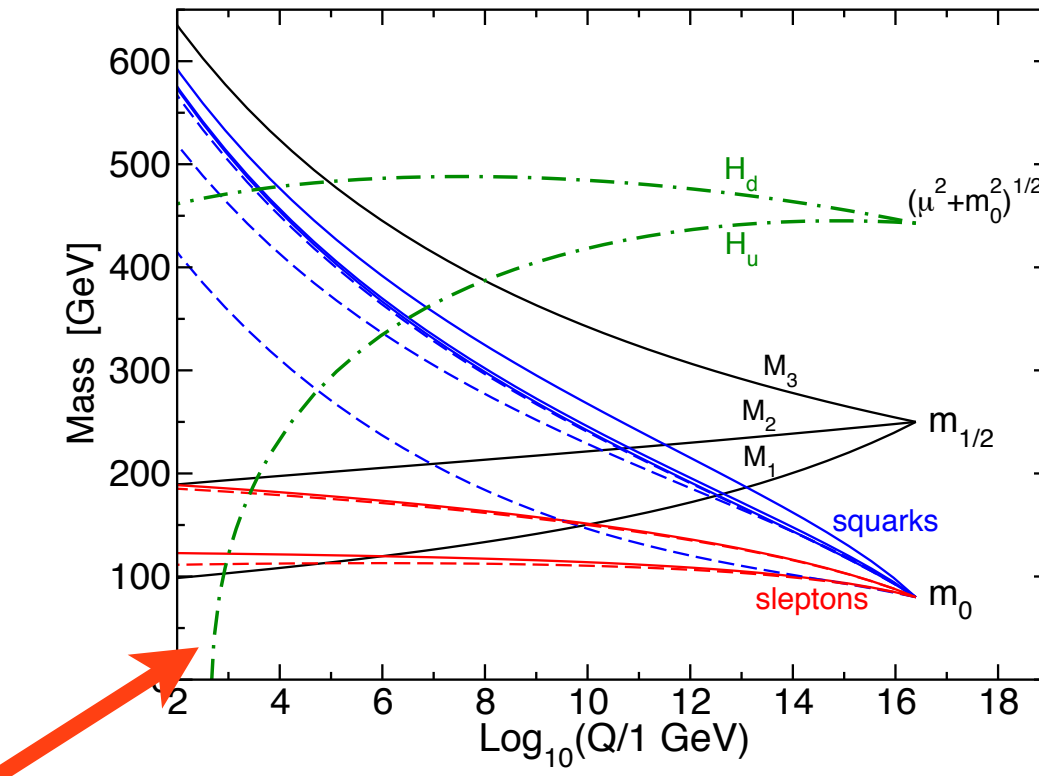
Supersymmetry



- For each SM fermion(boson), there is a supersymmetric (SUSY) partner boson(fermion) with all other quantum numbers identical
 - SM spin-1/2 Weyl fermion \leftrightarrow SUSY spin-0 scalar sfermion
 - SM spin-1 gauge boson \leftrightarrow SUSY spin-1/2 Weyl fermion gaugino
 - SUSY correction to m_H^2 exactly cancels SM correction to all orders due to relative sign between boson and fermion \Rightarrow hierarchy problem removed



Strengths of SUSY



- When evolved down to M_Z by renormalization group equations, **SUSY predicts $\mu^2 < 0$, as required by EWSB**
- Due to dependence on top Yukawa coupling, which is large because m_t is much larger than the lighter fermion masses
- Could explain why top quark is so much heavier than other fermions
- Nearly exact unification of forces at 10^{16} GeV
- **Predicts new feebly interacting, stable particle \Rightarrow dark matter?**

SUSY breaking

- No superpartners yet discovered, so SUSY must be spontaneously broken at a high energy scale
- Two popular ways to break SUSY
 - Gravity mediation: hidden SUSY-breaking sector connects to observable SM+SUSY sector through gravitational-strength interactions
 - **Gauge mediation (GMSB):** ordinary SM gauge interactions connect the hidden and observable sectors
 - **Flavor blindness automatically enforced** because gauge couplings are identical for the three families
 - Hidden and visible sectors connected by heavy messenger particles
 - **Gravitino (superpartner to graviton) mass \sim eV-keV**

$$\begin{aligned} \mathcal{L}_{\text{soft}}^{\text{MSSM}} = & -\frac{1}{2} \left(M_3 \tilde{g} \tilde{g} + M_2 \tilde{W} \tilde{W} + M_1 \tilde{B} \tilde{B} + \text{c.c.} \right) \\ & - \left(\tilde{\bar{u}} \mathbf{a}_u \tilde{Q} H_u - \tilde{\bar{d}} \mathbf{a}_d \tilde{Q} H_d - \tilde{\bar{e}} \mathbf{a}_e \tilde{L} H_d + \text{c.c.} \right) \\ & - \tilde{Q}^\dagger \mathbf{m}_Q^2 \tilde{Q} - \tilde{L}^\dagger \mathbf{m}_L^2 \tilde{L} - \tilde{\bar{u}} \mathbf{m}_{\bar{u}}^2 \tilde{\bar{u}}^\dagger - \tilde{\bar{d}} \mathbf{m}_{\bar{d}}^2 \tilde{\bar{d}}^\dagger - \tilde{\bar{e}} \mathbf{m}_{\bar{e}}^2 \tilde{\bar{e}}^\dagger \\ & - m_{H_u}^2 H_u^* H_u - m_{H_d}^2 H_d^* H_d - (b H_u H_d + \text{c.c.}) . \end{aligned}$$

$$\begin{bmatrix} \tilde{\bar{e}}_R \\ \tilde{\bar{\mu}}_R \\ \tilde{\bar{\tau}}_R \end{bmatrix} \begin{bmatrix} c_{ee} & c_{e\mu} & c_{e\tau} \\ c_{\mu e} & c_{\mu\mu} & c_{\mu\tau} \\ c_{\tau e} & c_{\tau\mu} & c_{\tau\tau} \end{bmatrix} \begin{bmatrix} \tilde{e}_R & \tilde{\mu}_R & \tilde{\tau}_R \end{bmatrix}$$

↓

if not proportional to the unit matrix,
will lead to, for example, $\mu \rightarrow e\gamma$

R-parity

- R-parity is a multiplicative quantum number that is +1 for SM particles and -1 for SUSY particles
- R-parity conservation ($R = 1$ at each vertex) enforces baryon and lepton number conservation
- Four phenomenological consequences
 1. In colliders, SUSY particles are produced in pairs ($+1 \times +1 \rightarrow -1 \times -1$)
 2. All SUSY particles decay to at least one other SUSY particle ($-1 \rightarrow -1 \times +1$)
 3. **Lightest SUSY particle (LSP) is absolutely stable \Rightarrow dark matter candidate**
 4. **eV-keV gravitino is LSP and only interacts gravitationally \Rightarrow escapes undetected \Rightarrow M_{ET}**

GMSB phenomenology

$$m_{\tilde{\chi}_1^0} = M_1 - \frac{m_Z^2 \sin^2 \theta_W (M_1 + \mu \sin 2\beta)}{\mu^2 - M_1^2} + \dots \quad (3.18)$$

$$m_{\tilde{\chi}_2^0} = M_2 - \frac{m_W^2 (M_2 + \mu \sin 2\beta)}{\mu^2 - M_2^2} + \dots \quad (3.19)$$

$$m_{\tilde{\chi}_3^0} = |\mu| + \frac{m_Z^2 (\text{sgn}(\mu) - \sin 2\beta)(\mu + M_1 \cos^2 \theta_W + M_2 \sin^2 \theta_W)}{2(\mu + M_1)(\mu + M_2)} + \dots \quad (3.20)$$

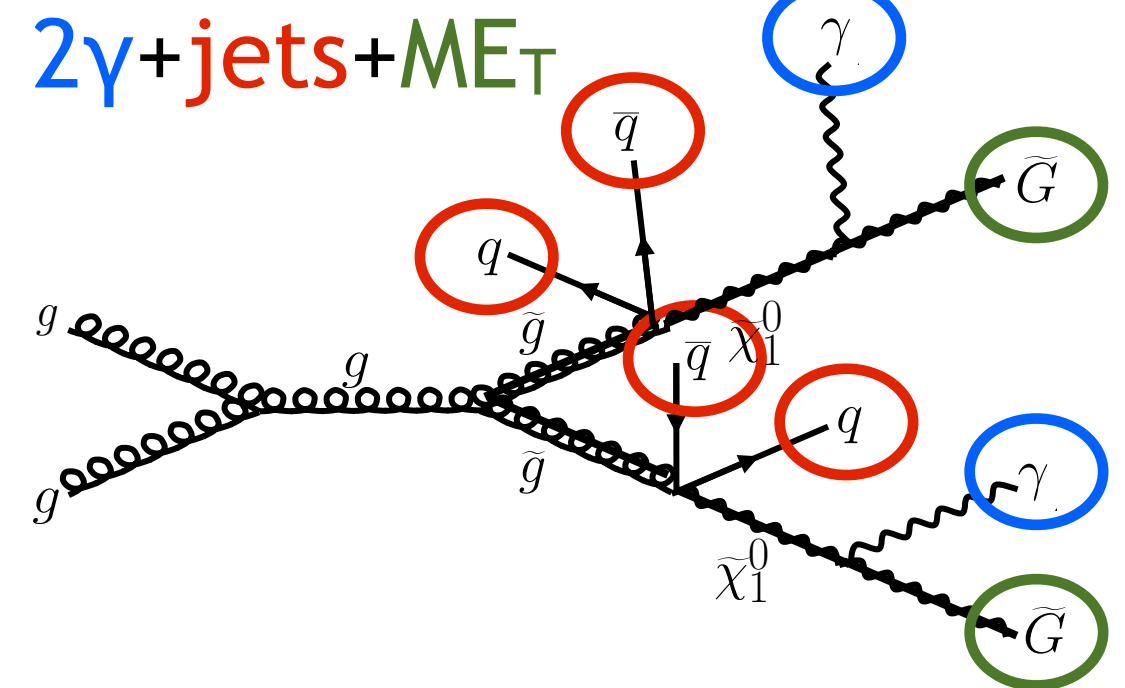
$$m_{\tilde{\chi}_4^0} = |\mu| + \frac{m_Z^2 (\text{sgn}(\mu) + \sin 2\beta)(\mu - M_1 \cos^2 \theta_W - M_2 \sin^2 \theta_W)}{2(\mu - M_1)(\mu - M_2)} + \dots \quad (3.21)$$

$$m_{\tilde{\chi}_1^\pm} = M_2 - \frac{m_W^2 (M_2 + \mu \sin 2\beta)}{\mu^2 - M_2^2} + \dots \quad (3.22)$$

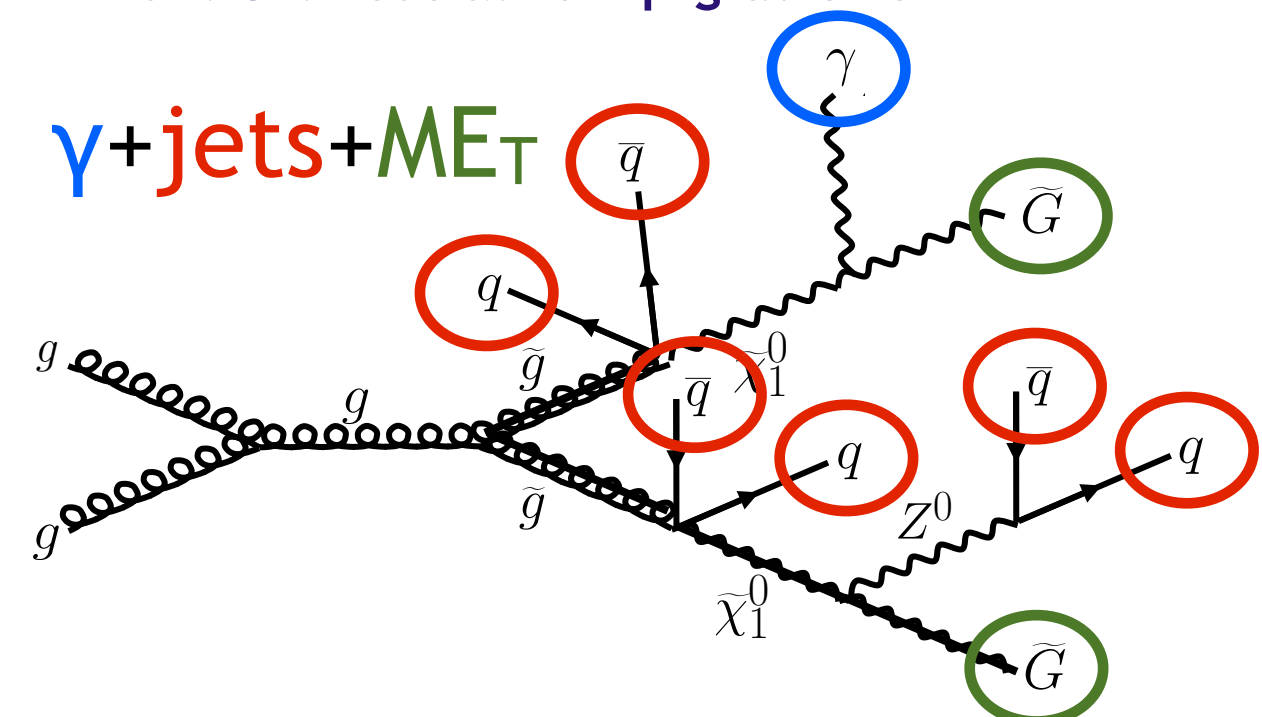
$$m_{\tilde{\chi}_2^\pm} = |\mu| + \frac{m_W^2 \text{sgn}(\mu)(\mu + M_2 \sin 2\beta)}{\mu^2 - M_2^2} + \dots \quad (3.23)$$

- Bino, wino, and higgsino mix to form physical neutralinos and charginos
- **Gravitino LSP \Rightarrow all decay chains proceed through neutralino(chargino) \rightarrow X + gravitino**
- Two mixing scenarios
 1. **Bino NLSP:** $M_1 \sim$ few hundred GeV; $M_2, |\mu| \gg M_1 \Rightarrow$ only lightest neutralino produced in colliders, decays to $\gamma/Z/H +$ gravitino (Z/H only if heavy enough)
 2. **Wino NLSP:** $M_2 \sim$ few hundred GeV; $M_1, |\mu| \gg M_2 \Rightarrow$ lightest neutralino and chargino produced in colliders, chargino decays to $W +$ gravitino

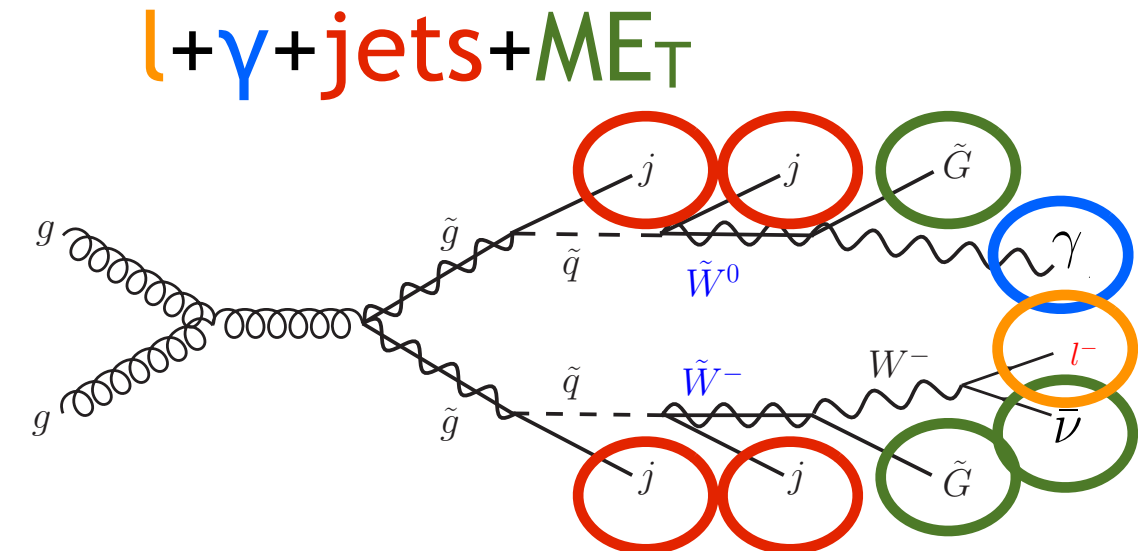
GMSB final states



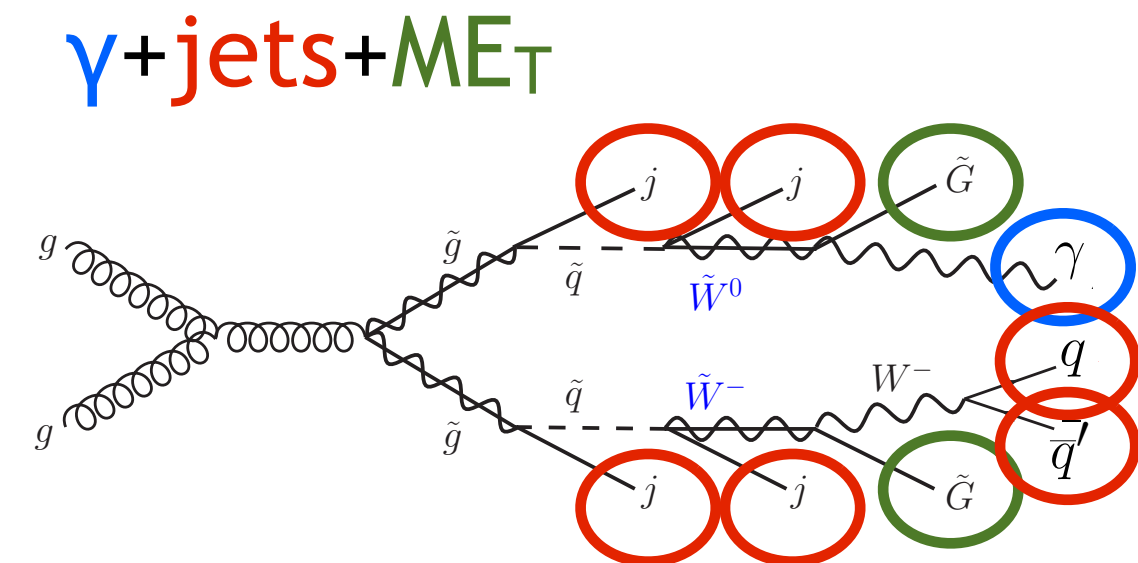
Bino NLSP: neutralino $\rightarrow \gamma + \text{gravitino}$



Bino NLSP: neutralino $\rightarrow \gamma + \text{gravitino}$ or
neutralino $\rightarrow Z(\rightarrow \text{jets}) + \text{gravitino}$

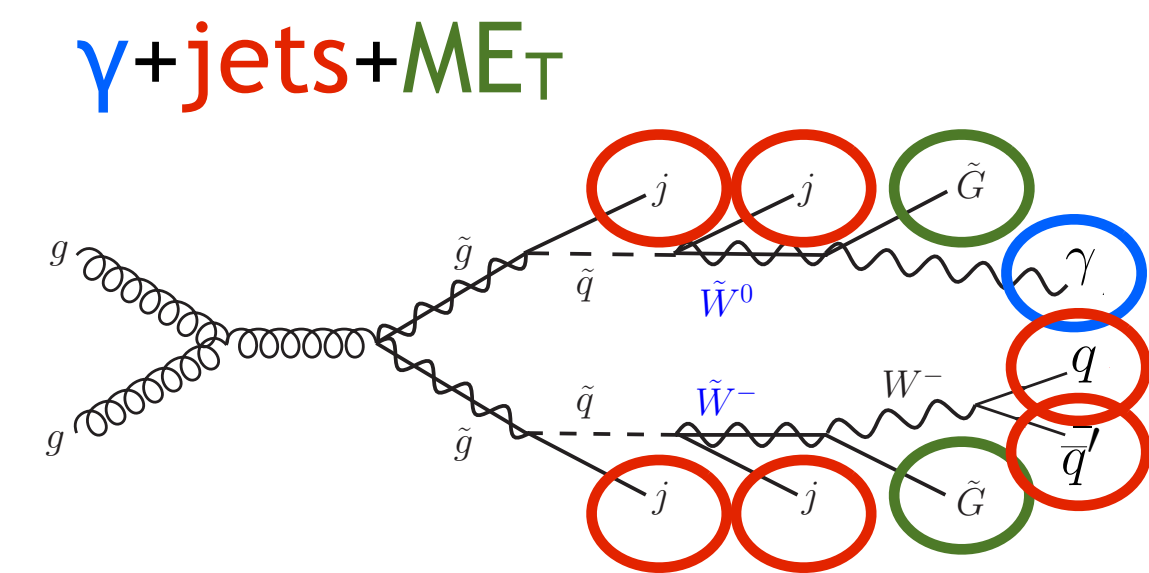
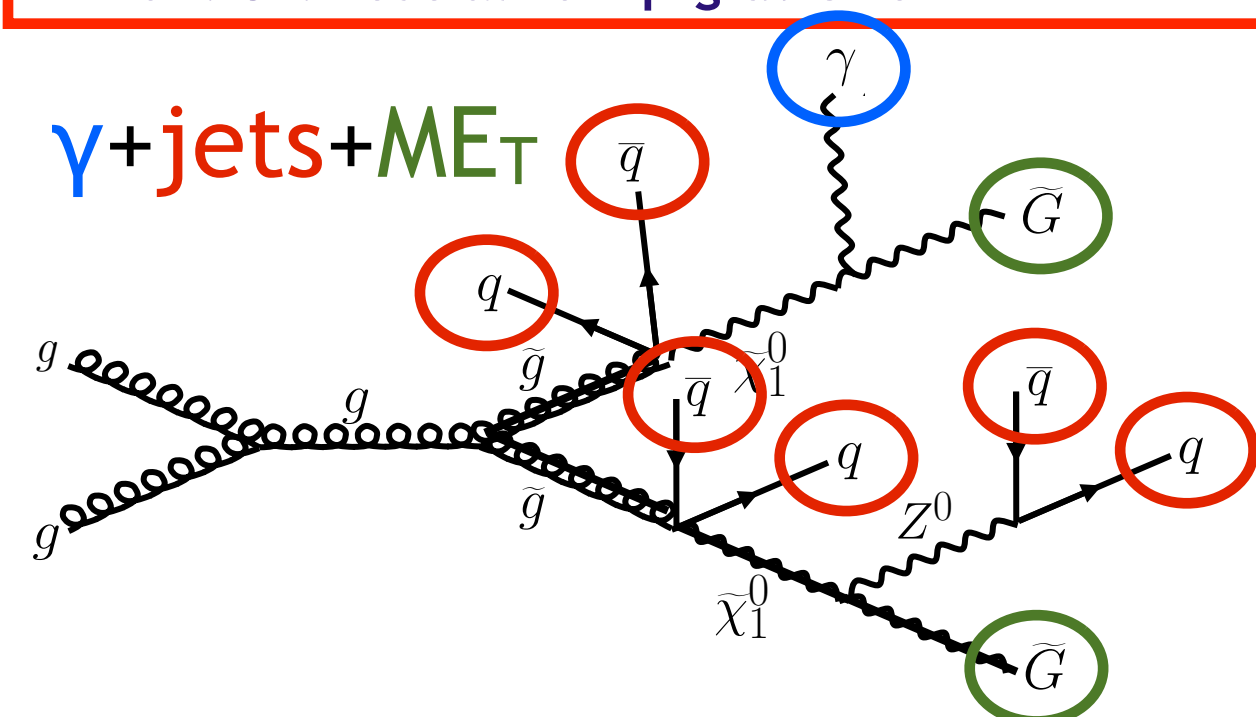
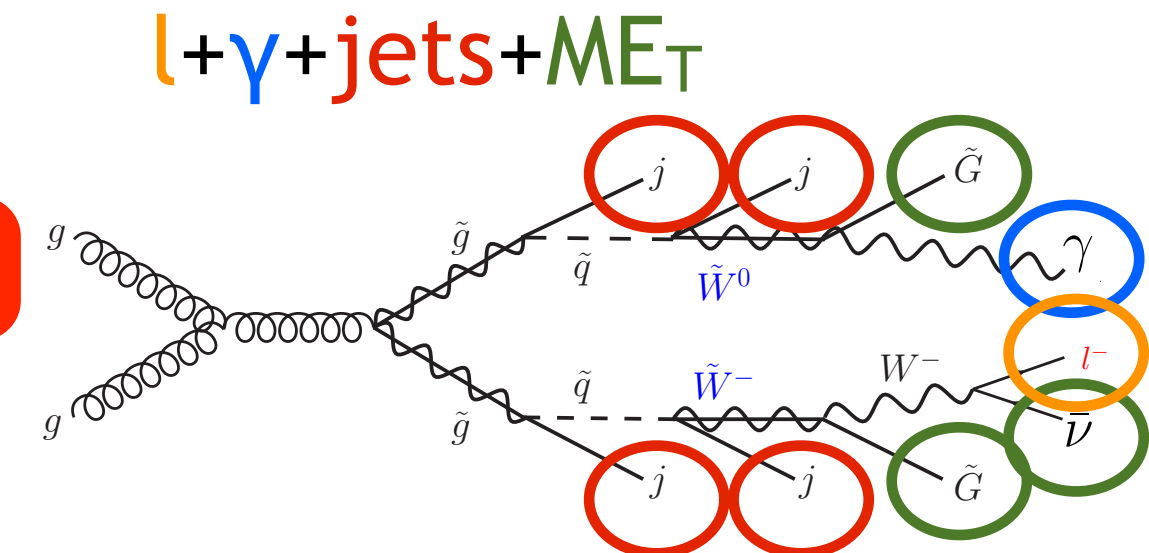
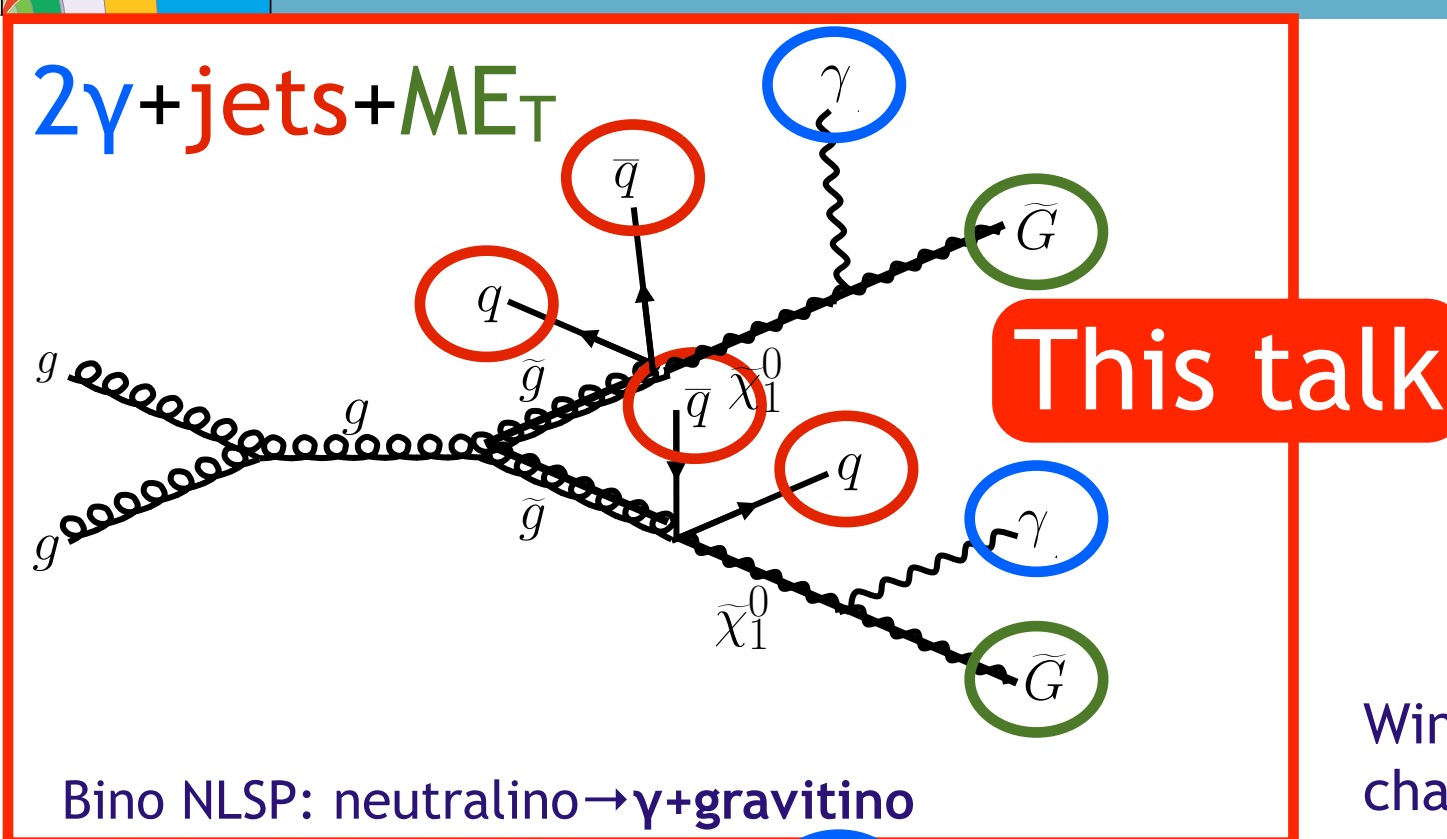


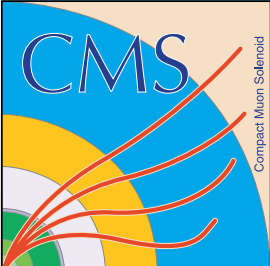
Wino NLSP: neutralino $\rightarrow \gamma + \text{gravitino}$ and
chargino $\rightarrow W(\rightarrow l\nu) + \text{gravitino}$



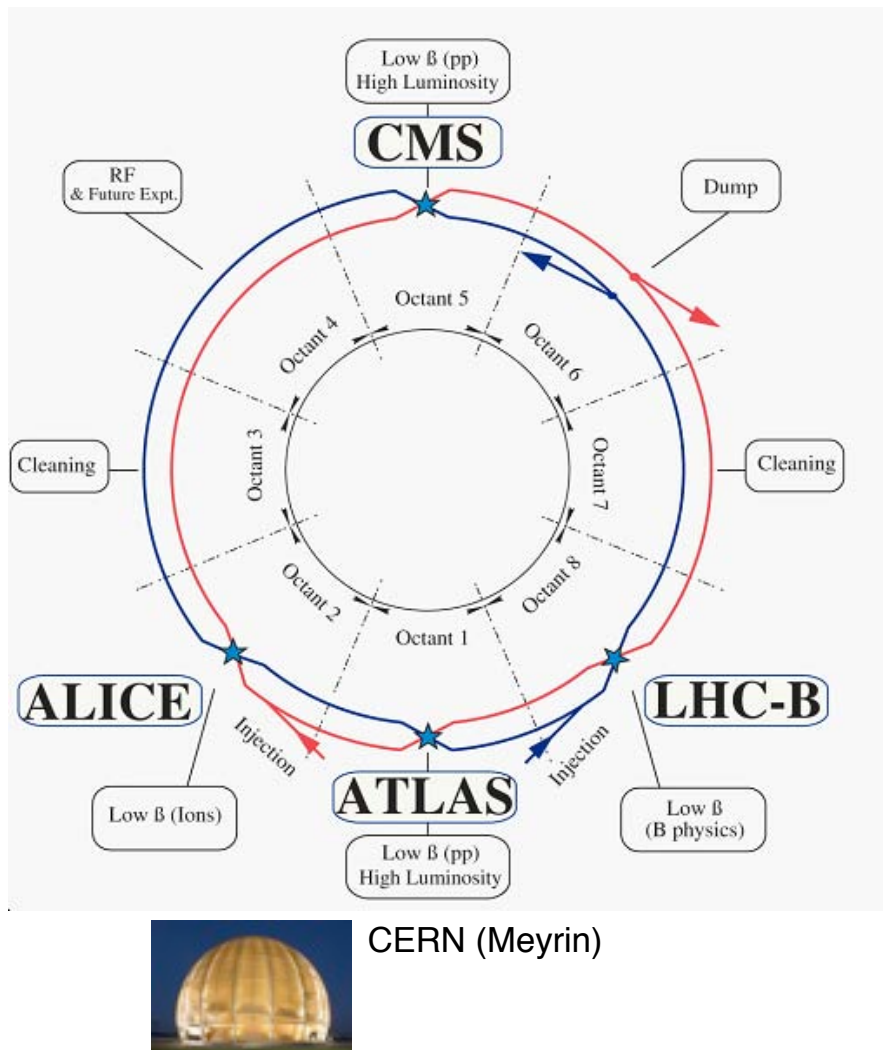
Wino NLSP: neutralino $\rightarrow \gamma + \text{gravitino}$ and
chargino $\rightarrow W(\rightarrow \text{jets}) + \text{gravitino}$

GMSB final states





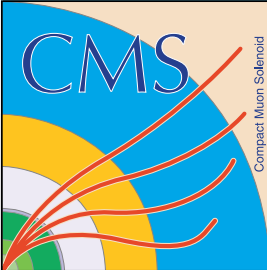
The Large Hadron Collider



Geneva Airport

$$L = \frac{N_b^2 n_b f_{\text{rev}} \gamma_r}{4\pi \epsilon_n \beta^*} F$$

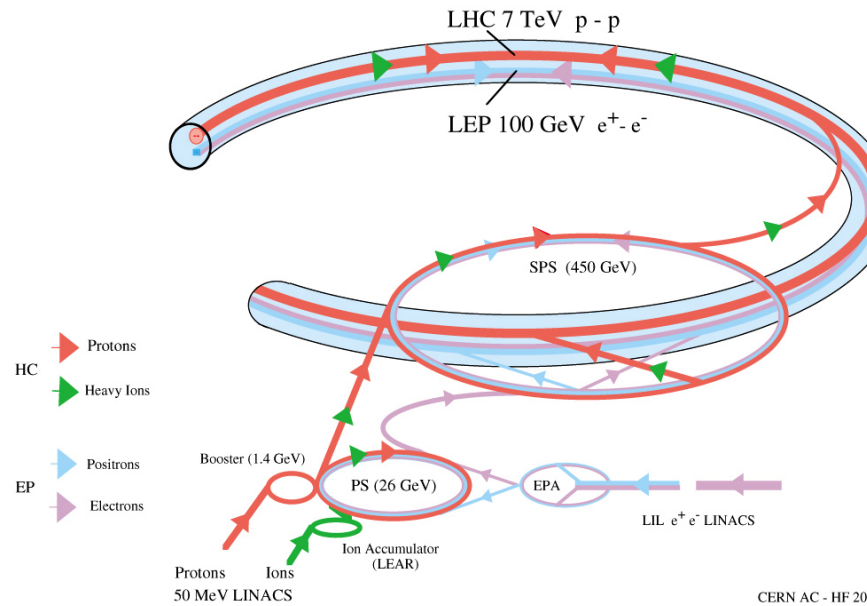
- 7 TeV center-of-mass energy pp collider synchrotron with instantaneous luminosity $3.55 \times 10^{33} \text{ cm}^{-2} \text{ s}^{-1}$ (design 10^{34})
- Highest energy collider to date (need to produce heavy particles, e.g. SUSY or Higgs)
- Highest luminosity hadron collider to date (new particles are rare)
- 26.7 km ring located 100 m underground on the French-Swiss border at the European Organization for Nuclear Research (CERN) in Geneva, Switzerland
- 4 experimental collision points, 2 high-luminosity points for general purpose detectors



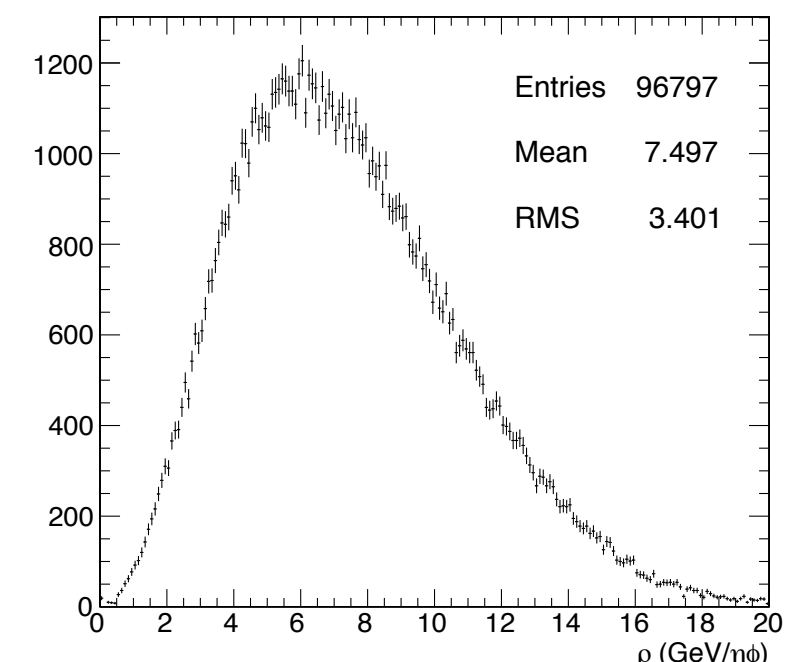
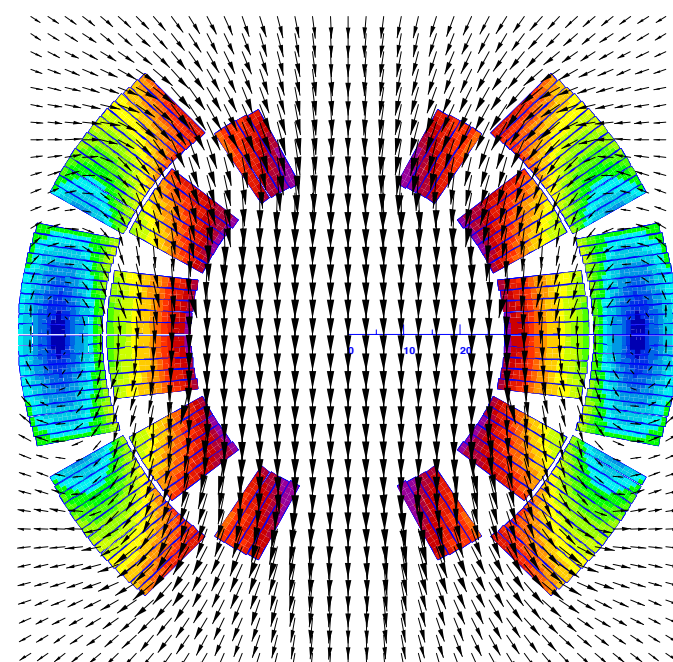
The Large Hadron Collider



The LHC injection complex

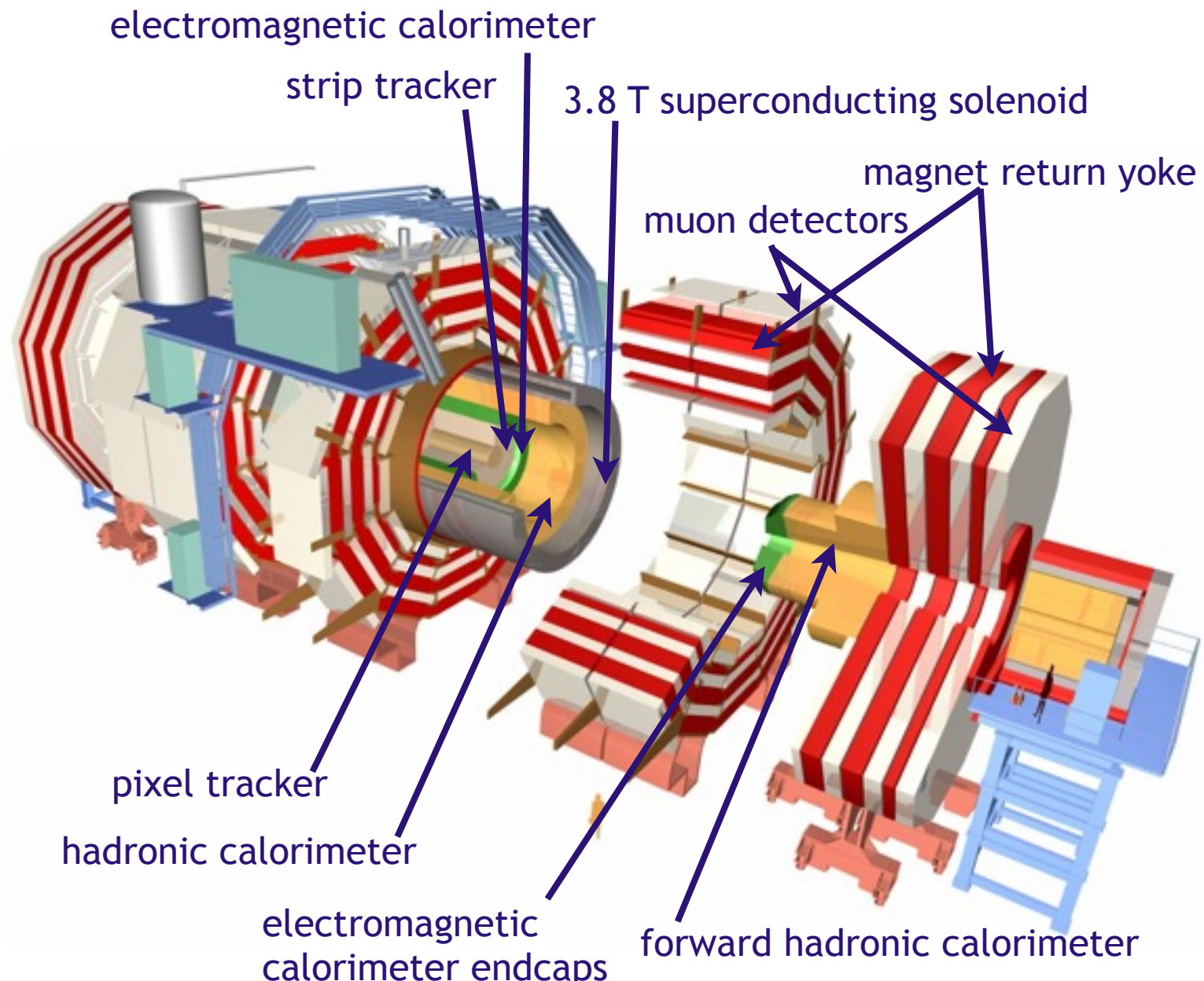


- Superconducting dipole magnets operated in 1.9 K superfluid helium bath
- Twin-bore dipoles to fit in the existing ring for the Large Electron Positron collider
- 50 ns bunch separation (25 ns design), ~7 pileup interactions mean (~20 design)
- Bunch length < 2 ns, defined by 400 MHz superconducting radiofrequency cavities



The Compact Muon Solenoid

- 4π hermetic general purpose detector
- 3.8 T superconducting solenoid enclosing the tracking detectors and calorimetry
- Detection of charged and neutral hadrons, photons, electrons, muons, taus, and particles that escape the detector (through transverse momentum imbalance)

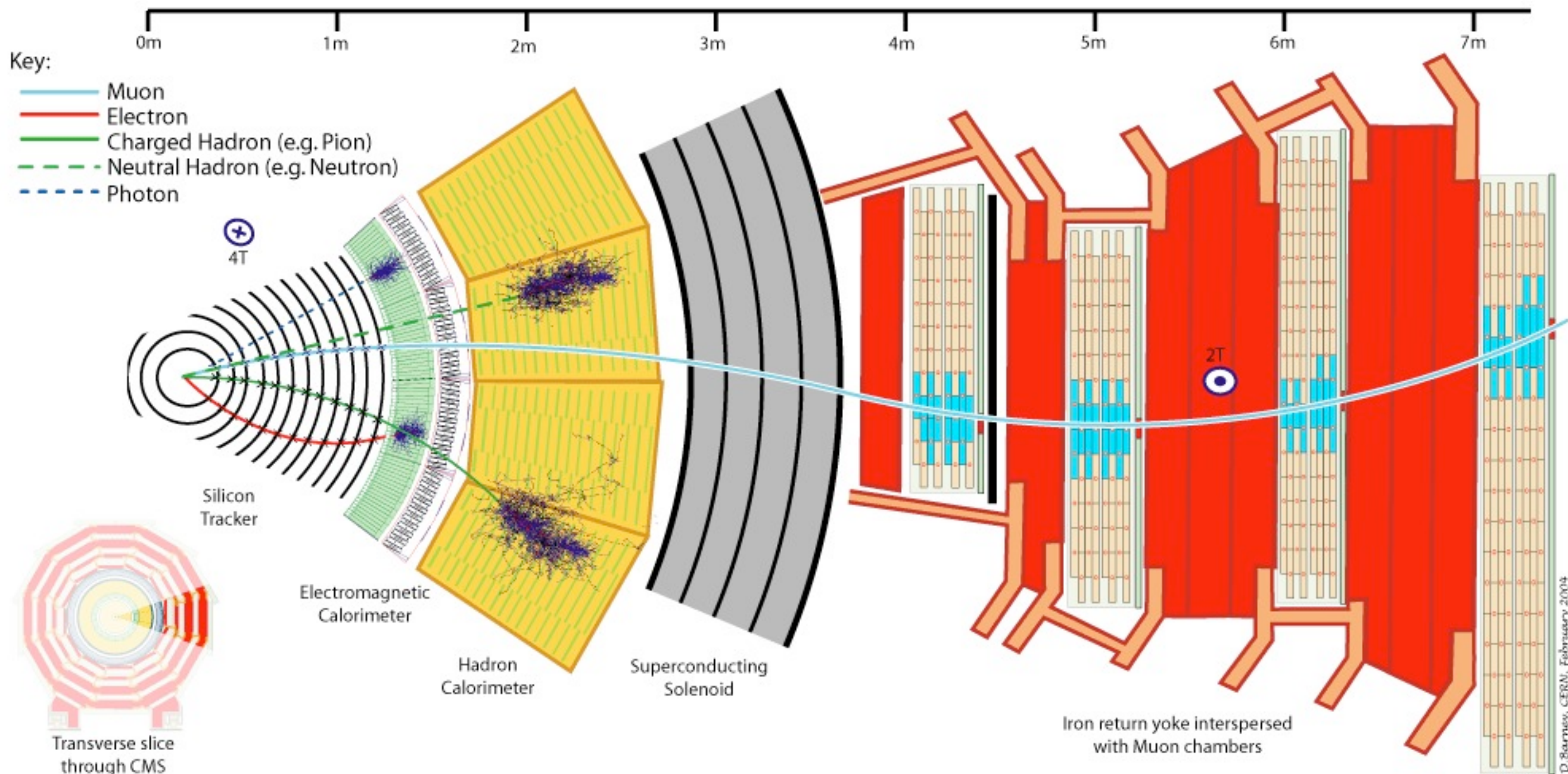


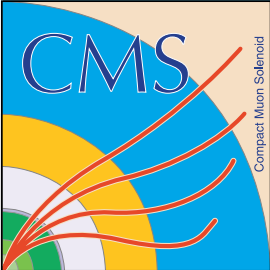
diameter: 15 m
length: 21 m

Detection principles

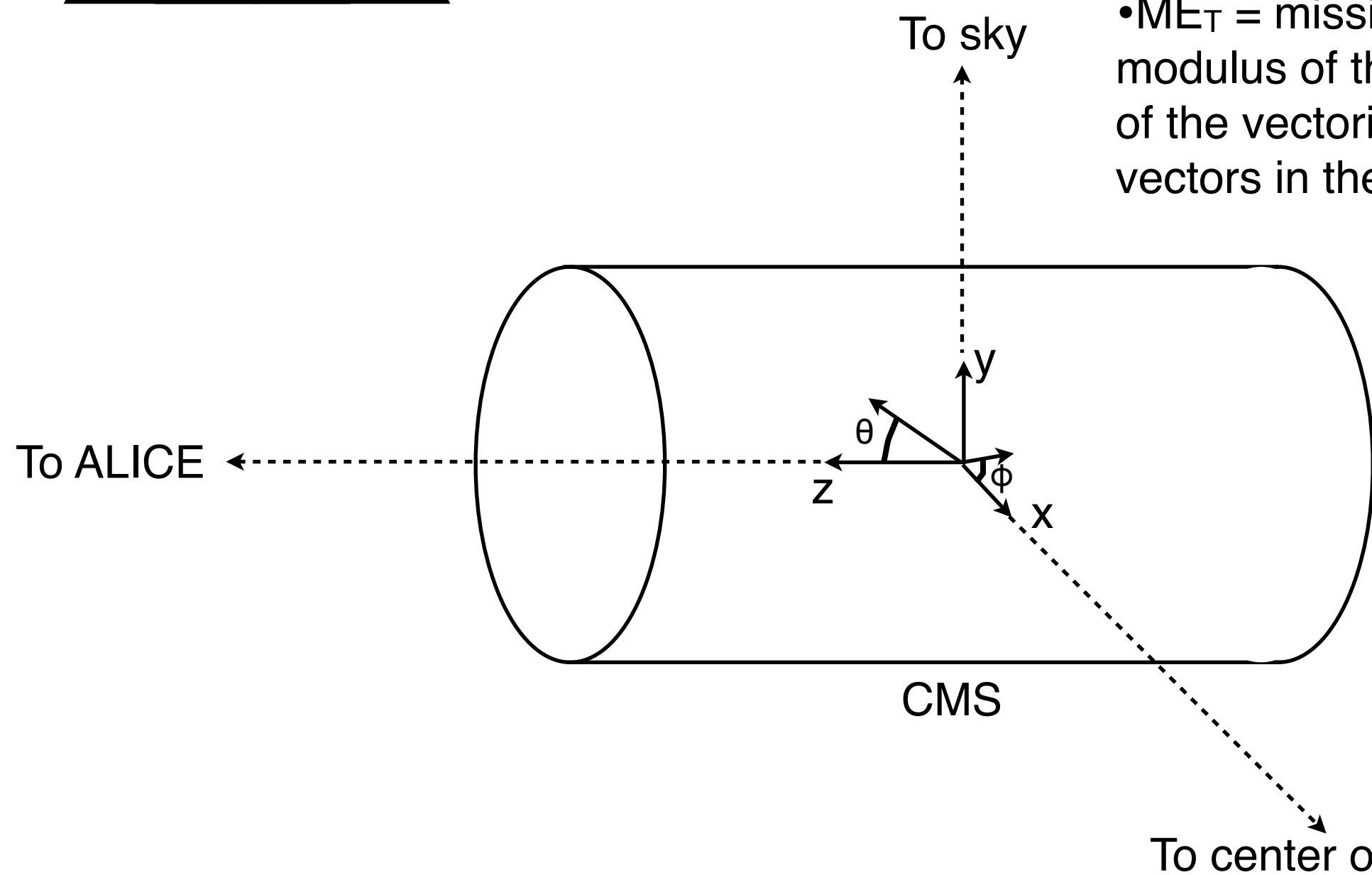


UNIVERSITY
of VIRGINIA

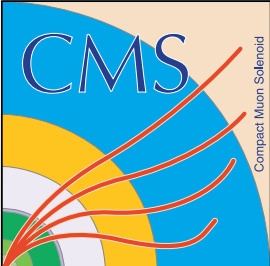




CMS coordinate system



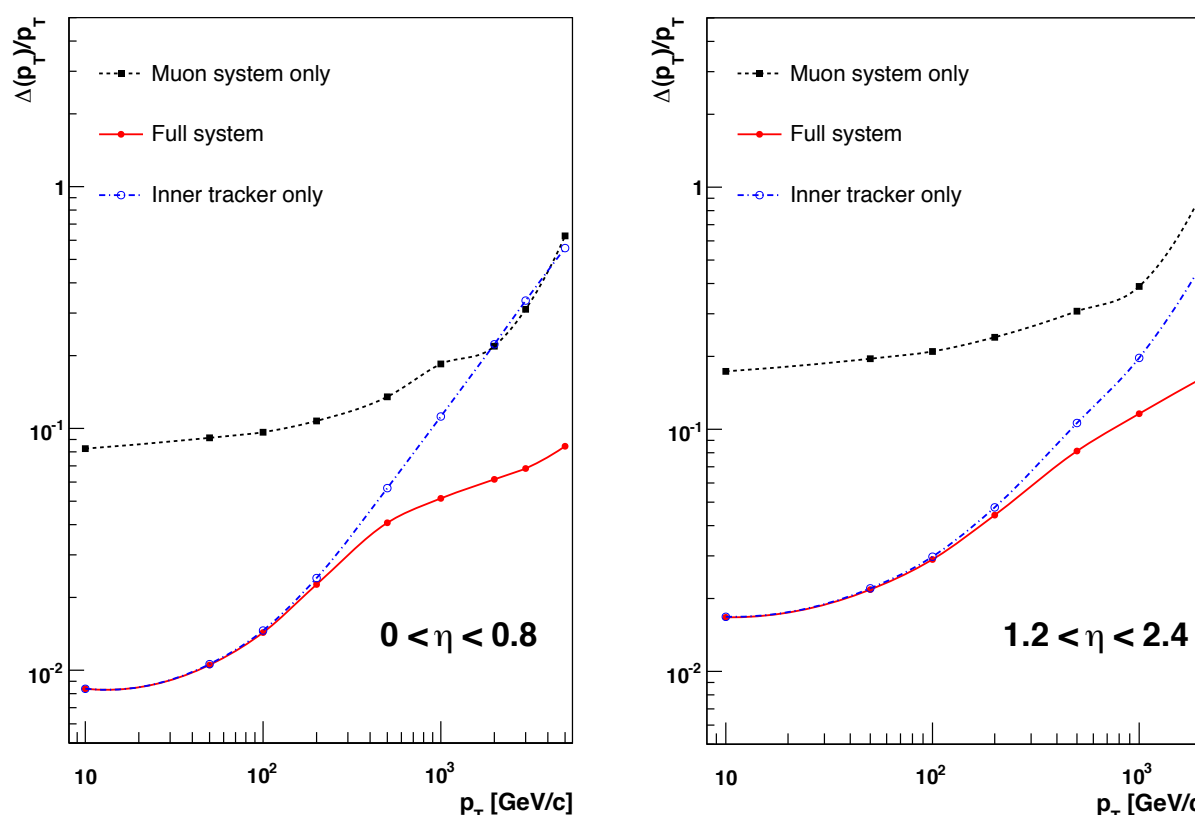
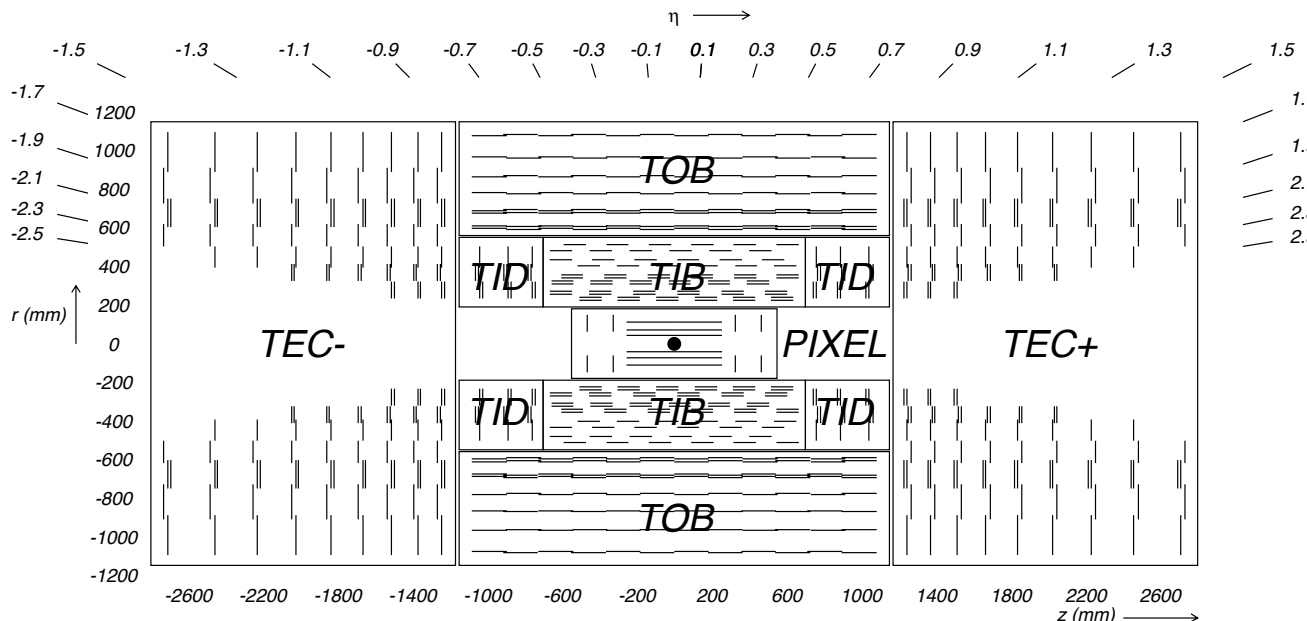
- $\eta = -\ln \tan (\theta/2)$
- $\eta \sim$ pseudorapidity for relativistic particles
- $M\mathbf{E}_T =$ missing transverse energy = modulus of the transverse component of the vectorial sum of all particle 4-vectors in the event



Tracker



UNIVERSITY
of VIRGINIA

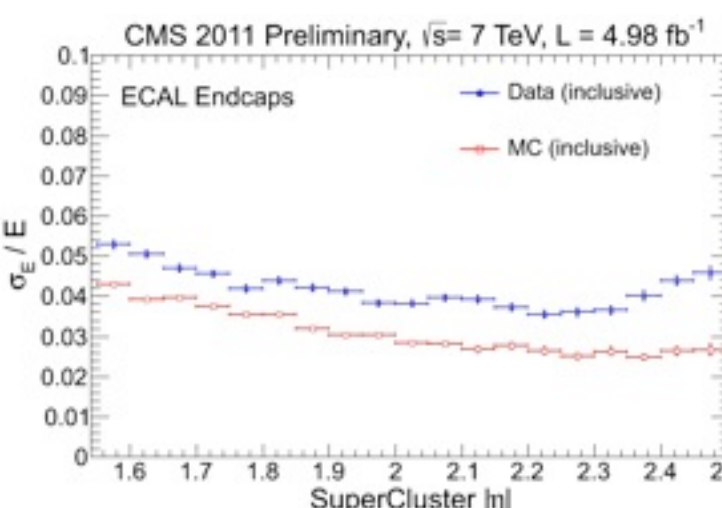
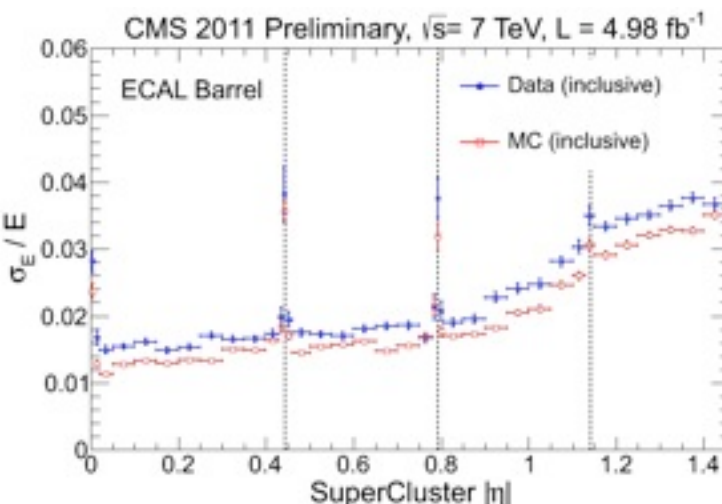


- Silicon pixels up to $r = 10.2$ cm, strips up to $r = 1.1$ m (3 layers pixels + >10 layers strips)
- Efficient reconstruction of many charged tracks per event and tagging of displaced vertices from b quarks
- $15\text{-}20 \mu\text{m } r\cdot\phi$ and z pixel resolution, $15\text{-}45 \mu\text{m } r\cdot\phi$ strip resolution
- Strip signal:noise ~ 20

Electromagnetic calorimeter

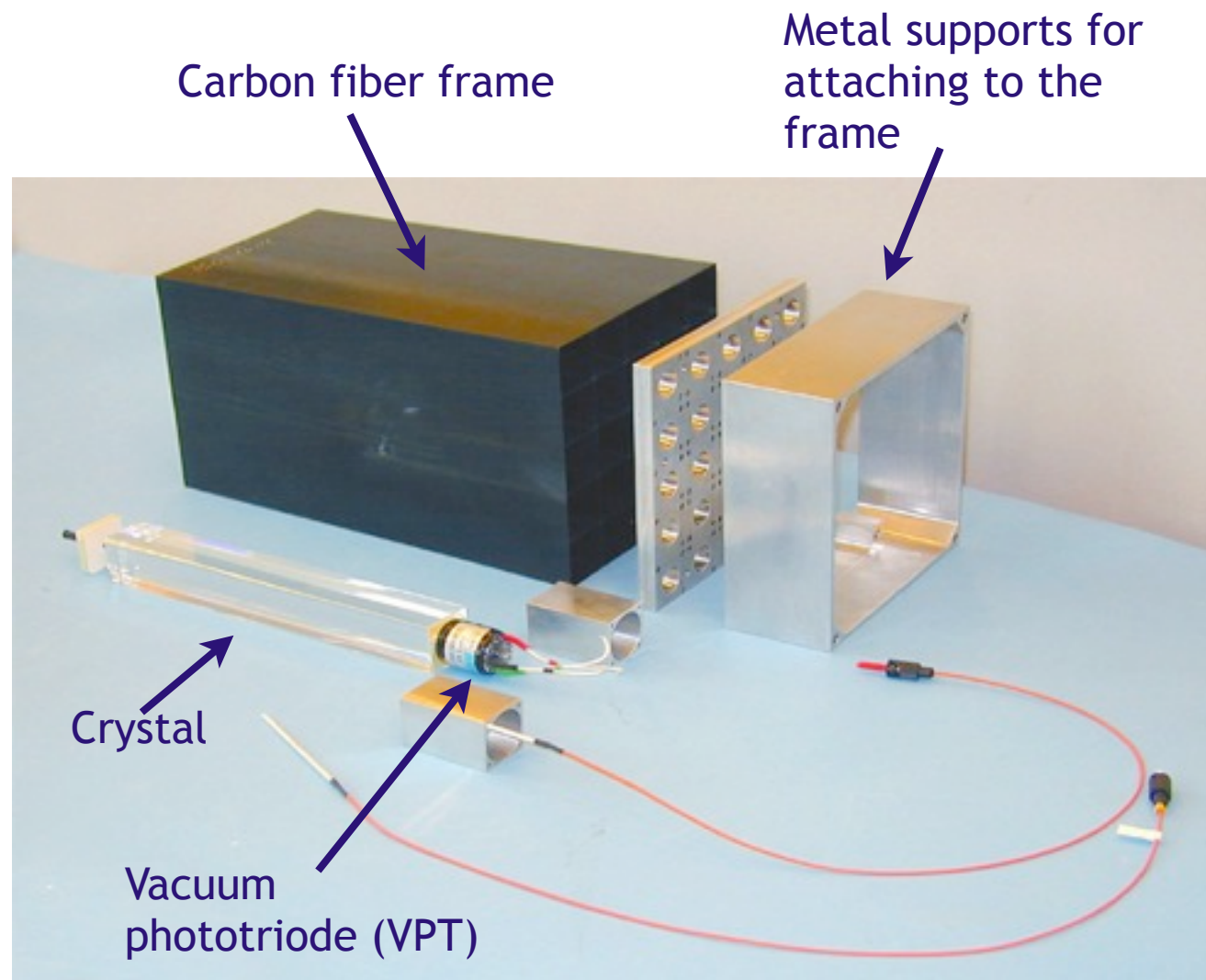


- Constructed of ~75,000 compact, dense (8.3 g/cm^3), relatively radiation hard scintillating lead tungstate (PbWO_4) crystals \Rightarrow absorber is scintillator
- Crystal dimensions: ~1 Molière radius (~22 mm) x ~1 Molière radius x ~25 X_0 (~9 mm) \Rightarrow most of an electromagnetic shower is contained within 1 crystal
- Short scintillation time (~80% of scintillation light is emitted in 25 ns, the LHC collision frequency) \Rightarrow can easily resolve events in different LHC buckets
- Efficient triggering of electrons and photons
- 10 samples read out for good amplitude and timing determination



Distinct challenges of the electromagnetic calorimeter endcaps

[4]



Disassembled EE supercrystal

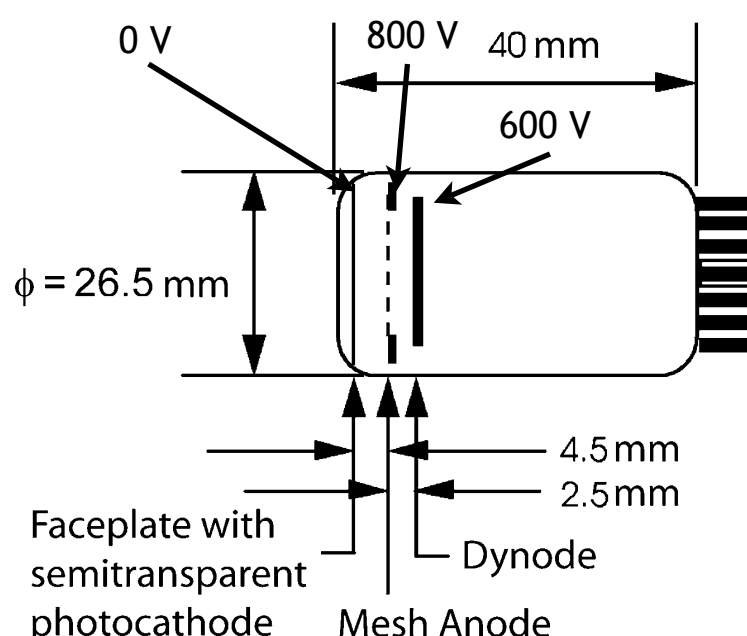
- Electromagnetic calorimeter (ECAL) endcaps (EE) extend crystal coverage from $\eta = 1.5$ out to $\eta = 3.0$
- Larger acceptance for rare $H \rightarrow \gamma\gamma$, $H \rightarrow ZZ$, and $H \rightarrow WW$ processes
- Calorimetry at high η (+ particle flow techniques) \Rightarrow better ME_T reconstruction \Rightarrow better sensitivity to SUSY processes
- EE faces a much harsher environment than the ECAL barrel (EB)
 - Strong magnetic field
 - Higher occupancy
 - More radiation damage
- **Significant design difference between EB and EE: choice of vacuum phototriode as photodetector**
- Calibrating EE is a considerable challenge

Vacuum phototriodes

Anode, dynode, and cathode HV wires

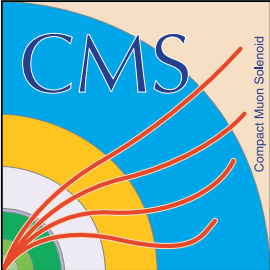


Faceplate



- Chosen for their radiation hardness and good performance in strong magnetic fields
- Cathode at 0 V, dynode at 600 V, and anode mesh between them at 800 V

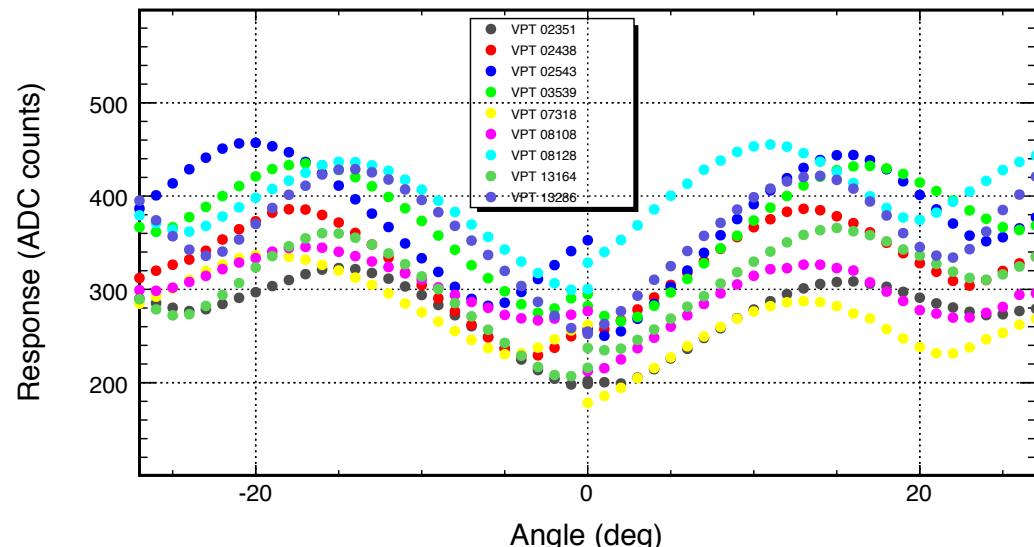
Schematic of a CMS VPT



VPT testing at UVa

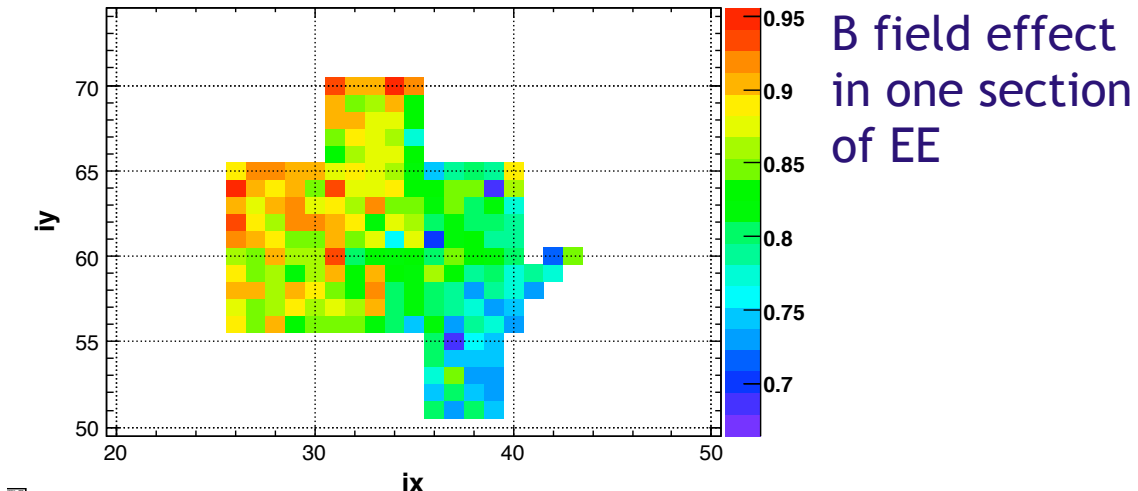


VPTs: 02351 02438 02543 03539 07318 08108 08128 13164 13286



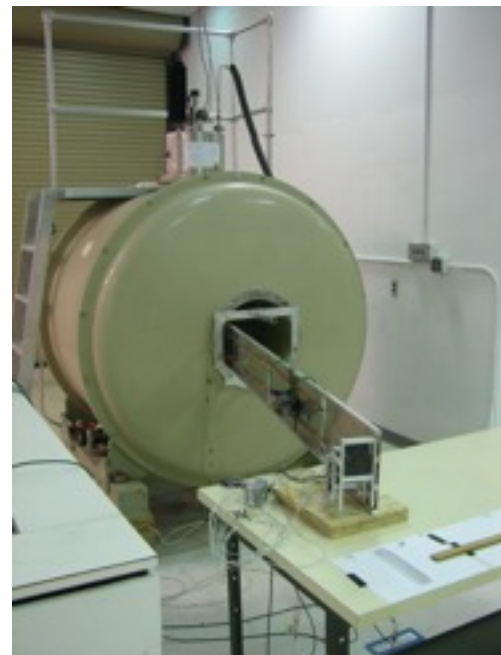
Response of 9 VPTs
vs. angle of VPT
with respect to the
magnetic field
direction

run 69486 (3.8 T) / run 70128 (0 T), blue LED



B field effect
in one section
of EE

- During the spring of 2008, extensive VPT testing was carried out in the UVa 4 T magnet, commissioned during winter 2008-2009
- Certified VPTs were installed on the endcap crystals
- Issues to be understood:
 - Response vs. angle with respect to the magnetic field direction: is it smooth and in rough agreement with theoretical calculation?
 - How do VPTs with skewed anodes or crinkled anodes compare to nominal?

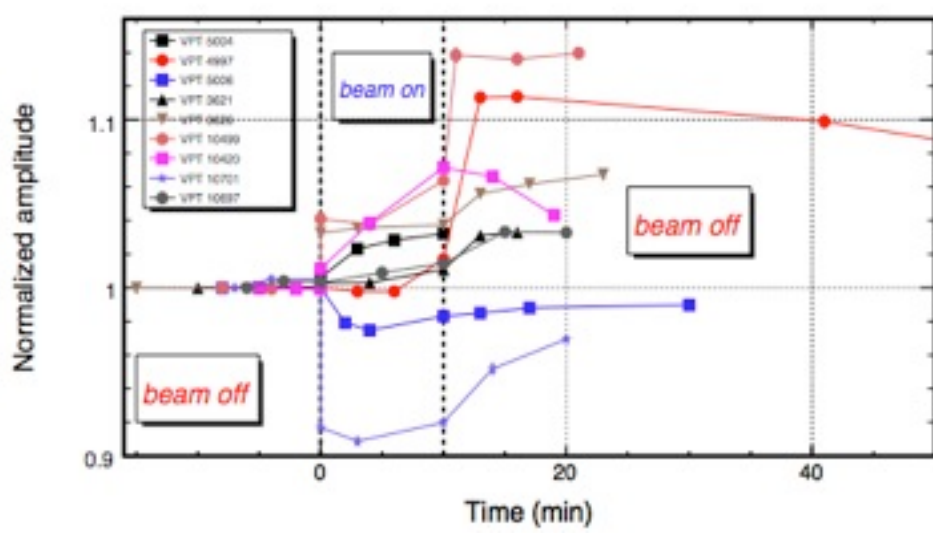


Apparatus for
measuring VPT
response vs. angle



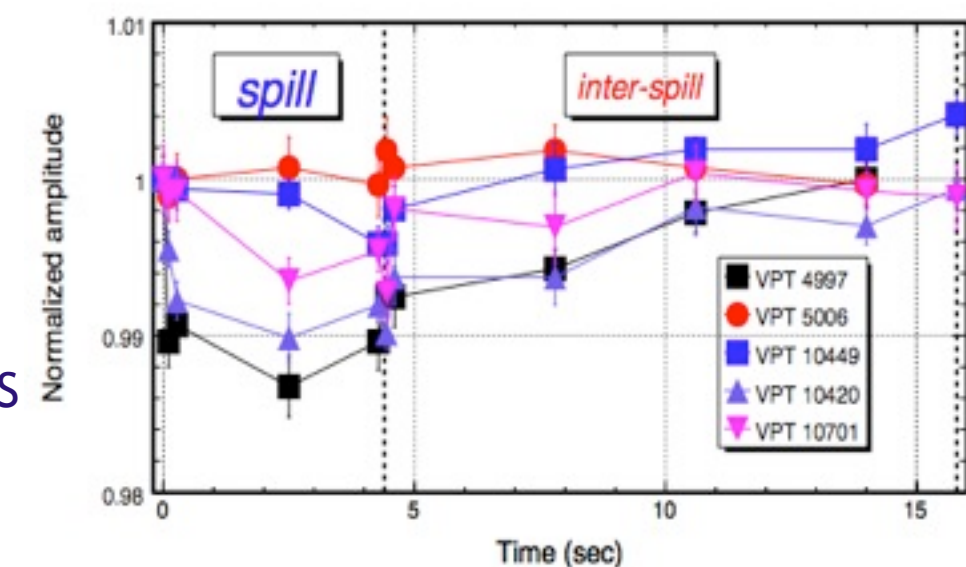
VPT stability

- VPTs first used in the OPAL electromagnetic calorimeter endcaps
- VPT gain varies with frequency/amplitude of incident light
 - Effect strongly suppressed in 4 T magnetic field
 - High→low frequency: gain increases
 - Low→high frequency: gain increases or decreases
- All VPT responses are different
- **Provide a constant rate of stability LED pulses to the VPTs to suppress gain changes at LHC on/off transitions**

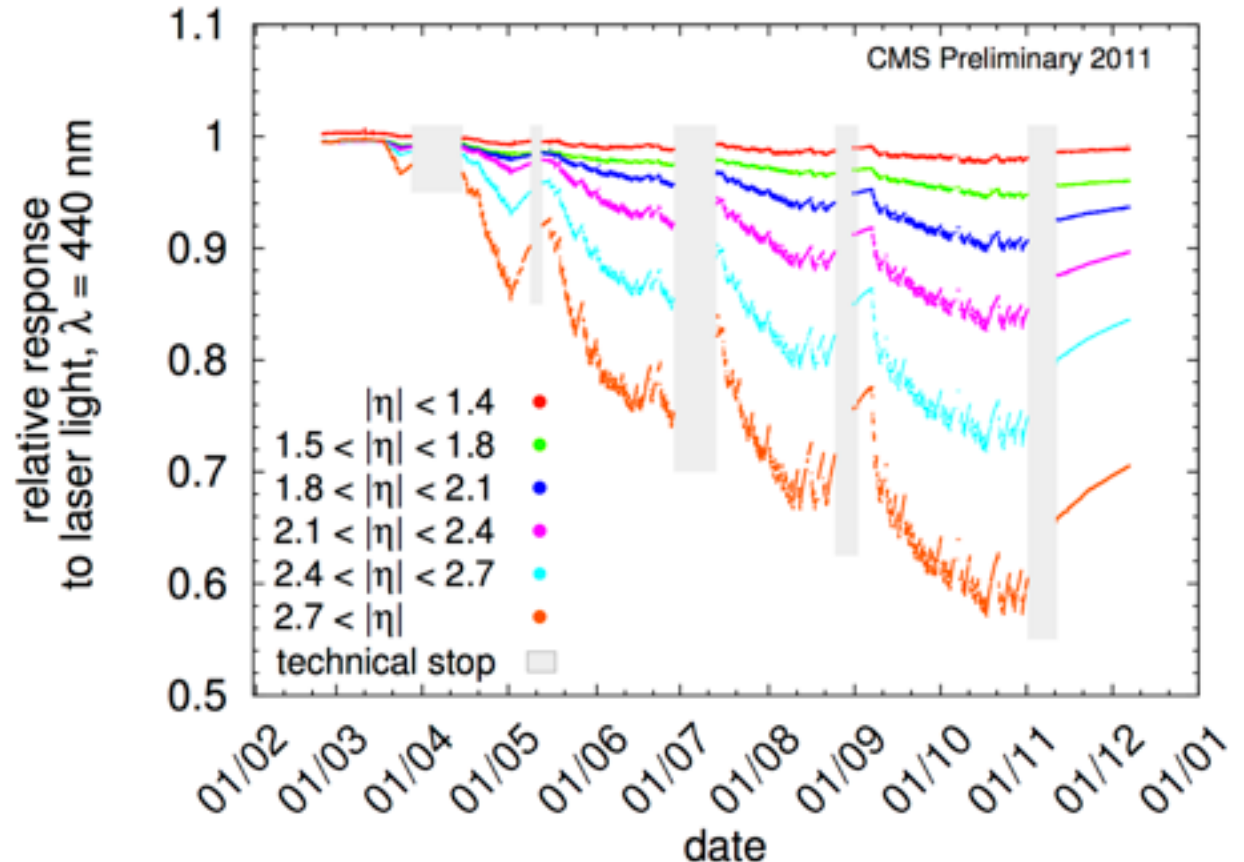


VPT response vs. time for different background pulsing rates

Response of VPTs to SPS spill simulation



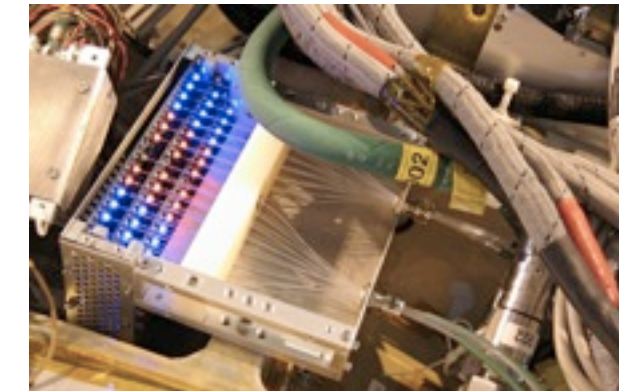
Radiation damage



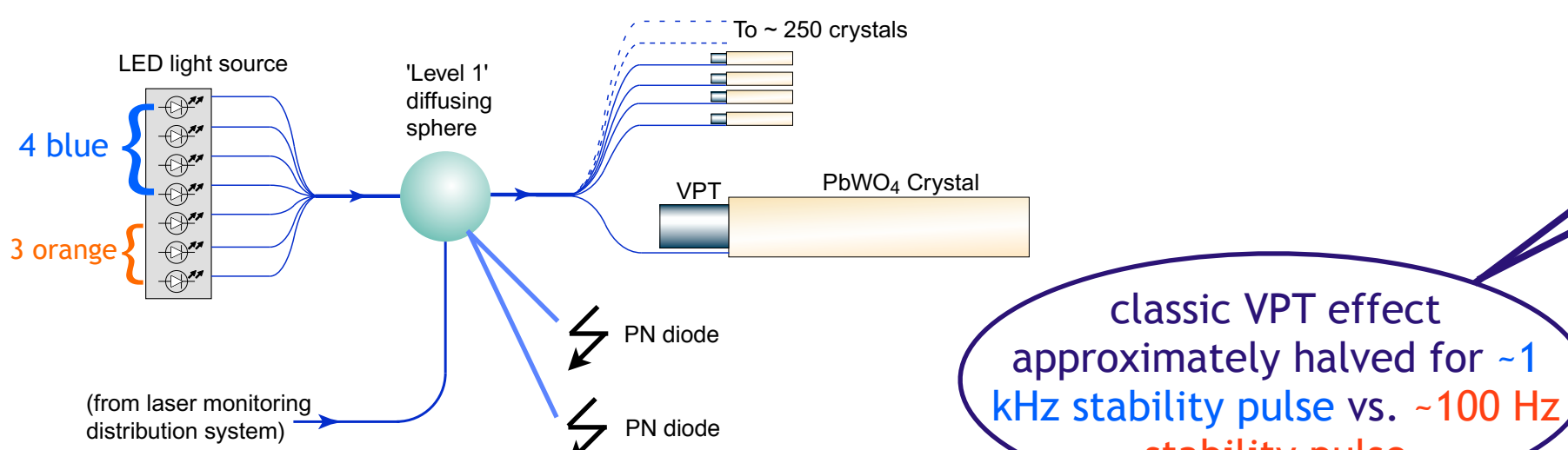
- Sustained ionizing radiation causes crystal radiation damage, reducing crystal transparency and ultimately the amount of light collected by the photodetectors
- Crystal transparency loss correlated with LHC integrated luminosity, and increases faster for higher instantaneous luminosity
- **Continuously pulse crystals from known light source to track and correct for transparency loss from radiation damage**

LED stability and calibration system

- Dual wavelength LED stability and monitoring system designed at UVa
- Blue (450 nm) LED: near the peak of crystal scintillation and VPT photocathode efficiency, so ideal for transmitting the maximum amount of light to VPTs for stability pulsing
- Orange (617 nm): transparent to crystals but still efficient for VPT photocathode, so ideal for disentangling crystal damage from VPT gain changes
- PN diodes for normalization



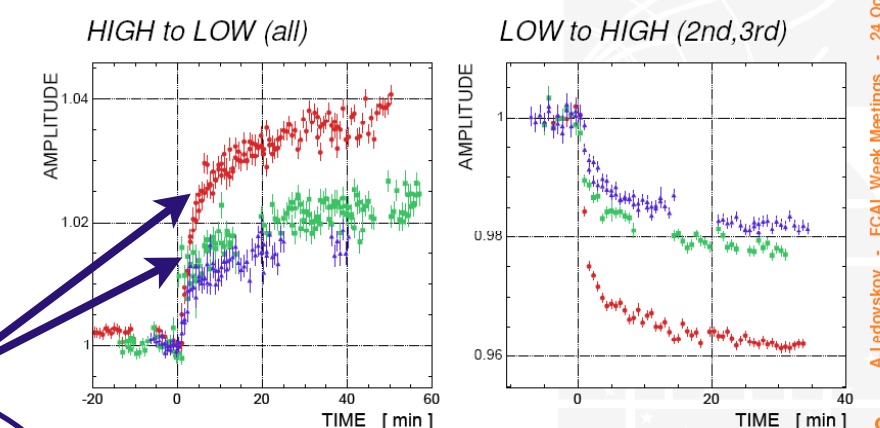
LED system on EE
dee patch panel



classic VPT effect
approximately halved for ~1
kHz stability pulse vs. ~100 Hz
stability pulse

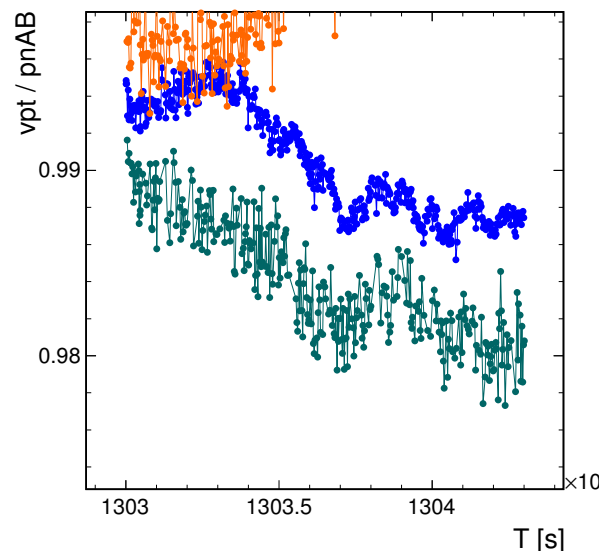
summary

	LED	Beam LOW	Beam HIGH
Red:	88.4 Hz	200-300 Hz	16-18 kHz
Green:	635 Hz	190-220 Hz	8.0-8.5 kHz
Blue:	932 Hz	220-260 Hz	15-16 kHz

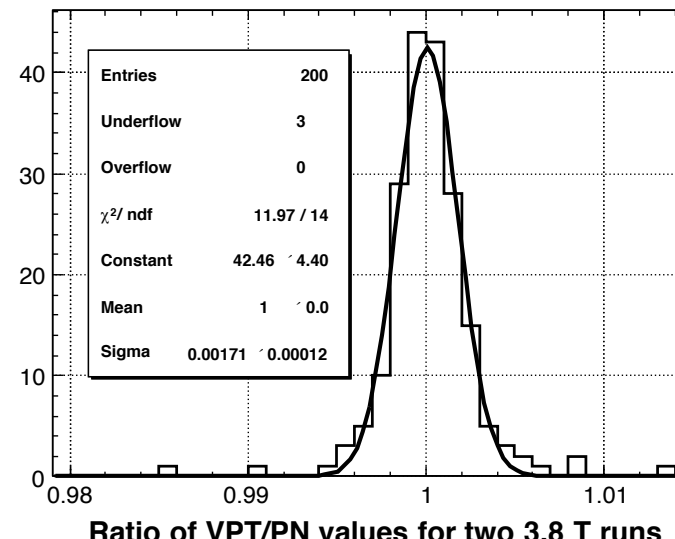


LED and VPT performance

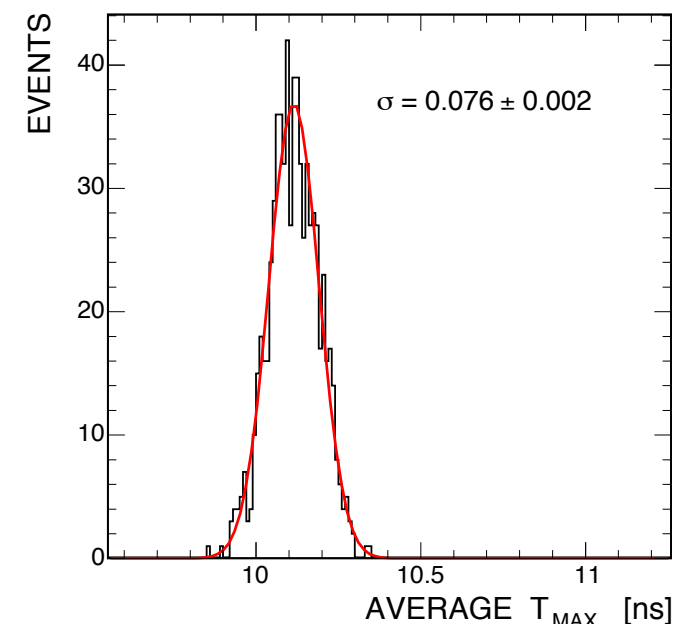
VPT/PN vs. time for blue laser (green) and blue LED (blue) Apr. 17 - May 2 2011



Ratio of PN-normalized VPT amplitudes for two different runs (channels experienced HV and B field cycling between runs)

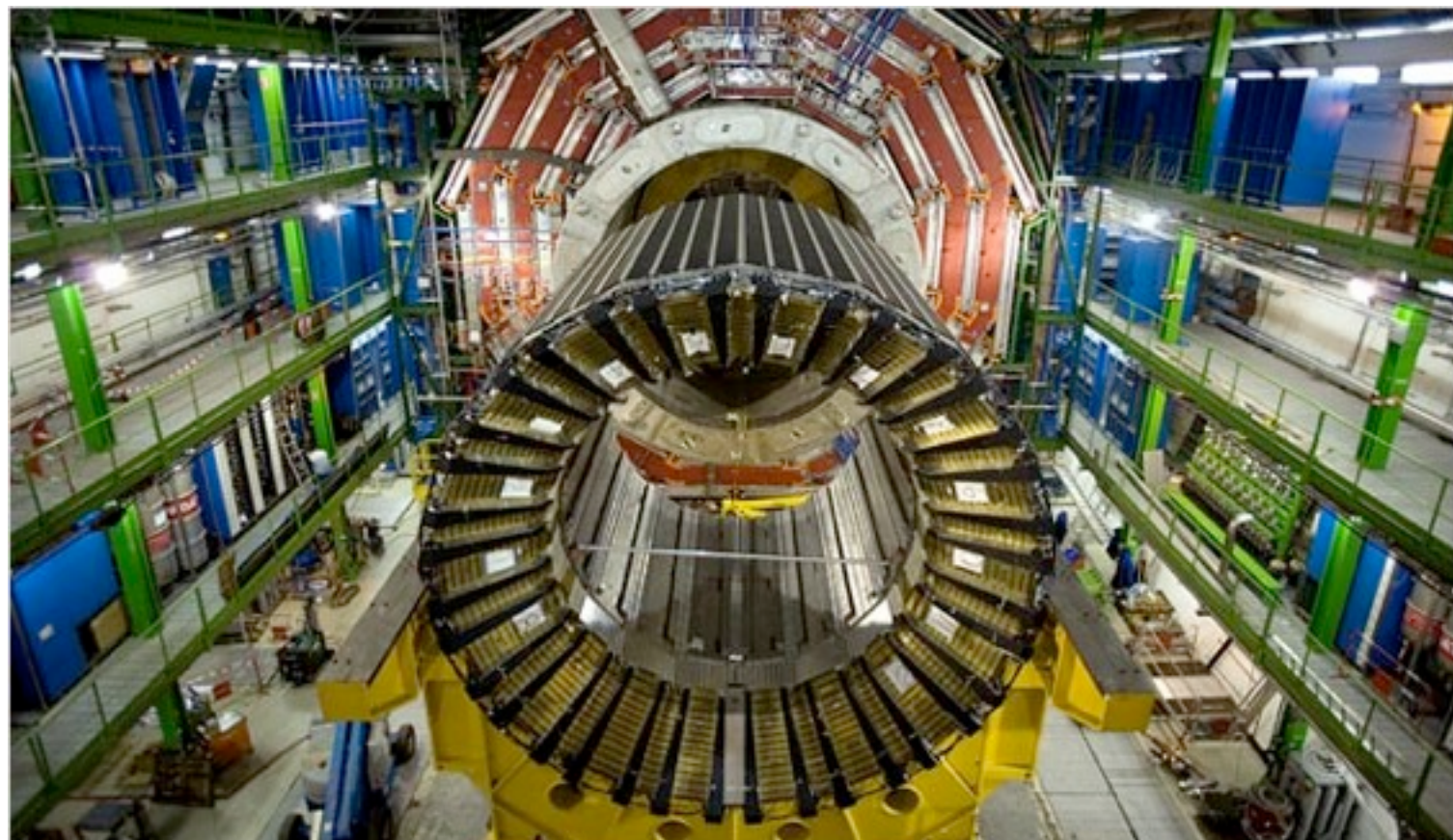


Distribution of average LED timing for a single diffusing sphere



- Stable, reliable LED system important for ECAL calibration
- VPT effect currently dwarfed by transparency loss, but system in place to mitigate gain changes in order to achieve best performance

Hadron calorimeter



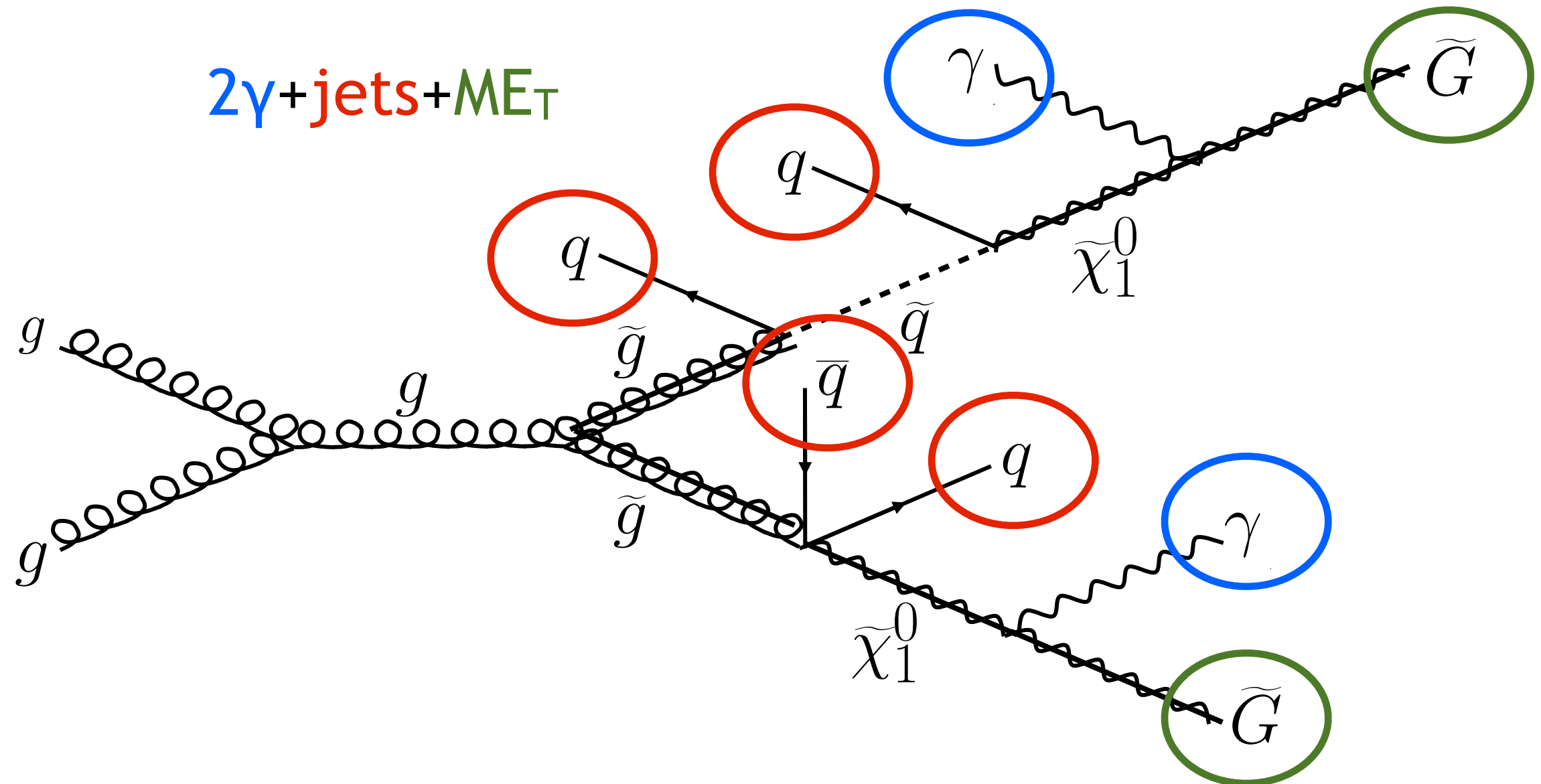
- Sampling calorimeter made of brass absorber interleaved with plastic scintillator
- 1 readout layer
- Forward hadron calorimeter (HCAL) constructed of quartz fibers distributed throughout steel absorber
- Covers ~12 hadronic interaction lengths
- Reconstruction of hadronic jets and MET

Muon detectors



- Gaseous ionization detectors (drift tubes, cathode strip chambers, and resistive plate chambers)
- 4 tracking points recorded and combined with silicon tracker measurements
- Efficient triggering of muons

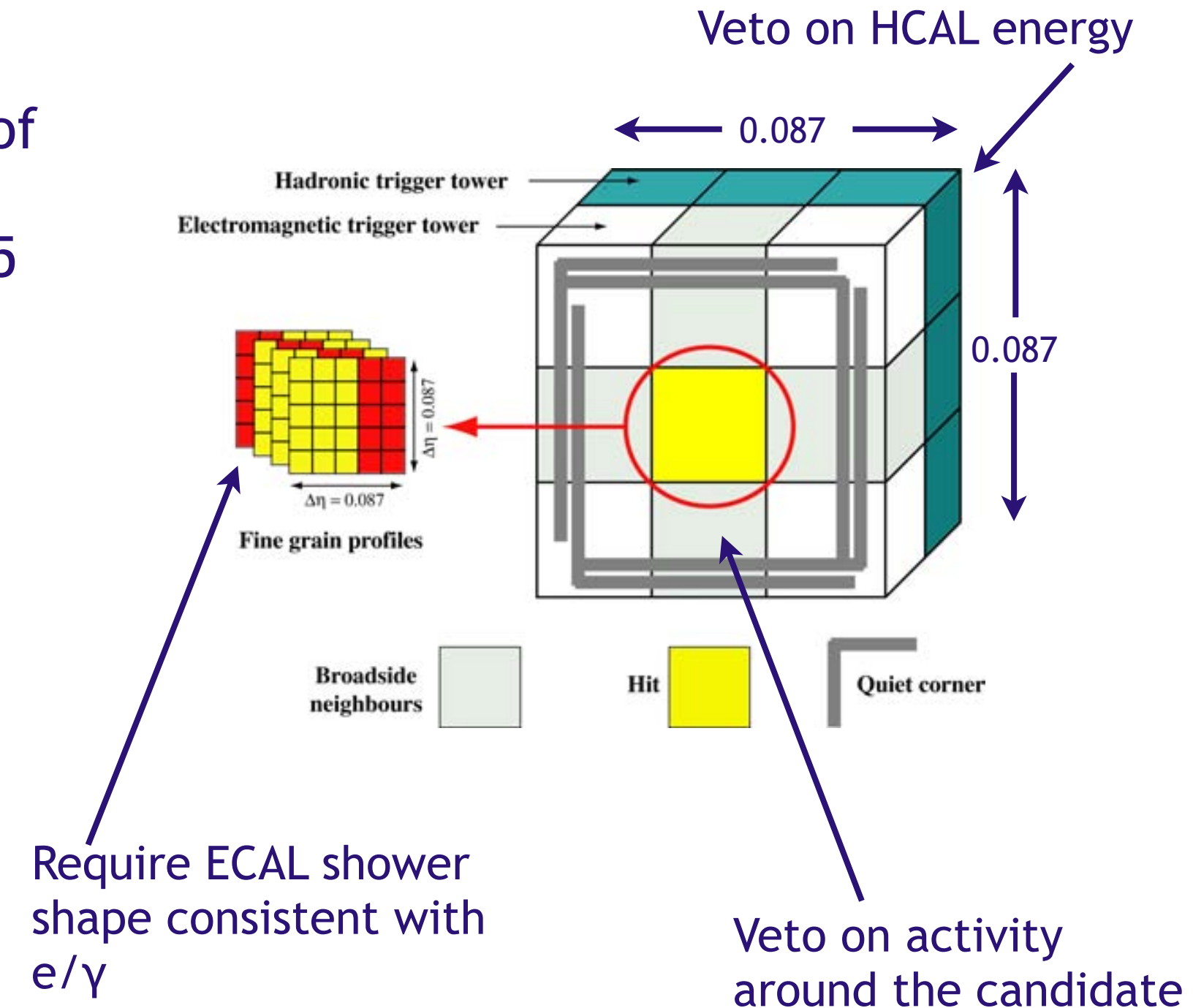
Event selection



How to find this in CMS?

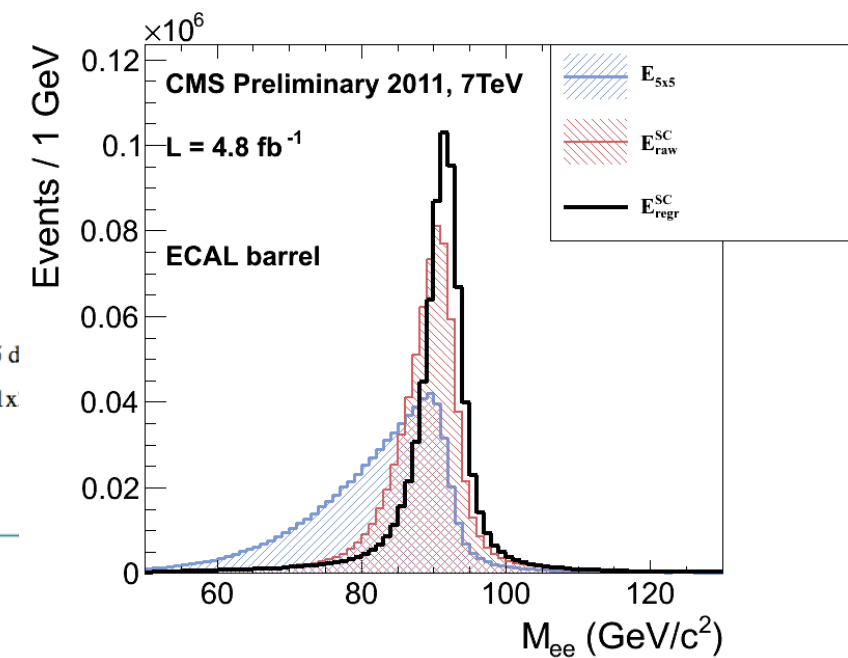
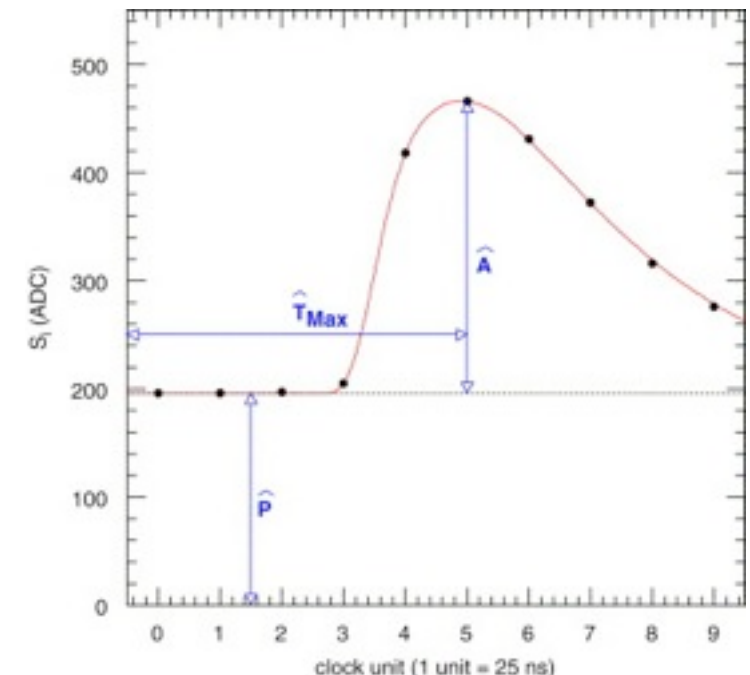
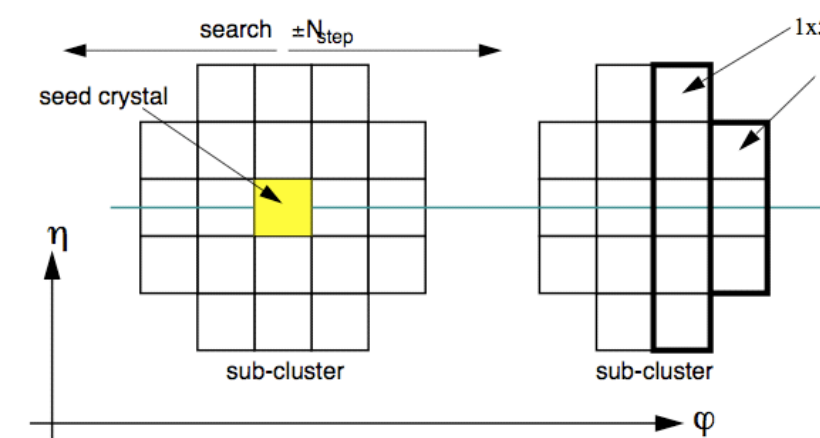
Trigger

- Trigger on the presence of ≥ 2 high E_T isolated ECAL energy deposits in a 5×5 array of crystals
- Trigger efficiency nearly 100% for selected $\gamma\gamma$ events
- Total data sample analyzed: 4.7 fb^{-1} , corresponding to entire 2011 run

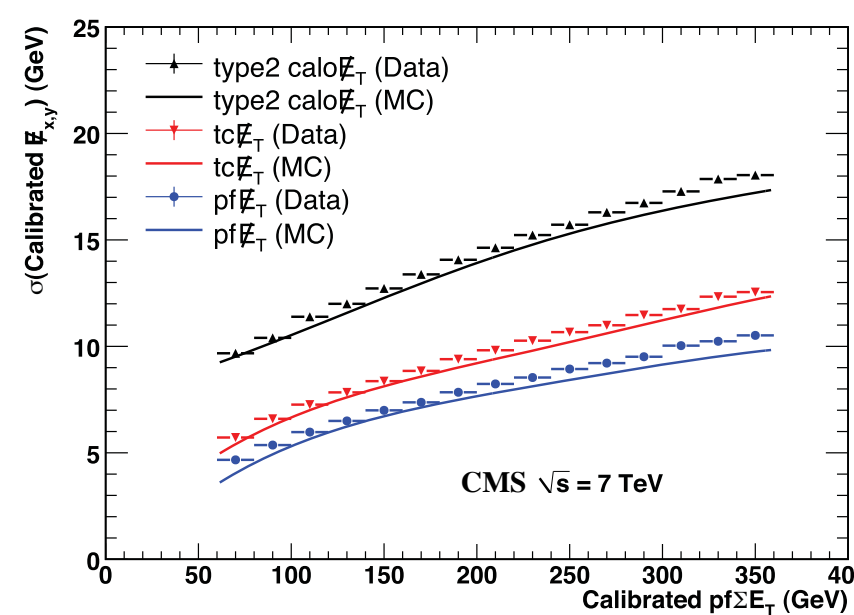
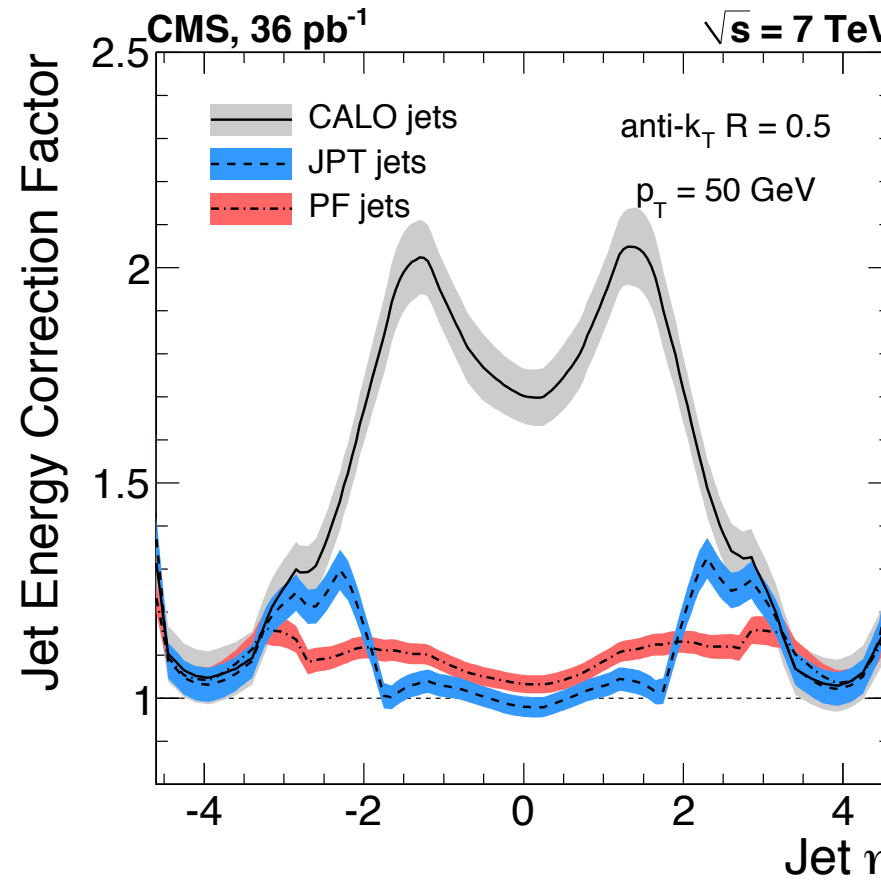


Photon reconstruction

- Pulse amplitude and timing determined from fit to digitized samples
- Amplitude calibrated to get a value in GeV
 - Correct for transparency loss and non-uniformity of response across crystals
 - Calibration exploits ϕ symmetry of detector, π^0/η decays to photons, and $E(\text{ECAL})/p(\text{tracker})$ for Z electrons
- Clustering
 - Dynamic window in ϕ to pick up $\gamma \rightarrow e^+e^-$ conversions and electron bremsstrahlung
 - Cluster corrections $f(E_T, \eta)$ for bremsstrahlung, tracker material, containment of showers, and residual E_T dependence taken from MC



Jet/ ME_T reconstruction



- Particle flow (PF) algorithm
 - Reconstruct fundamental objects (charged tracks, calorimeter clusters, outer muon tracks)
 - Link fundamental objects
 - Tracks to clusters
 - ECAL to HCAL clusters
 - Silicon muon track to outer muon track
 - Identify particles (muons, electrons, photons, charged and neutral hadrons) from the links
- Cluster jets according to anti- k_T R = 0.5 algorithm
- Jets corrected for noise, pileup, underlying event, and non-uniformity of response across η and in p_T
- ME_T built from PF candidates

Photon selection

- Single L1-seeded diphoton triggers with 36 and 22 GeV thresholds
- Combined detector isolation cuts in $\Delta R = 0.3$ cone to improve acceptance in jet-rich events
- Shower shape cuts further reduce jet fakes and anomalous energy deposits
- Pileup subtraction from isolation cone using Fastjet [15]
- Minimum ΔR between the photons to avoid isolation cone overlap
- $\sim \pm 3$ ns timing cut removes cosmics and beam halo
- Pixel veto rejects electrons

HLT match	IsoVL
E_T	$> 40 / > 25$ GeV
SC $ \eta $	$< 1.44 / 42$
H/E	< 0.05
$R9$	< 1
Pixel seed	No/No
$I_{\text{comb}}, \sigma_{i\eta i\eta}$	< 6 GeV $\&$ < 0.011
JSON	Yes
No. good PVs	≥ 1
ΔR_{EM}	> 0.6
$\Delta\phi_{\text{EM}}$	≥ 0.05

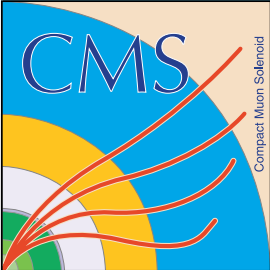
Jet selection

Variable	Cut
Algorithm	L1FastL2L3Residual corrected PF
p_T	$> 30 \text{ GeV}$
$ \eta $	< 2.6
Neutral hadronic energy fraction	< 0.99
Neutral electromagnetic energy fraction	< 0.99
Number of constituents	> 1
Charged hadronic energy	$> 0.0 \text{ GeV}$ if $ \eta < 2.4$
Number of charged hadrons	> 0 if $ \eta < 2.4$
Charged electromagnetic energy fraction	< 0.99 if $ \eta < 2.4$

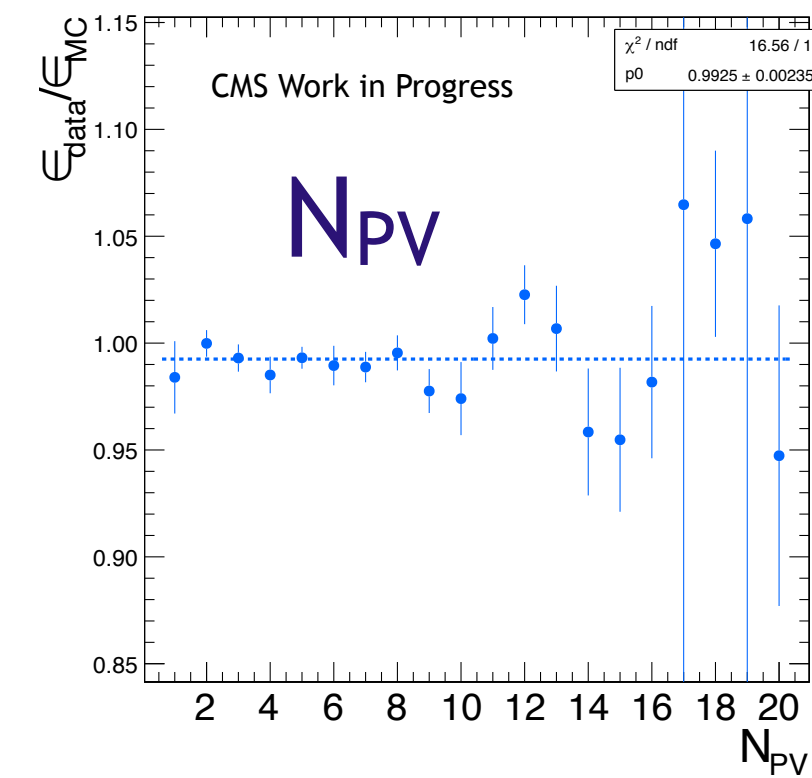
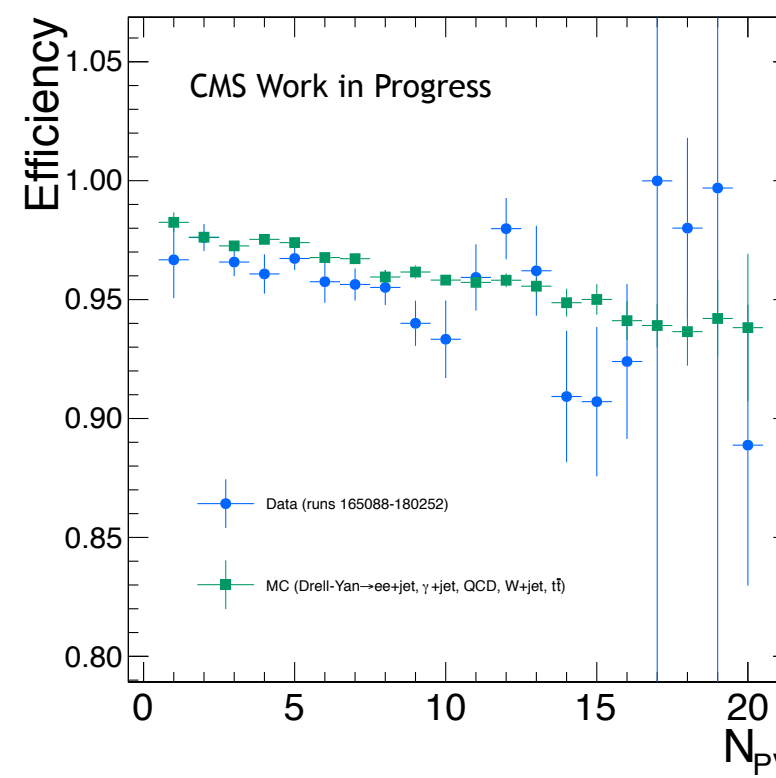
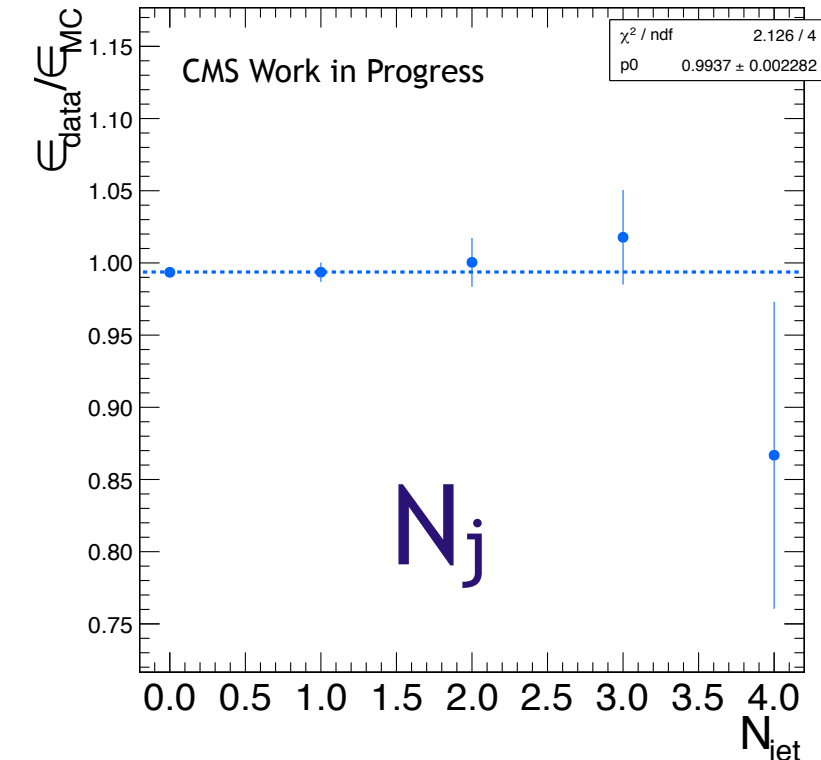
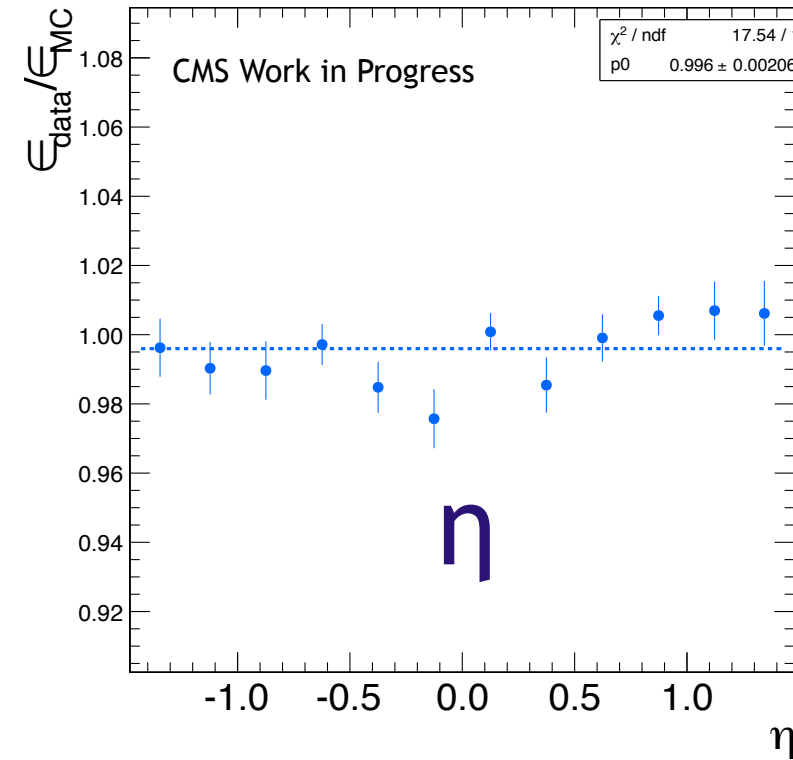
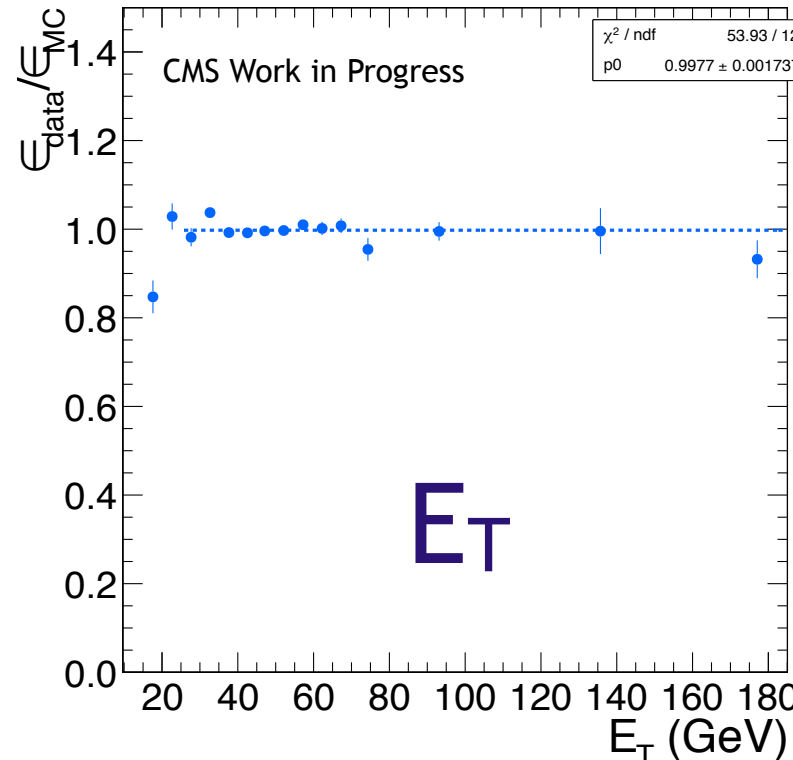
- ≥ 1 jet not overlapping any electron, photon, or fake (loosely isolated) photon

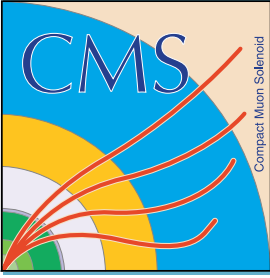
Photon ID efficiency

- Photon ID efficiencies taken from MC and corrected by $(\text{data electron efficiency}) / (\text{MC electron efficiency})$
 - Use $Z \rightarrow ee$ events to measure the electron efficiencies
 - Photon ID cuts designed to behave similarly for electrons and photons
- Signal MC acceptance \times efficiency multiplied by 1 factor of $\varepsilon_{\text{data}} / \varepsilon_{\text{MC}}$ per photon
- Pixel match veto efficiency estimated from MC: $(96.4 \pm 0.5)\%$ (stat. \oplus syst. due to tracker material budget variation)
- Data/MC efficiency scale factor: 0.99 ± 0.04 , with errors due to:
 - Z signal and background shape variation
 - Signal fit over/underestimation
 - Pileup effects
 - MC electron/photon difference



Photon ID scale factor dependence





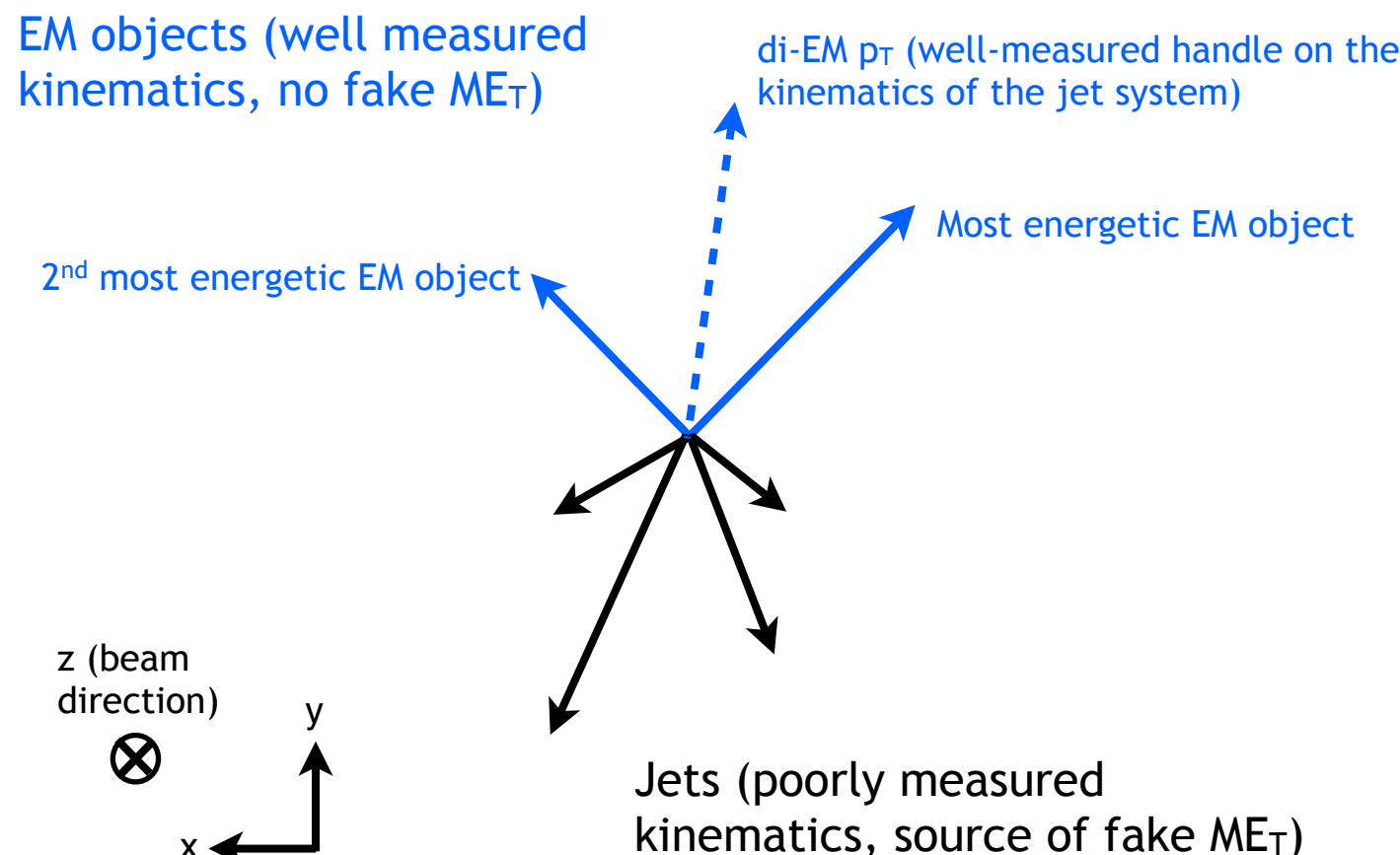
UNIVERSITY
of
VIRGINIA

Analysis

Backgrounds

- Dominant: QCD with fake ME_T
 - Diphoton
 - $\gamma + \text{jet}$: 1 jet misidentified as a photon
 - Multijet: at least 2 jets misidentified as photons
- Subdominant: electroweak processes with real ME_T
 - $W(\rightarrow e\nu)\gamma$: electron misidentified as a photon
 - $W(\rightarrow e\nu) + \text{jet}$: electron and jet misidentified as photons

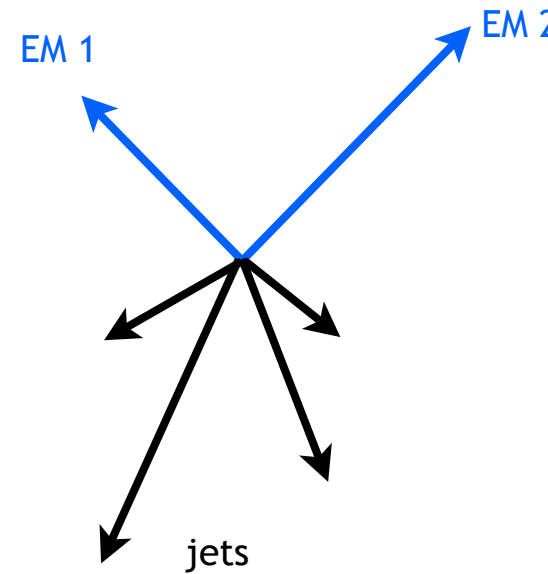
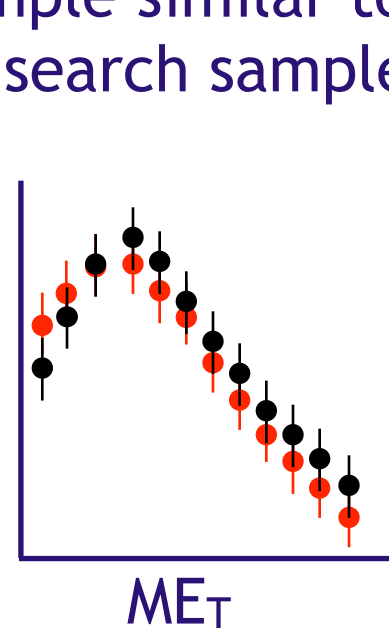
Estimating the QCD background



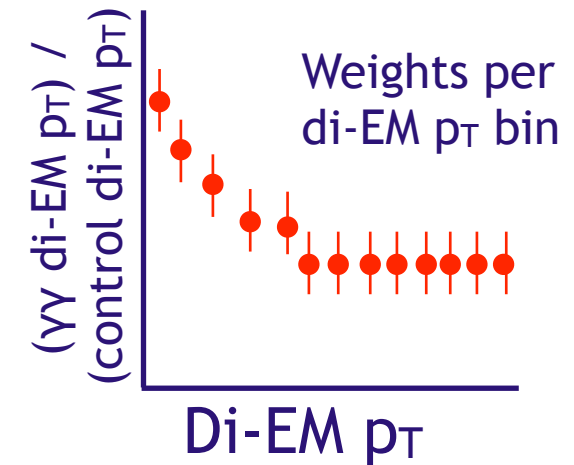
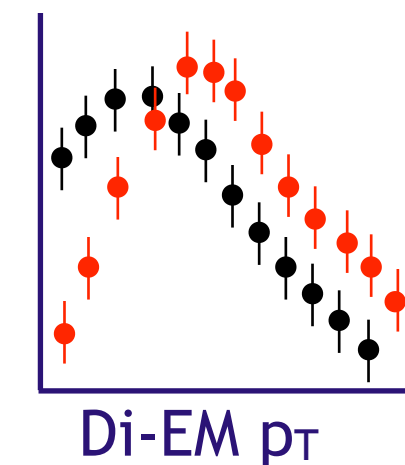
- **EM superior to hadronic energy resolution** \Rightarrow fake MET due entirely to jet mis-measurement
- **Measure QCD background from data**—control sample with well-measured EM objects to model the QCD fake MET spectrum
- **Reweighting** events in control sample based on di-EM p_T (kinematics) and N_j (hadronic activity)
- **Normalize** the predicted QCD fake MET spectrum to a signal-depleted region with $\text{MET} < 20 \text{ GeV}$

Reweighting

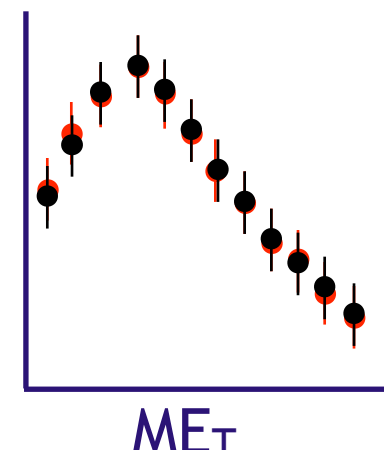
Step 1: Find a control sample similar to the $\gamma\gamma$ search sample



Step 2: p_T of di-EM system different between control and $\gamma\gamma$ samples \Rightarrow different ME_T \Rightarrow assign weight to control event based on di-EM p_T

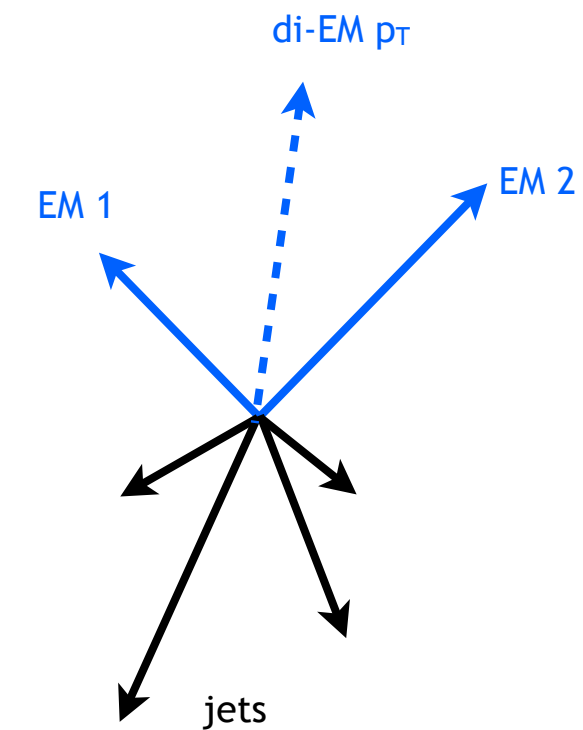


Step 4: Weight each event in control ME_T distribution with weights from steps 2-3.



Step 3: Repeat step 2 for events with 0 jets, 1 jet, and ≥ 2 jets.

$\gamma\gamma$ sample
control sample

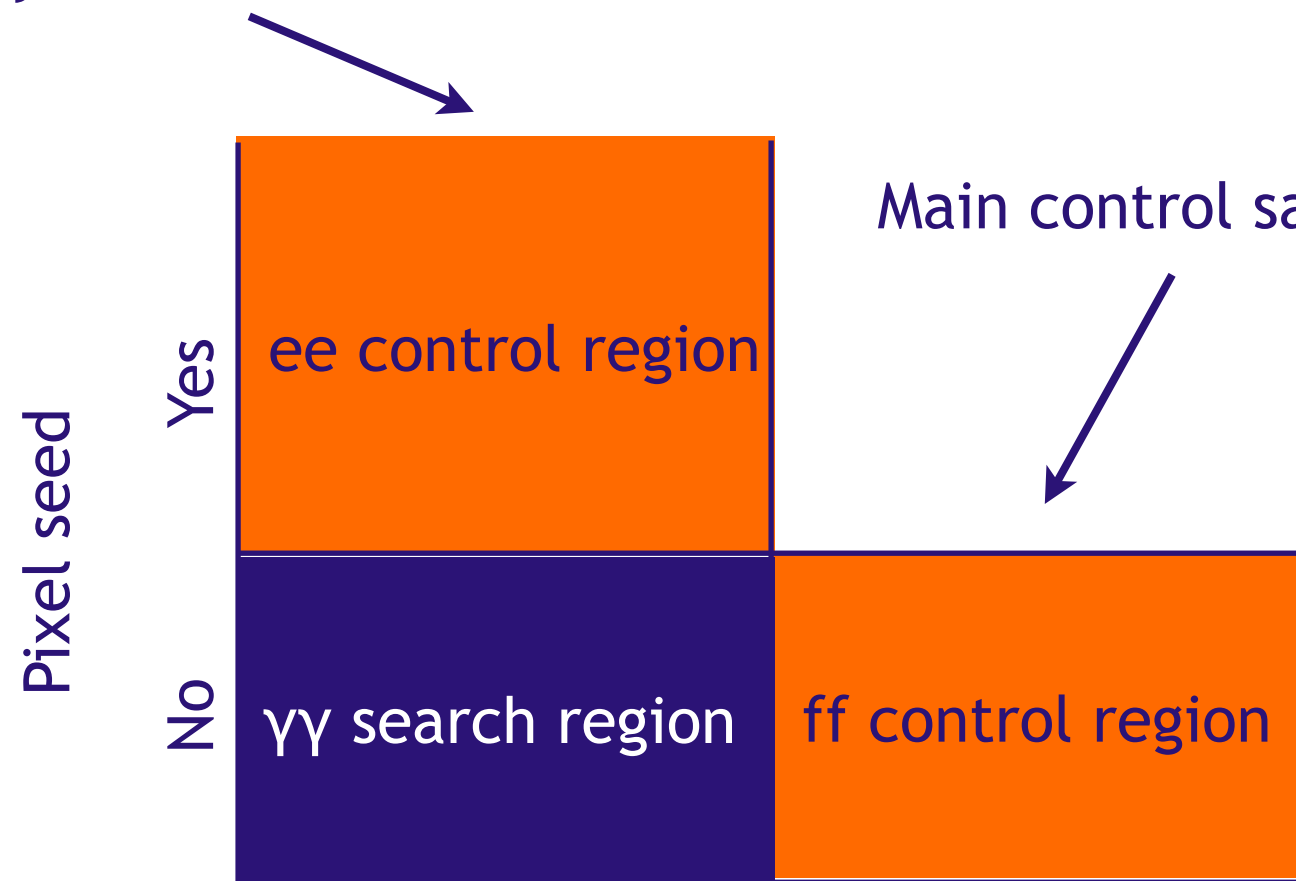


QCD control samples



UNIVERSITY
of VIRGINIA

Secondary control sample
used for comparison and
systematic studies

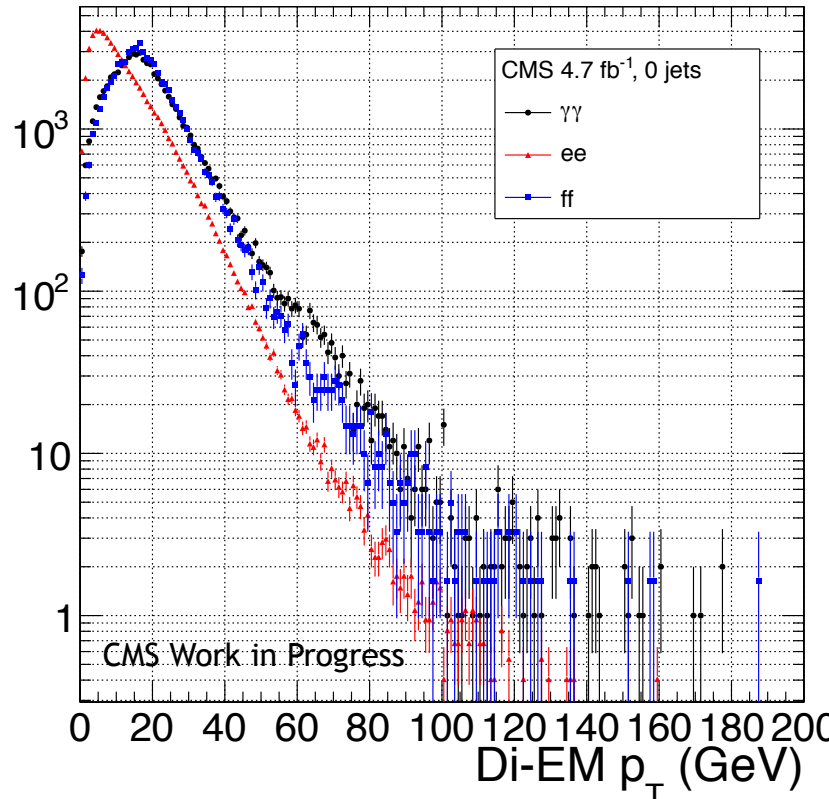


Tight ← Isolation / shower shape → Loose

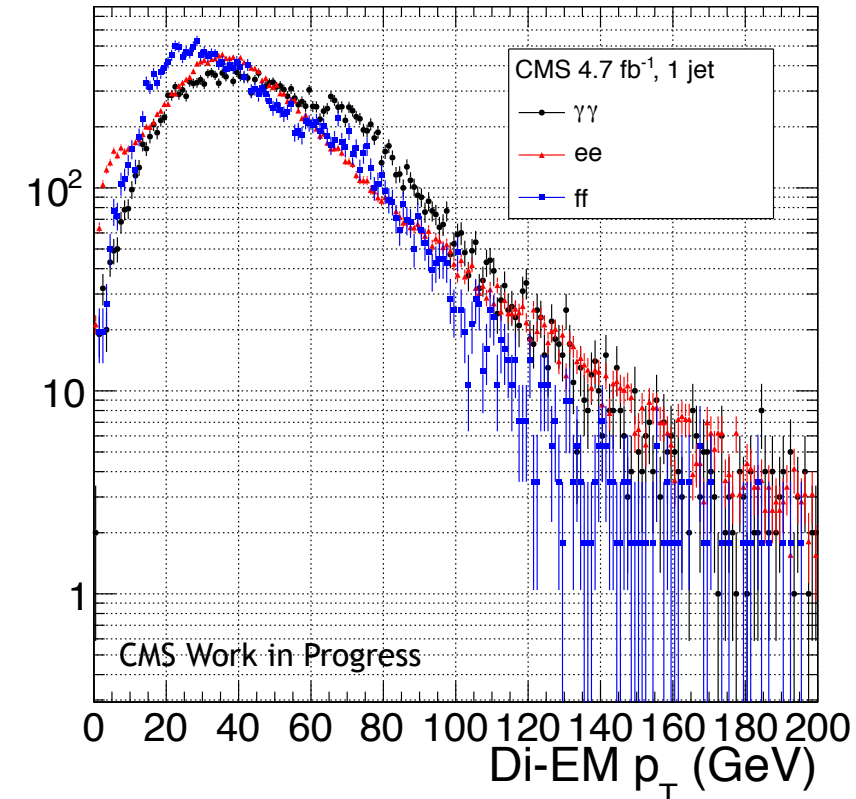
- Z dielectron (ee)
 - $81 \text{ GeV} \leq m_{ee} < 101 \text{ GeV}$
 - Photon with inverted pixel seed veto
 \Rightarrow similar energy resolution as photons
- Di-EM p_T reweighting significant because the kinematics of Z and QCD diphoton production are different
- Subtract tt contribution to ee sample using invariant mass sidebands
- Electromagnetic dijets (ff)
 - Photon with inverted isolation or shower shape, below a maximum allowed isolation
 - Tends to have a little bit of HCAL energy, so use PF E_T instead of ECAL E_T
 - Similar kinematics to diphoton sample, so reweighting has small effect

Di-EM p_T spectra

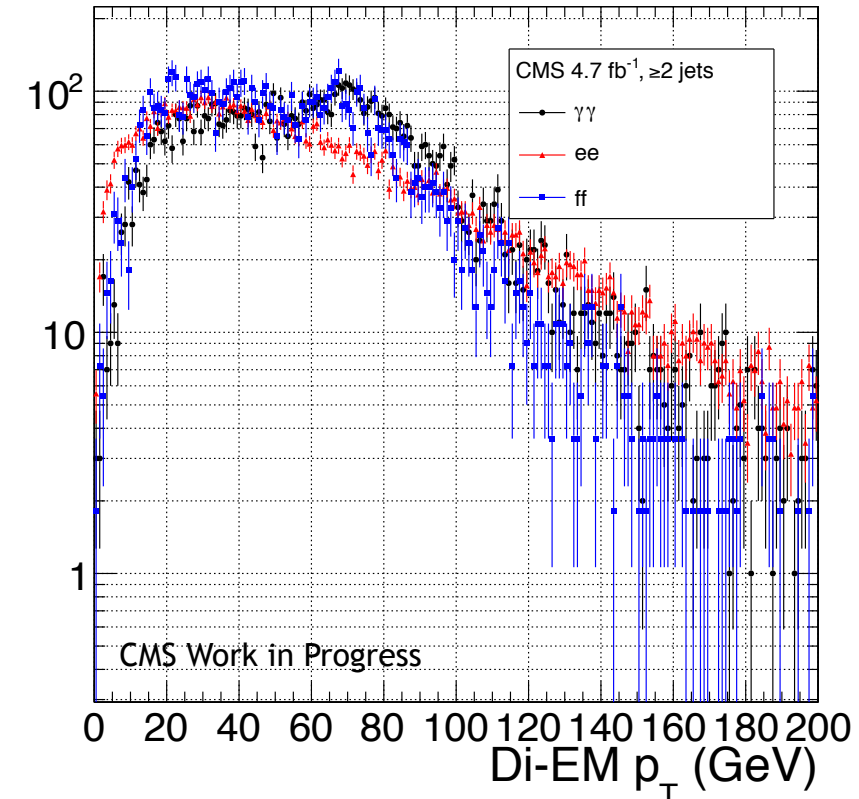
0 jets



1 jet



≥ 2 jets

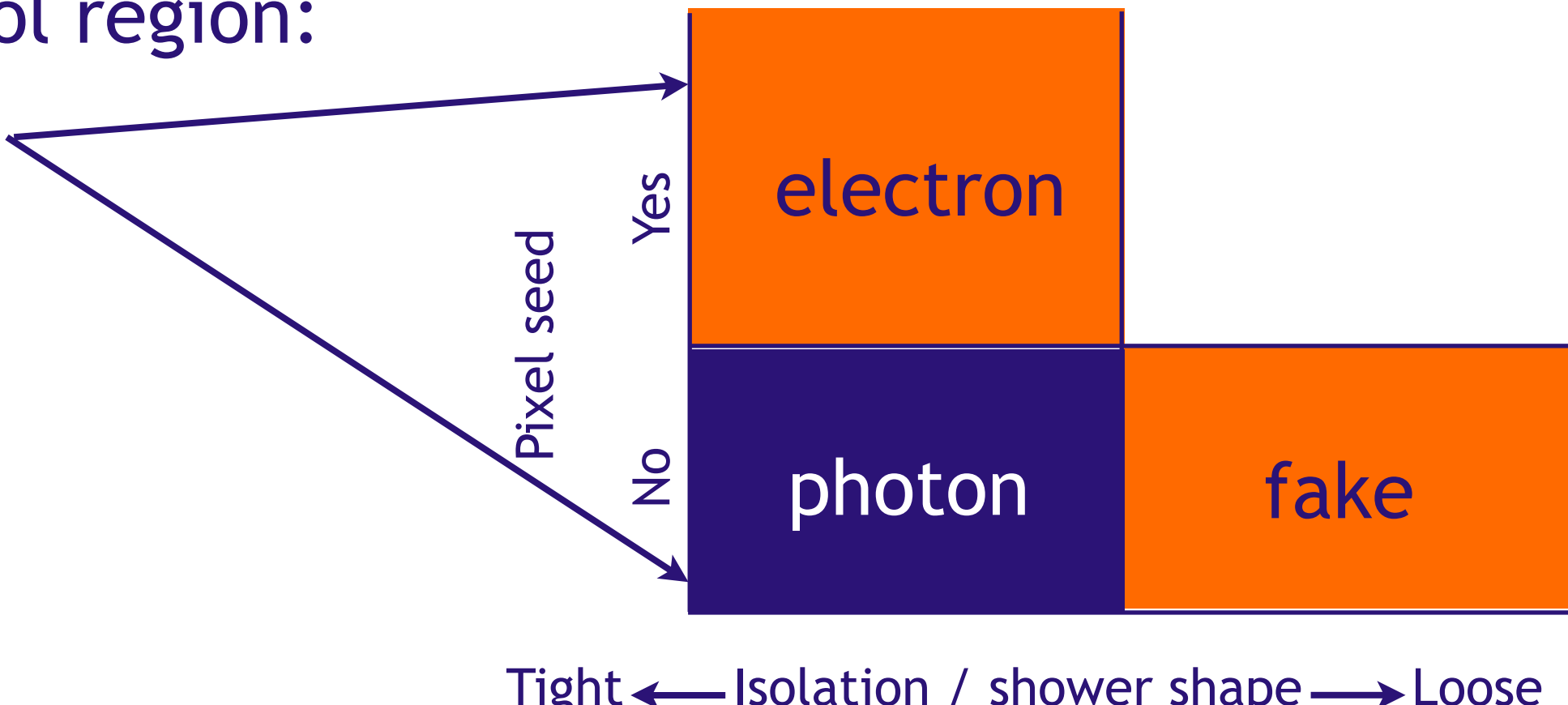


- ee (red) and ff (blue) spectra area-normalized to $\gamma\gamma$ (black) spectrum
- $W_{ij} = (N_{\text{control}}/N_{\gamma\gamma})(N_{\gamma\gamma}^{ij}/N_{\text{control}}^{ij})$
 - i runs over di-EM p_T bins
 - j runs over N_j bins

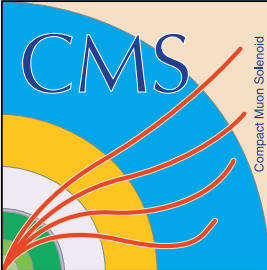
Estimating the electroweak background

$e\gamma$ control region:

1 e + 1 γ



- $W(\rightarrow e\nu)\gamma$ and $W(\rightarrow e\nu) + \text{jet}$ can fake $\gamma\gamma$ if the electron pixel seed is missed
- Estimate the electron \rightarrow photon mis-ID rate $f_{e\rightarrow\gamma}$ by fitting for the Z contribution in the ee and $e\gamma$ samples
- $f_{e\rightarrow\gamma} = 0.014 \pm 0.000(\text{stat.}) \pm 0.004(\text{syst.})$
 - Systematic error due to small p_T dependence of the mis-ID rate
- Scale $e\gamma$ sample by $f_{e\rightarrow\gamma}/(1 - f_{e\rightarrow\gamma})$



Errors on ee and ff QCD predictions



Source of error	Fractional uncertainty (%)				
	[50, 60)	[60, 70)	[70, 80)	[80, 100)	≥ 100
Total	3.9	8.1	16	25	25
Statistics	3.6	7.8	16	24	22
No. events	3.6	7.7	15	24	20
In norm. region	0.43	0.44	0.46	0.55	0.51
In this E_T bin	3.5	7.7	15	24	20
Reweighting	0.73	1.2	3.5	4.3	7.7
In norm. region	0.19	0.19	0.2	0.24	0.23
In this E_T bin	0.71	1.2	3.5	4.3	7.7
Systematics	2.6	4.4	1.2	7.5	14
$f_{e \rightarrow \gamma}$ (in norm. region)	0.0012	0.0012	0.0013	0.0015	0.0014
m_{ee} background shape	1.4	2	0.72	5.5	12
Jet energy scale	2.2	3.9	0.96	5.1	6.9

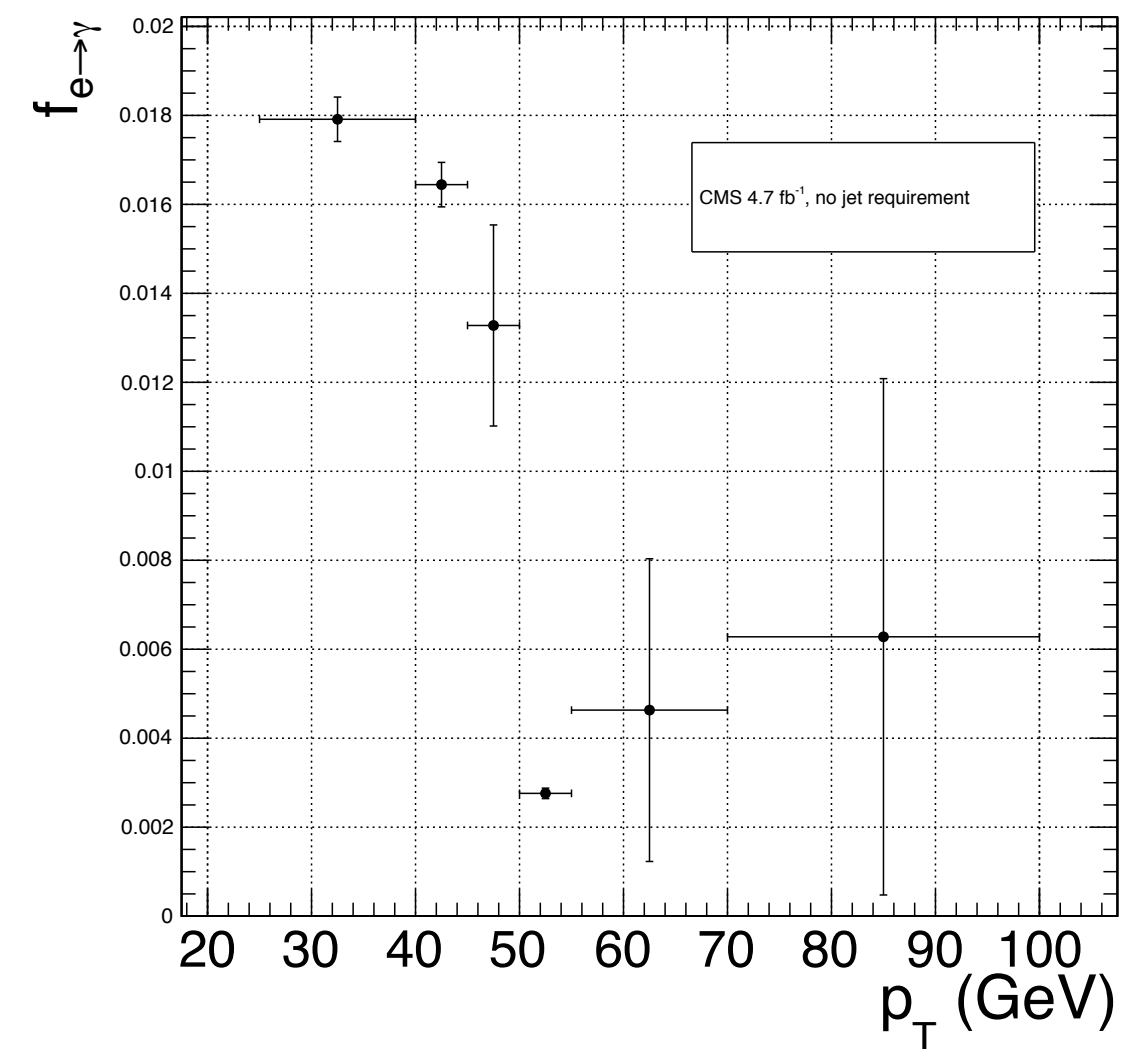
Source of error	Fractional uncertainty (%)				
	[50, 60)	[60, 70)	[70, 80)	[80, 100)	≥ 100
Total	15	25	61	34	64
Statistics	7.2	14	30	33	38
No. events	7.1	14	29	33	36
In norm. region	0.64	0.64	0.64	0.64	0.64
In this E_T bin	7.1	14	29	33	36
Reweighting	0.85	2.7	5.1	6.9	13
In norm. region	0.27	0.27	0.27	0.27	0.27
In this E_T bin	0.81	2.6	5.1	6.9	13
Systematics	13	21	53	6.6	52
ee/ff difference	13	21	53	5.5	52
$f_{e \rightarrow \gamma}$ (in norm. region)	0.0012	0.0012	0.0012	0.0012	0.0012
Jet energy scale	0.099	1.7	1.8	3.5	1.8

- Tables show uncertainties for ≥ 0 -jet selection only
- $MET \geq 50$ GeV used as the GMSB-sensitive region
- For ee, statistical error dominates but is still a little smaller than statistical error on ff
- Difference between ee and ff prediction taken as a systematic error on ff QCD prediction—this is the dominant uncertainty

Error on electroweak background prediction

Source of error	Fractional uncertainty (%)				
	[50, 60)	[60, 70)	[70, 80)	[80, 100)	≥ 100
Total	29	29	30	30	30
Statistics	3.6	5.2	6.7	7.2	6.5
Systematics ($f_{e \rightarrow \gamma}$)	29	29	29	29	29

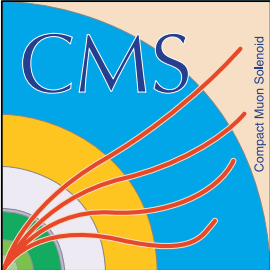
- Table shows uncertainties for ≥ 0 -jet selection only
- Dominated by p_T dependence of $f_{e \rightarrow \gamma}$



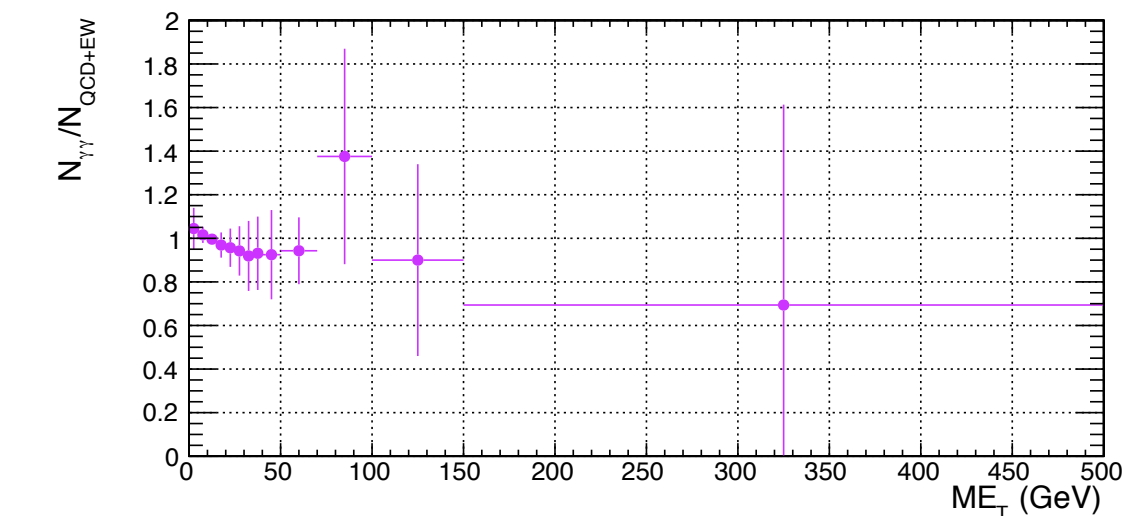
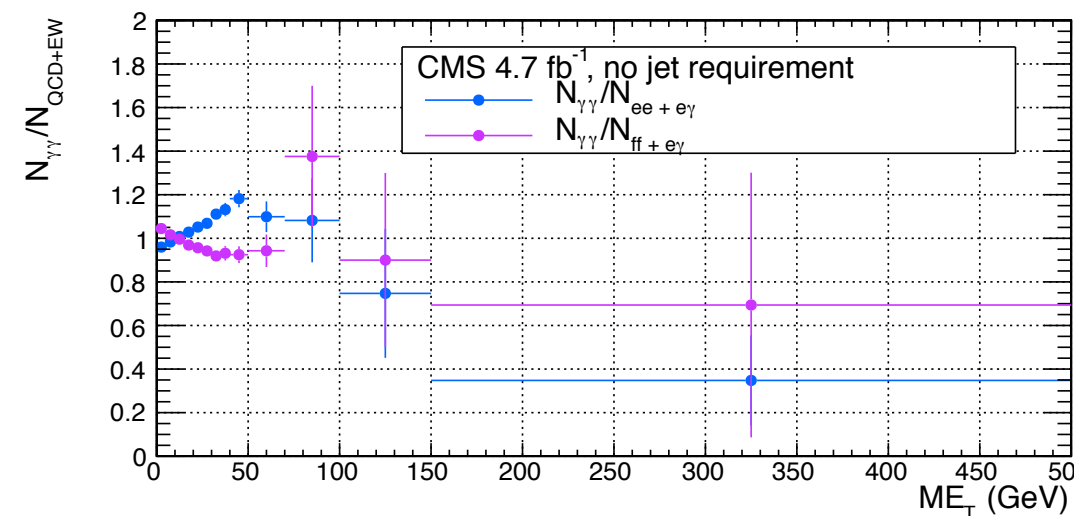
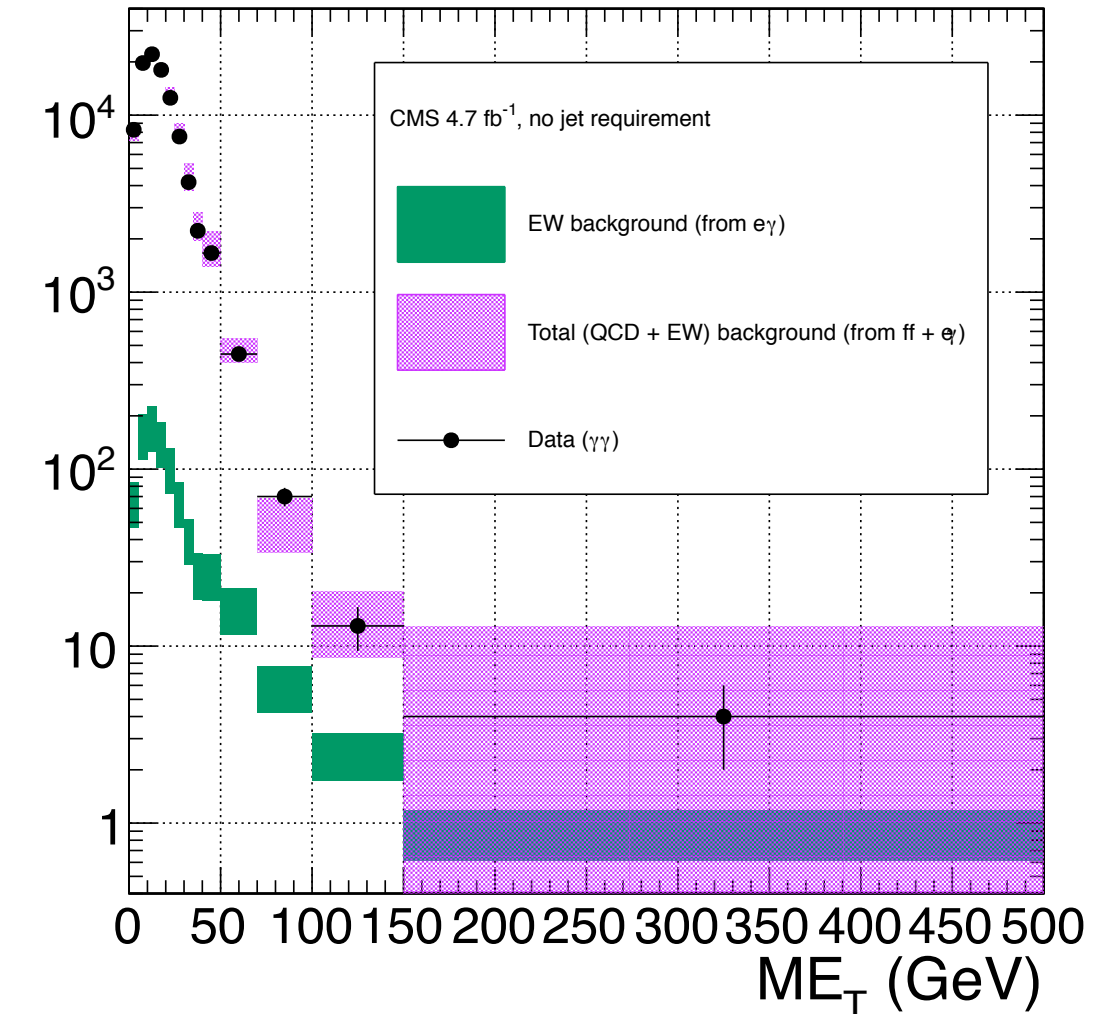
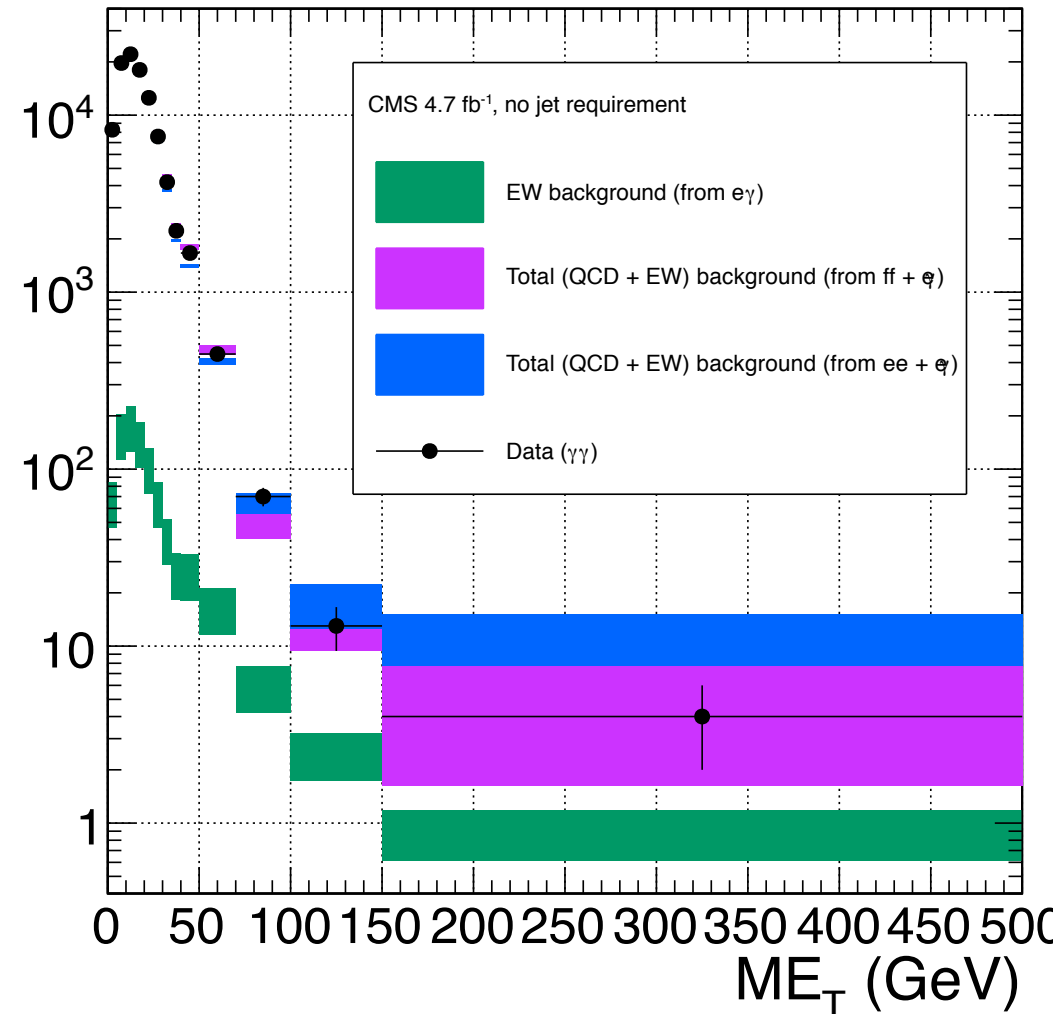
Total error

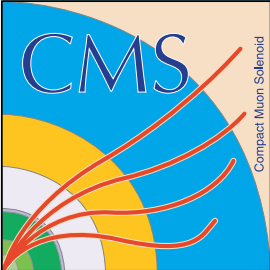
Source of error	Fractional uncertainty (%)				
	[50, 60)	[60, 70)	[70, 80)	[80, 100)	≥ 100
Total ($ee + e\gamma$)	3.9	7.8	15	22	22
Statistics	3.4	7.3	14	21	18
QCD	3.4	7.3	14	21	18
Electroweak	0.13	0.3	0.53	0.79	0.76
Systematics	2.7	4.5	2.6	7.4	13
QCD	2.5	4.1	1.1	6.7	12
Electroweak	1	1.7	2.3	3.2	3.4
Total ($ff + e\gamma$)	14	24	54	30	54
Statistics	6.9	13	26	29	30
QCD	6.9	13	26	29	30
Electroweak	0.11	0.24	0.79	0.83	1.1
Systematics	12	20	47	6.7	43
QCD	12	20	47	5.8	43
Electroweak	0.9	1.3	3.4	3.4	4.8

- Table shows uncertainties for ≥ 0 -jet selection only



Results (≥ 0 jets)

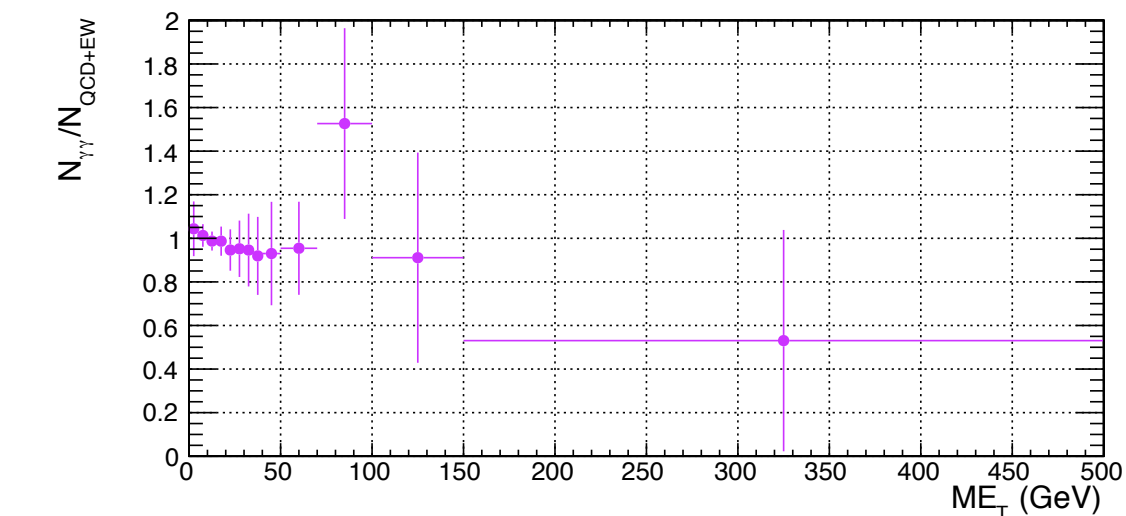
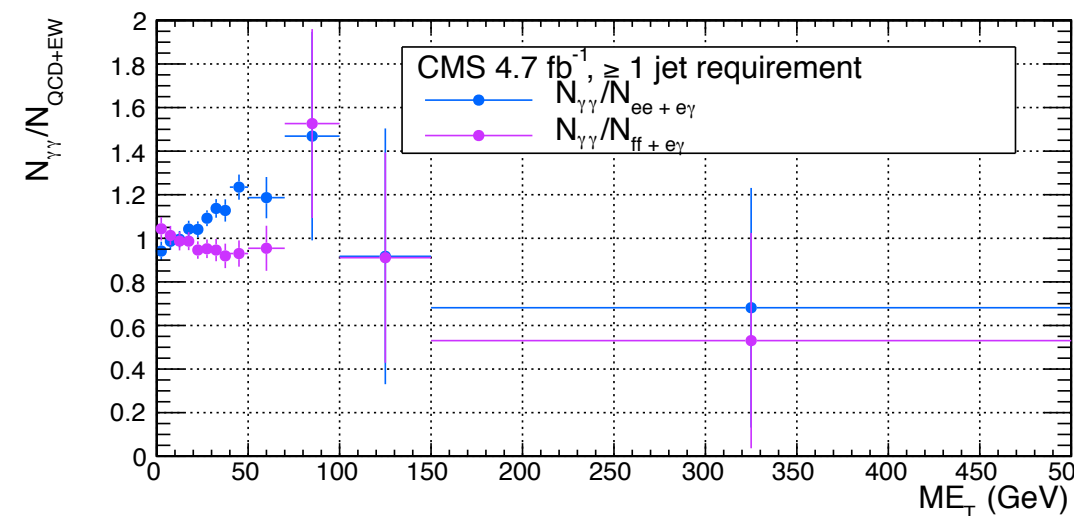
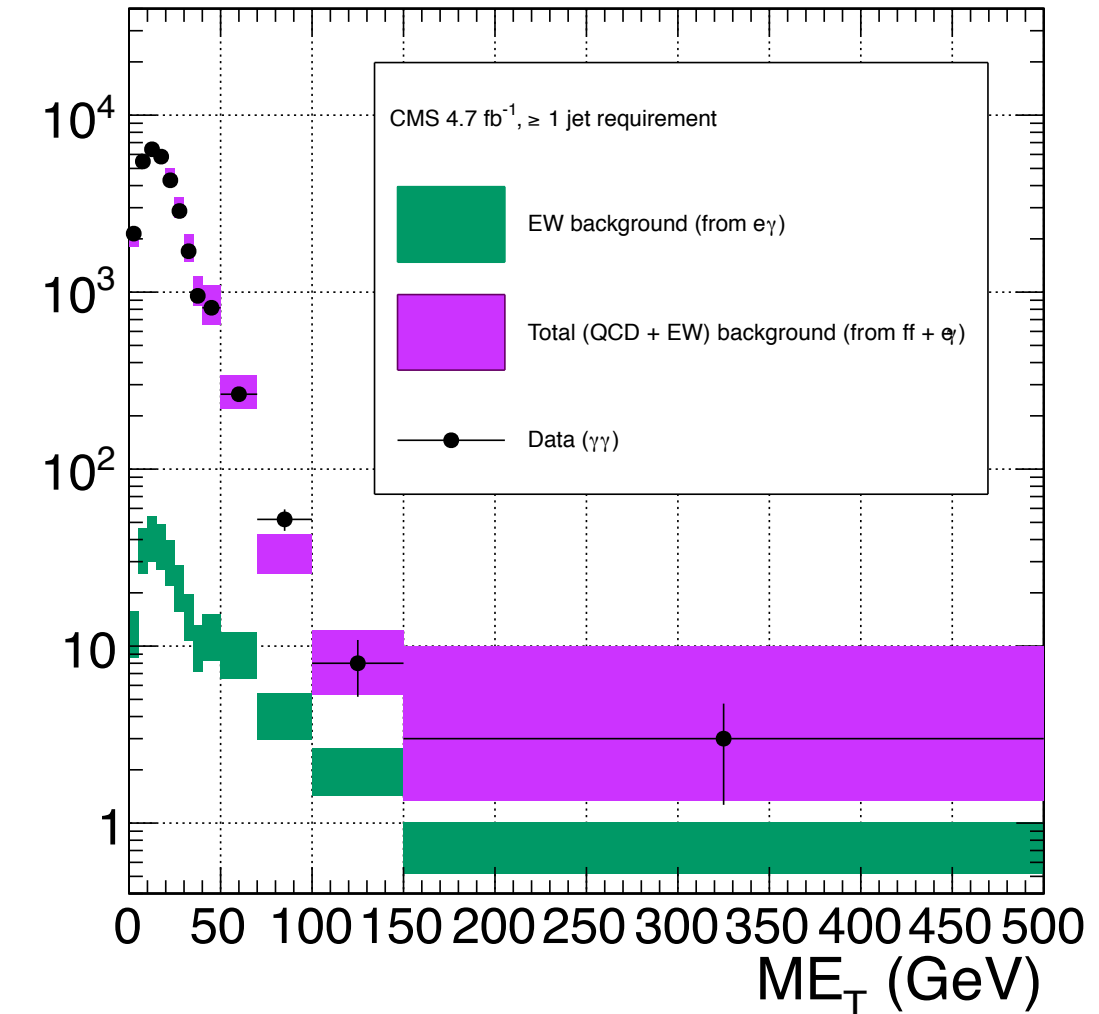
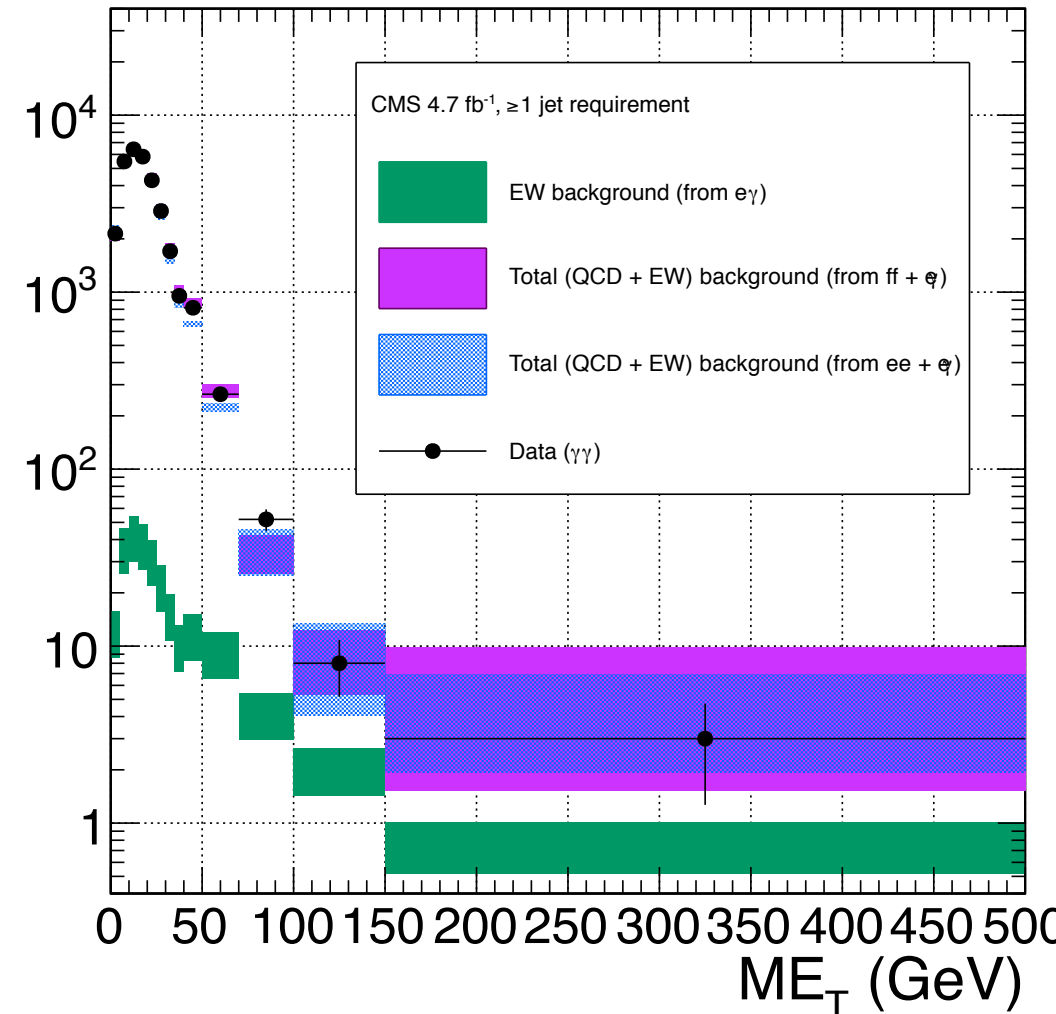




Results (≥ 1 jet)



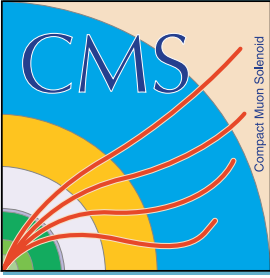
UNIVERSITY
of VIRGINIA



Results

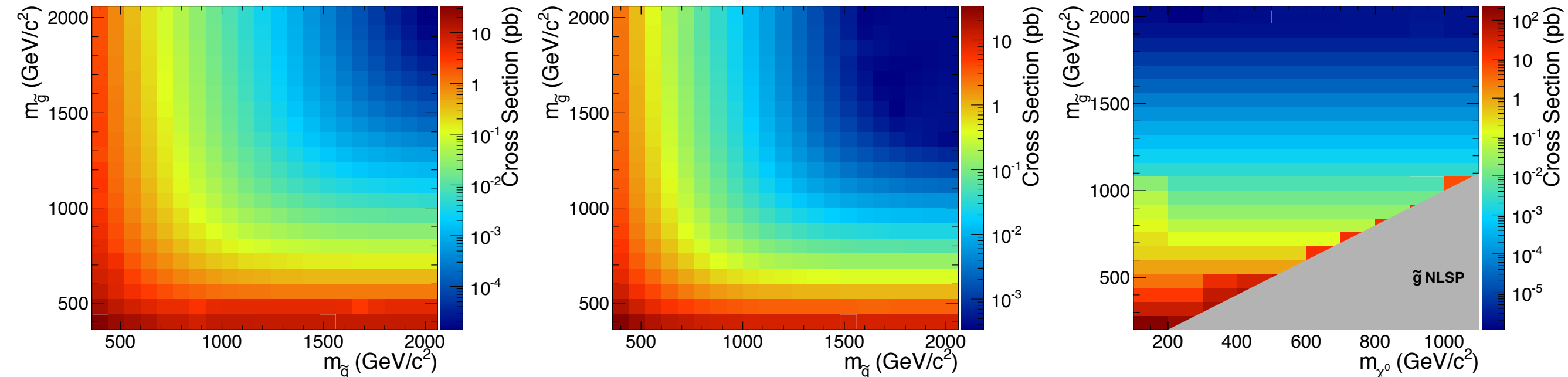
Source	No. events				
	[50, 60)	[60, 70)	[70, 80)	[80, 100)	≥ 100
Observation $(\gamma\gamma)$	354	93	37	33	17
Predicted background $(ff + e\gamma)$	361 ± 51.5	113 ± 27.1	26.9 ± 14.5	23.9 ± 7.23	20.2 ± 10.9
Predicted background $(ee + e\gamma)$	317 ± 14.1	90.2 ± 7.77	39.6 ± 5.75	25.1 ± 5.66	28.9 ± 6.70
$m_{\tilde{q}} = 720 \text{ GeV}$ $M_3 = 720 \text{ GeV}$ $M_1 = 375 \text{ GeV}$	13.3 ± 2.13	17.7 ± 2.46	15.3 ± 2.33	42.9 ± 3.82	966 ± 18.3
$m_{\tilde{q}} = 1440 \text{ GeV}$ $M_3 = 1440 \text{ GeV}$ $M_1 = 375 \text{ GeV}$	0.008 ± 0.003	0.009 ± 0.003	0.012 ± 0.003	0.030 ± 0.005	1.92 ± 0.04

- Table shows numbers for ≥ 0 -jet selection only
- No significant excess observed



Interpretation

Simplified GMSB model scans



$M_2 = 3.5 \text{ TeV}$,
 $M_1 = 375 \text{ GeV}$,
 M_3 vs. m_{squark}

$M_1 = 3.5 \text{ TeV}$,
 $M_2 = 375 \text{ GeV}$,
 M_3 vs. m_{squark}

$m_{\text{squark}} = 2.5 \text{ TeV}$,
 M_3 vs. M_1

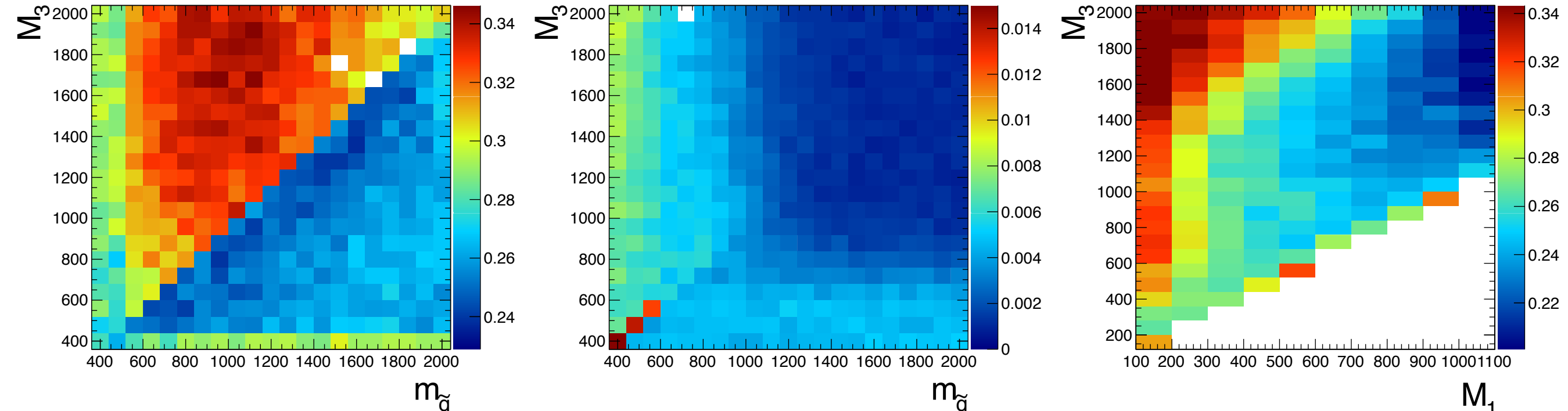
- M_1 = bino mass parameter
- M_2 = wino mass parameter
- M_3 = gluino mass parameter
- All mass parameters not mentioned set to 2.5 or 3.5 TeV

Upper limit calculation

- CL_S 95% with profile likelihood test statistic
 - $q_{\mu}^* \equiv -2 \ln (\mathcal{L}(\text{data} | \mu, \theta_{\mu}^*) / \mathcal{L}(\text{data} | \mu^*, \theta^*))$, $0 \leq \mu^* \leq \mu$
 - μ = signal strength, θ = nuisance parameters
 - μ^* and θ^* are the global maximum likelihood estimators (MLE) of \mathcal{L}
 - θ_{μ}^* is the MLE of \mathcal{L} evaluated at μ
- Nuisance parameters modeled with log-normal distribution
- Traditional frequentist interval: $p_{\mu} \leq 0.05 \Rightarrow \text{exclude } \mu$
- CL_S: $p_{\mu} / (1 - p_0) \leq 0.05 \Rightarrow \text{exclude } \mu$
- CL_S avoids excluding signals to which there is little sensitivity

Nuisance parameters

Uncertainty	Value
Integrated luminosity uncertainty	4.5% in all ME_T bins
Photon efficiency uncertainty on signal acceptance	8% in all ME_T bins
Pileup simulation uncertainty on signal acceptance	2.6% in all ME_T bins
Systematic uncertainty on QCD background	5.5%-53%
Systematic uncertainty on electroweak background	29%-30%
Statistical uncertainty on signal acceptance	1.8%-100%
Statistical uncertainty on QCD background	7.2%-38%
Statistical uncertainty on electroweak background	3.6%-7.2%



$M_2 = 3.5 \text{ TeV}$,
 $M_1 = 375 \text{ GeV}$,
 M_3 vs. m_{squark}

$M_1 = 3.5 \text{ TeV}$,
 $M_2 = 375 \text{ GeV}$,
 M_3 vs. m_{squark}

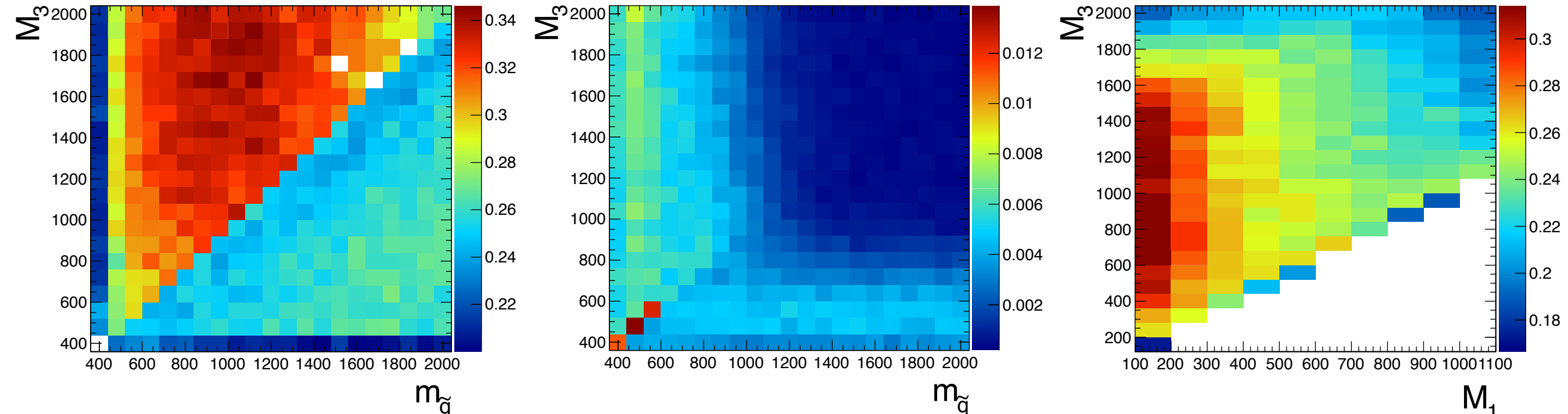
$m_{\text{squark}} = 2.5 \text{ TeV}$,
 M_3 vs. M_1

$$A \times \epsilon \equiv N_{\gamma\gamma}(\text{ME}_T \geq 50 \text{ GeV}) / N_{\text{gen}}$$

Acceptance × efficiency (≥ 1 jet)



UNIVERSITY
of VIRGINIA



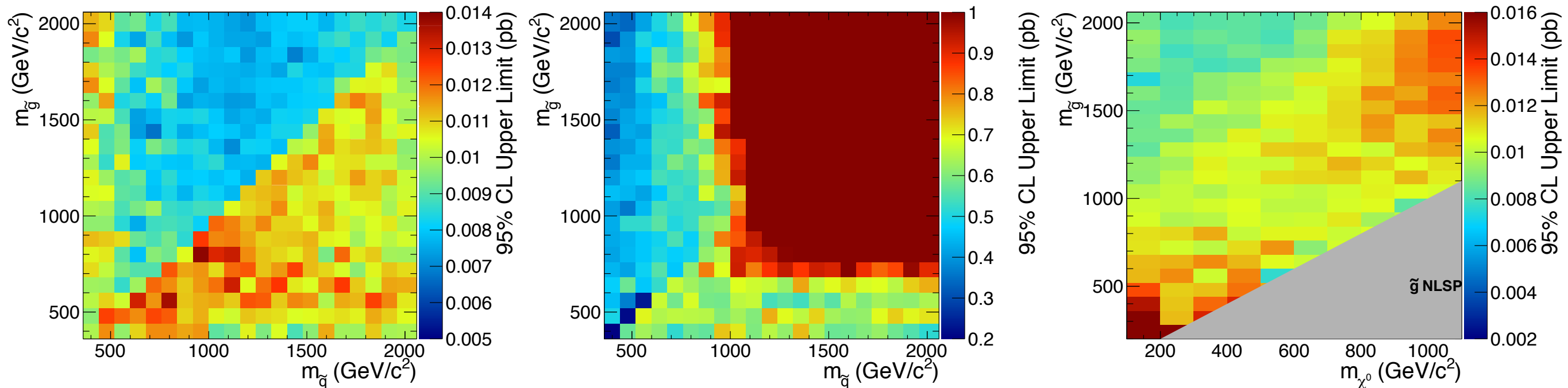
$M_2 = 3.5 \text{ TeV}$,
 $M_1 = 375 \text{ GeV}$,
 M_3 vs. m_{squark}

$M_1 = 3.5 \text{ TeV}$,
 $M_2 = 375 \text{ GeV}$,
 M_3 vs. m_{squark}

$m_{\text{squark}} = 2.5 \text{ TeV}$,
 M_3 vs. M_1

$$A \times \epsilon \equiv N_{\gamma\gamma}(\text{ME}_T \geq 50 \text{ GeV}) / N_{\text{gen}}$$

Cross section upper limits (≥ 0 jets)

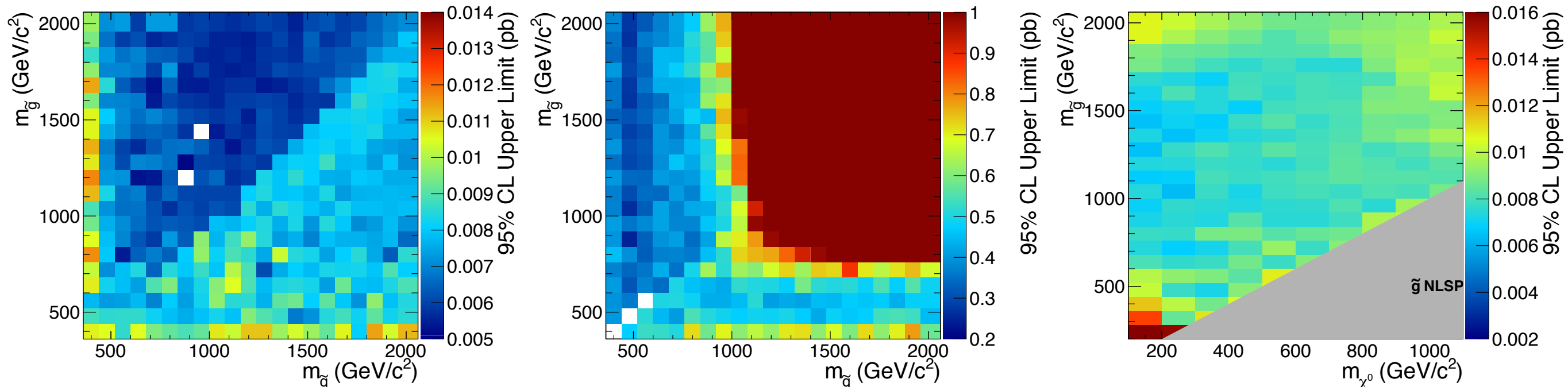


$M_2 = 3.5$ TeV,
 $M_1 = 375$ GeV,
 M_3 vs. m_{squark}

$M_1 = 3.5$ TeV,
 $M_2 = 375$ GeV,
 M_3 vs. m_{squark}

$m_{\text{squark}} = 2.5$ TeV,
 M_3 vs. M_1

Cross section upper limits (≥ 1 jet)



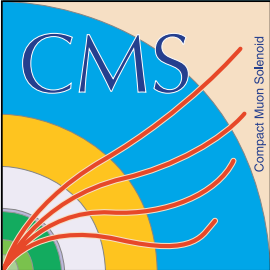
$M_2 = 3.5$ TeV,
 $M_1 = 375$ GeV,
 M_3 vs. m_{squark}

$M_1 = 3.5$ TeV,
 $M_2 = 375$ GeV,
 M_3 vs. m_{squark}

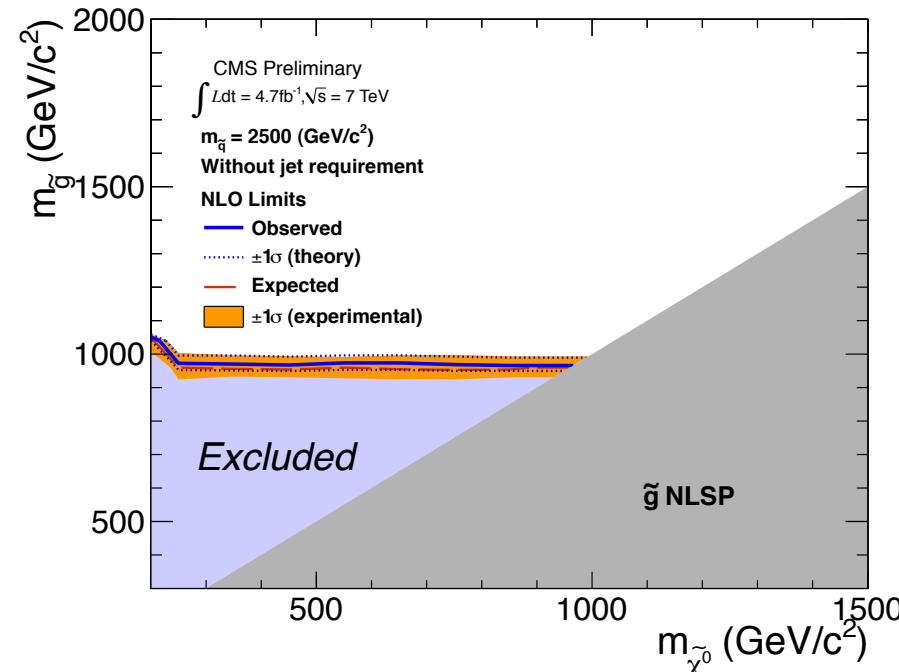
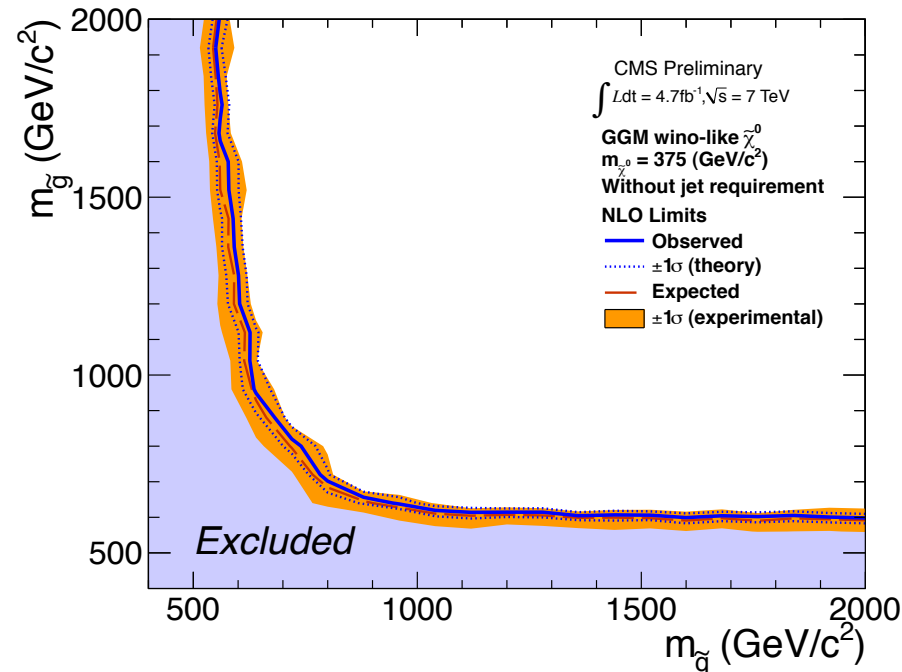
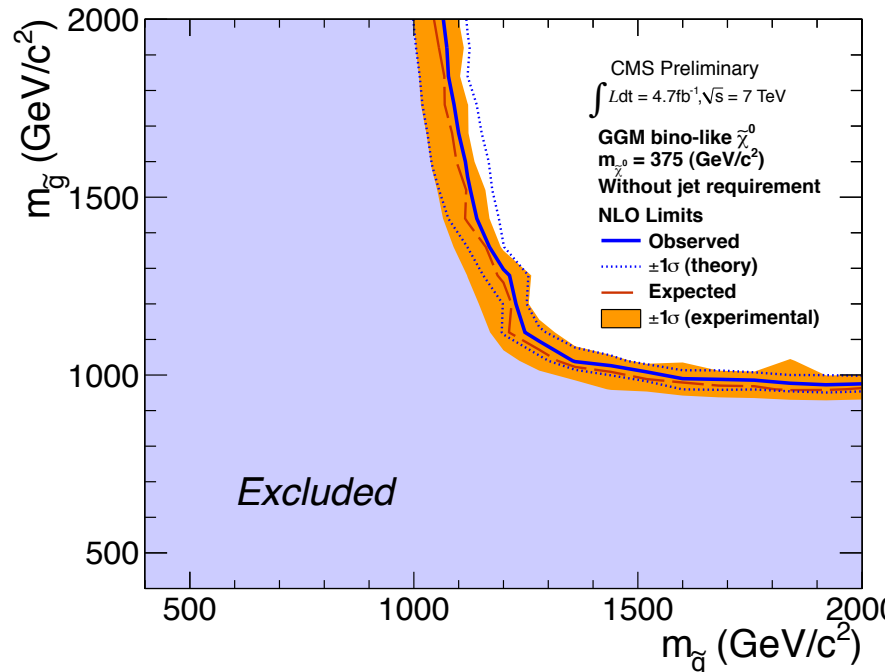
$m_{\text{squark}} = 2.5$ TeV,
 M_3 vs. M_1

Model exclusions

- If the observed cross section upper limit is less than the predicted cross section, the model is excluded
- Theoretical errors on predicted cross section
 - Uncertainty on parton distribution functions (PDF) used to model the signal (4%-100%)
 - Renormalization scale uncertainty (0.036%-25%)
 - PDF errors come from reevaluating the cross section for all “error” PDFs (1 error PDF for each 1σ +/- deviation of each parameter used in the PDF fit) for CTEQ6.6, MSTW08, and NNPDF2.0 PDFs
 - Renormalization scale halved and doubled to get error



Model exclusions (≥ 0 jets)

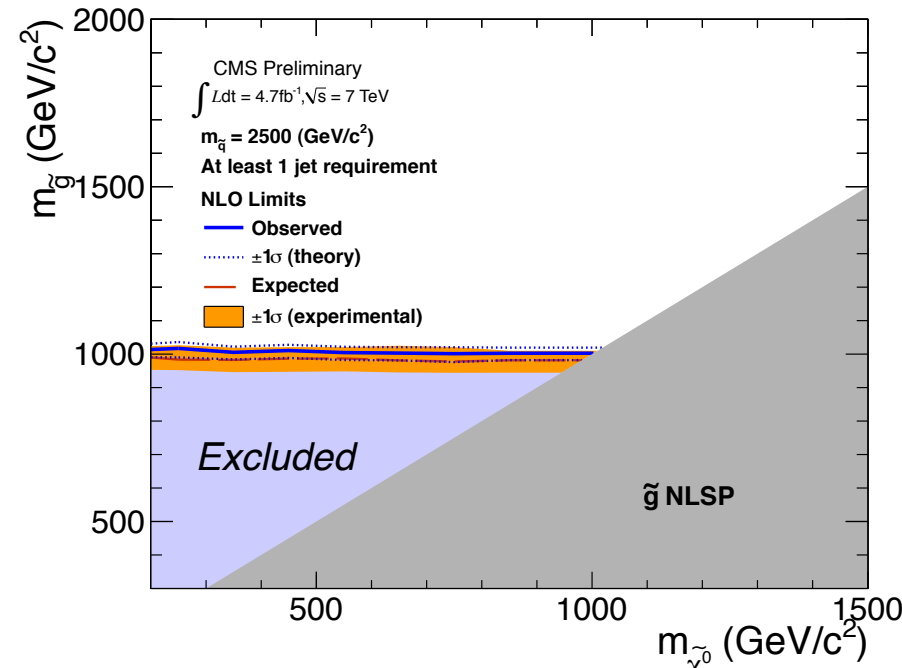
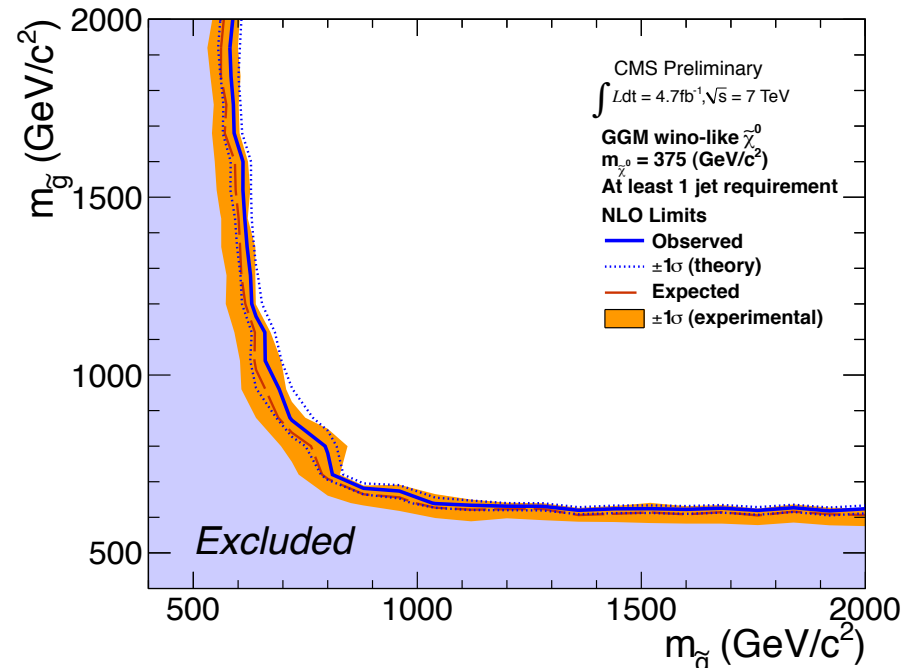
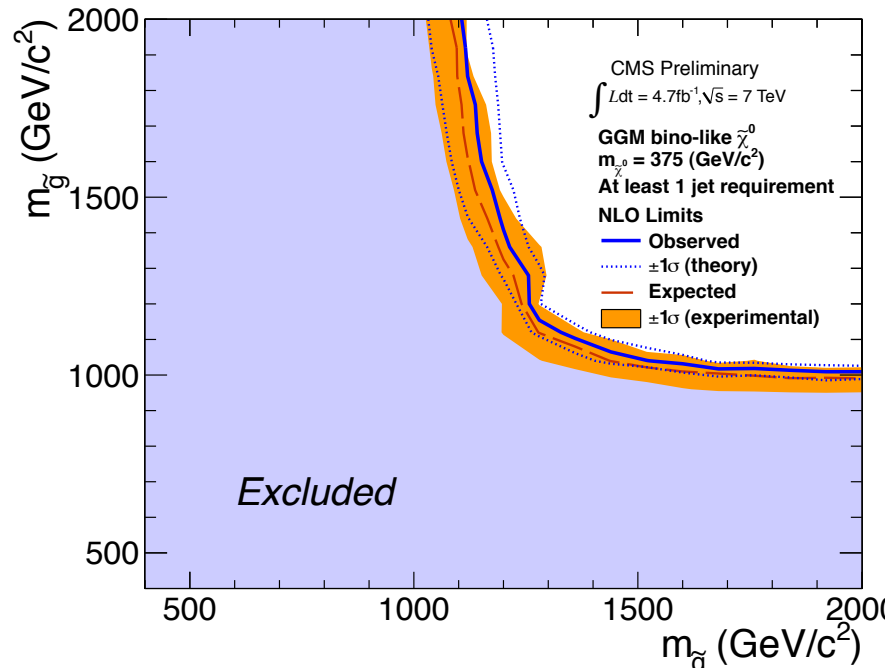


$M_2 = 3.5 \text{ TeV}$,
 $M_1 = 375 \text{ GeV}$,
 M_3 vs. m_{squark}

$M_1 = 3.5 \text{ TeV}$,
 $M_2 = 375 \text{ GeV}$,
 M_3 vs. m_{squark}

$m_{\text{squark}} = 2.5 \text{ TeV}$,
 M_3 vs. M_1

Model exclusions (≥ 1 jet)



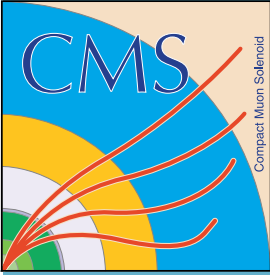
$M_2 = 3.5\text{ TeV}$,
 $M_1 = 375\text{ GeV}$,
 M_3 vs. m_{squark}

$M_1 = 3.5\text{ TeV}$,
 $M_2 = 375\text{ GeV}$,
 M_3 vs. m_{squark}

$m_{\text{squark}} = 2.5\text{ TeV}$,
 M_3 vs. M_1

Conclusions

- Top performing ECAL is an important instrument in the quest for new physics at CMS
 - Steadily moving toward design calibration precision
 - Utilized in Higgs, SUSY, and Exotica searches
- Searches in the diphoton final state are powerful tools for observing SUSY
 - Clean trigger objects
 - Dominant background estimated from data
- 4.7 fb^{-1} search has excluded gluinos and light squarks in the GMSB scenario below $\sim 1 \text{ TeV}$
 - Best exclusions to date on gauge mediation
 - As energy and luminosity increase, different variants on the diphoton search can be explored to give the best coverage of possible SUSY scenarios



UNIVERSITY
of
VIRGINIA

Backup

Previous VPT rate effect

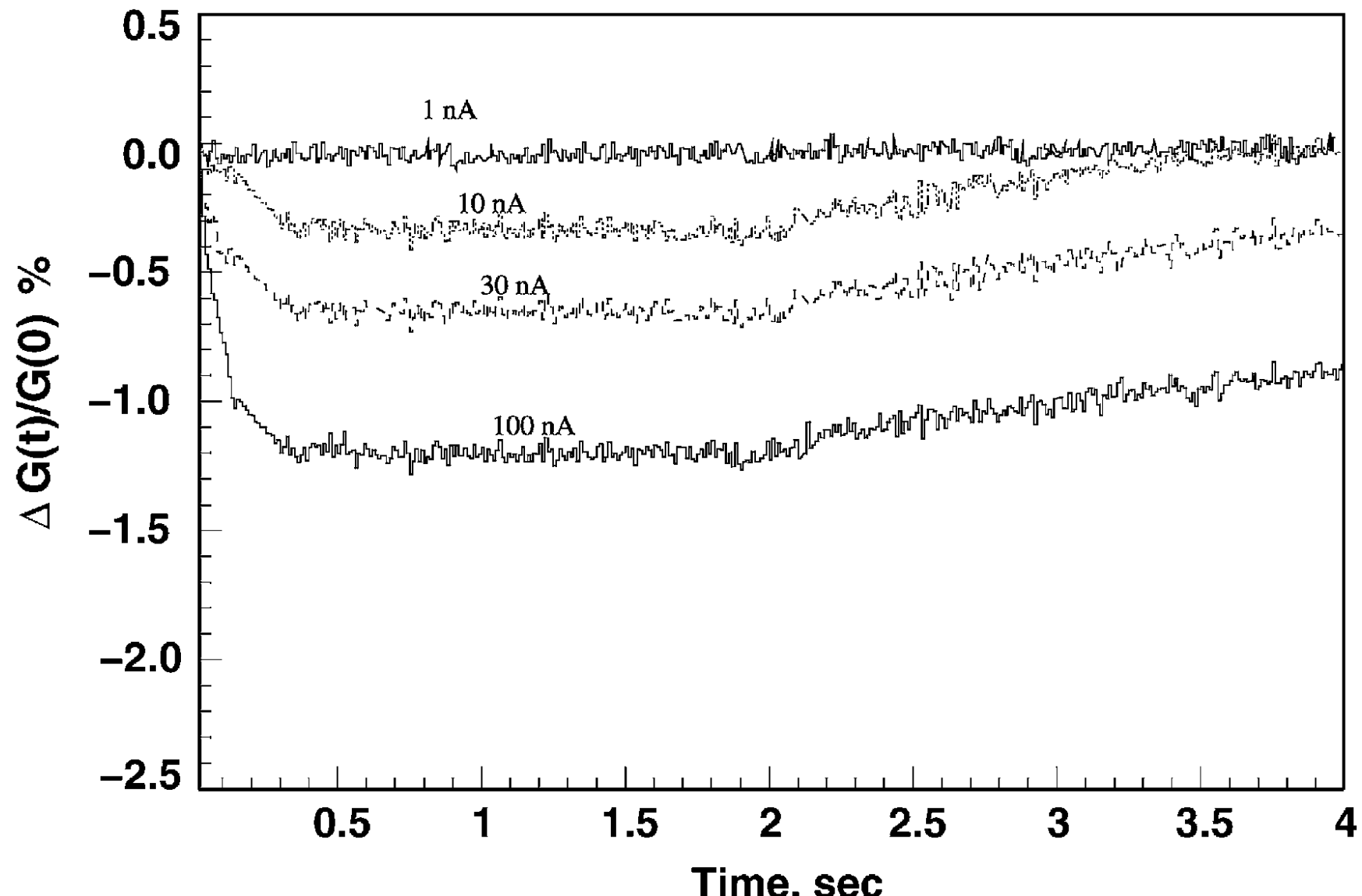


Fig. 5. Relative variation of the VPT gain averaged over 20 spills as a function of time for different average VPT anode currents.

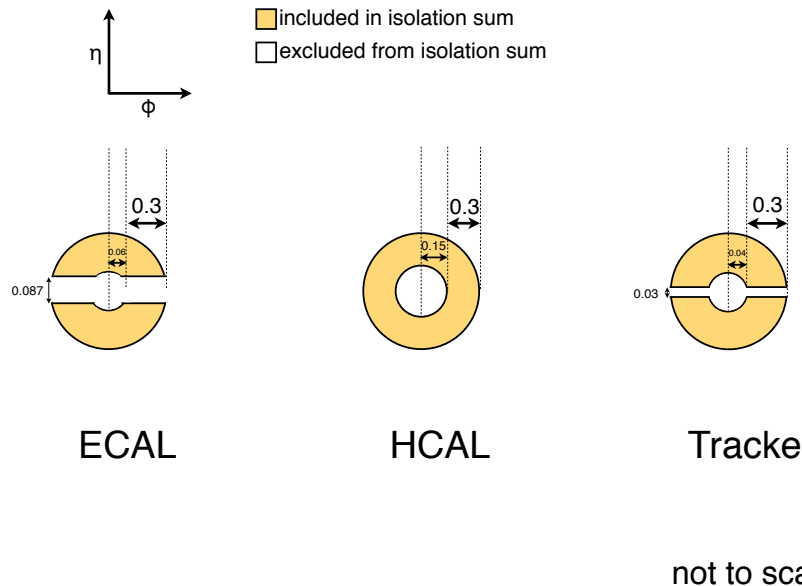
LED running modes

- Calibration sequence
 - Few hundred LED pulses read out (readout rate ~100 Hz) for each EE monitoring region
 - Continuous monitoring of the VPTs and crystals, to complement the laser monitoring
- Local run
 - Short sequence of a few hundred LED pulses triggered by ECAL-generated trigger and read out
 - Useful for debugging the system and checking the health of the ECAL
- Soaking
 - Fire the blue LED stability pulses all the time in the abort gaps to dampen VPT gain changes
 - Frequency up to ~11.4 kHz (use only 100 Hz right now)

Trigger definitions

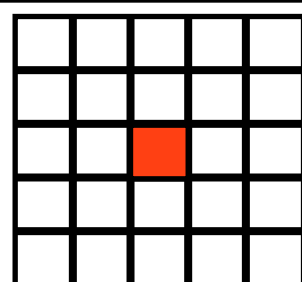
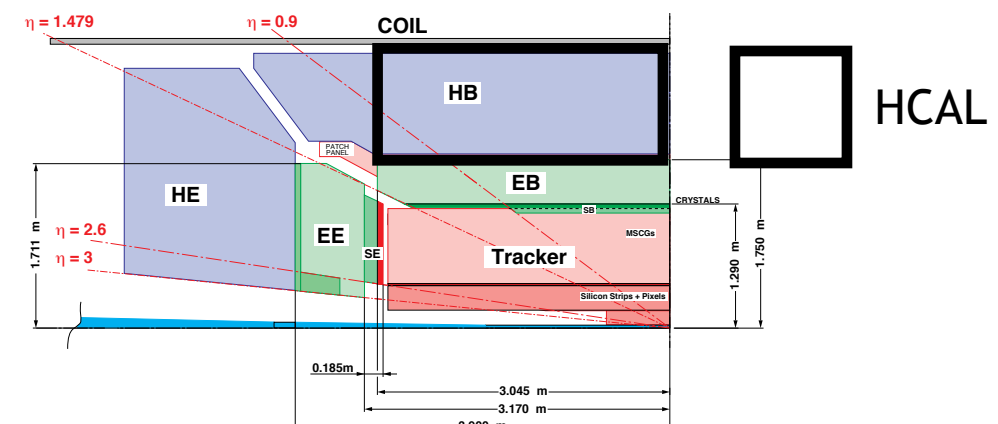
- IsoVL
 - $I_{ECAL} < 0.012E_T + 6 \text{ GeV}$
 - $I_{HCAL} < 0.005E_T + 4 \text{ GeV}$
 - $I_{track} < 0.002E_T + 4 \text{ GeV}$
- R9Id
 - $R9 > 0.85$

Photon isolation criteria



- $I_{\text{ECAL}} - 0.0792\rho + I_{\text{HCAL}} - 0.0252\rho + I_{\text{track}} < 6 \text{ GeV}$
- $\rho = \text{average energy density per unit area in the calorimeters as measured by Fastjet}$

$$\frac{\text{HCAL energy in } R < 0.15 \text{ cone around photon candidate}}{\text{ECAL energy of photon candidate}} < 0.05$$

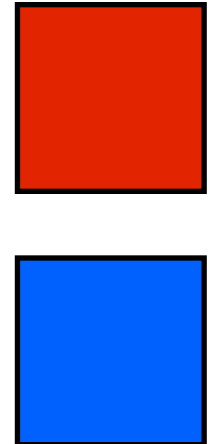
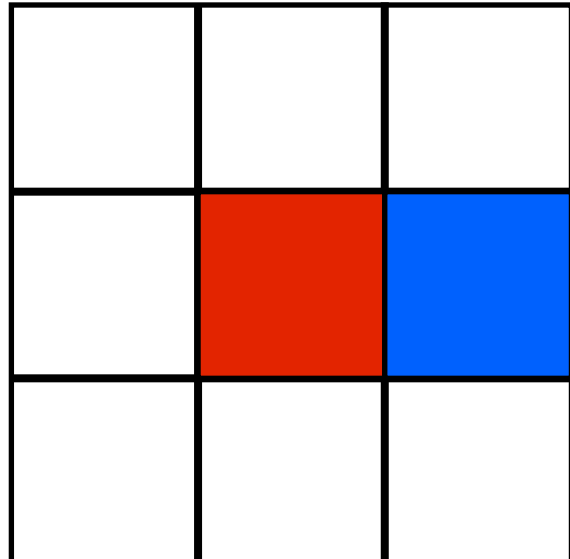


■ Highest energy
(photon seed) crystal

$$\sigma_{\eta\eta}^2 = \sum_{i=1}^{25} w_i (\eta_i - \bar{\eta})^2 / \sum_{i=1}^{25} w_i, \quad < 0.011$$

where $w_i = \max(0, 4.7 + \ln(E_i/E))$, E_i is the energy of the i^{th} crystal in a group of 5×5 centred on the one with the highest energy, and $\eta_i = \hat{\eta}_i \times \delta\eta$, where $\hat{\eta}_i$ is the η index of the i^{th} crystal and $\delta\eta = 0.0174$; E is the total energy of the group and $\bar{\eta}$ the average η weighted by w_i in the same group [20].

ECAL noise cleaning

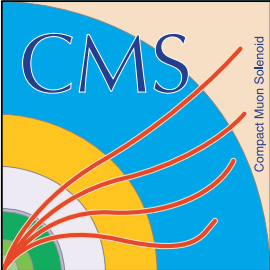


Highest energy crystal

2nd highest energy crystal

$$\frac{E_{\text{red}} + E_{\text{blue}}}{E_{3 \times 3}} > 0.95 \Rightarrow \text{reject}$$

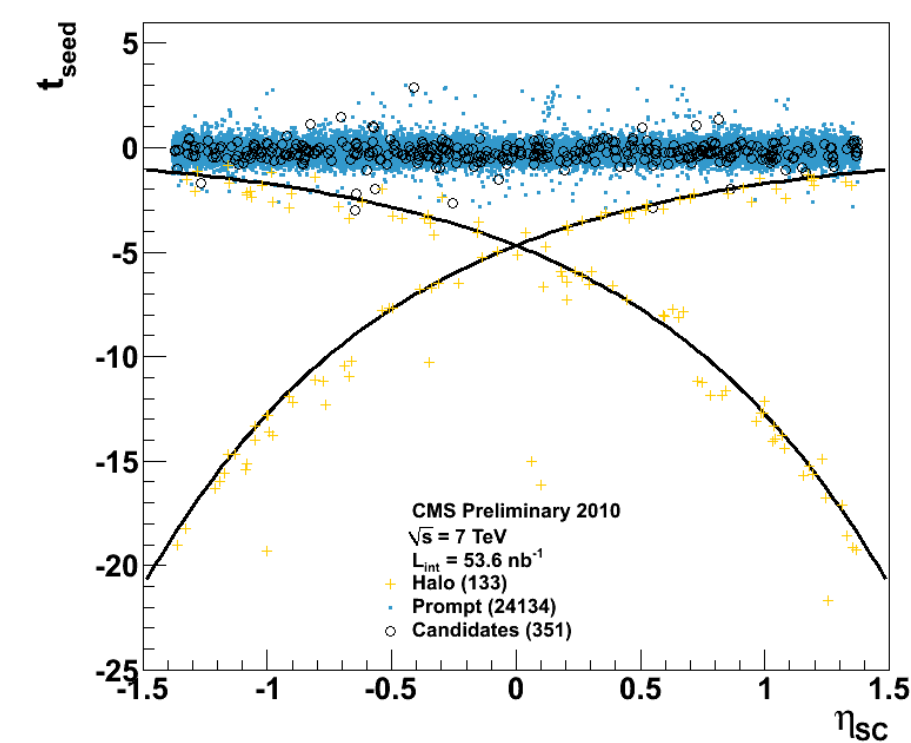
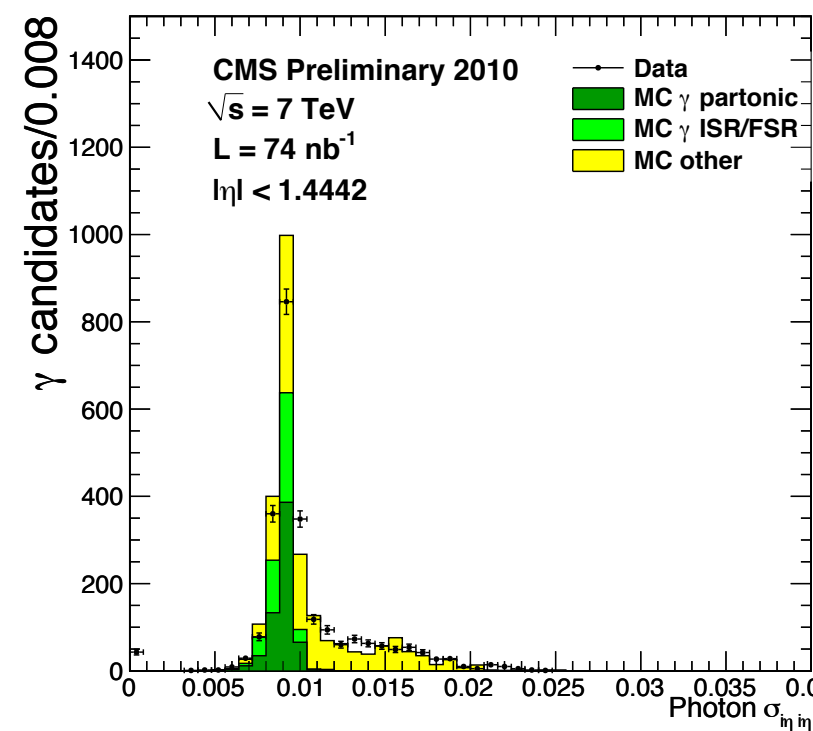
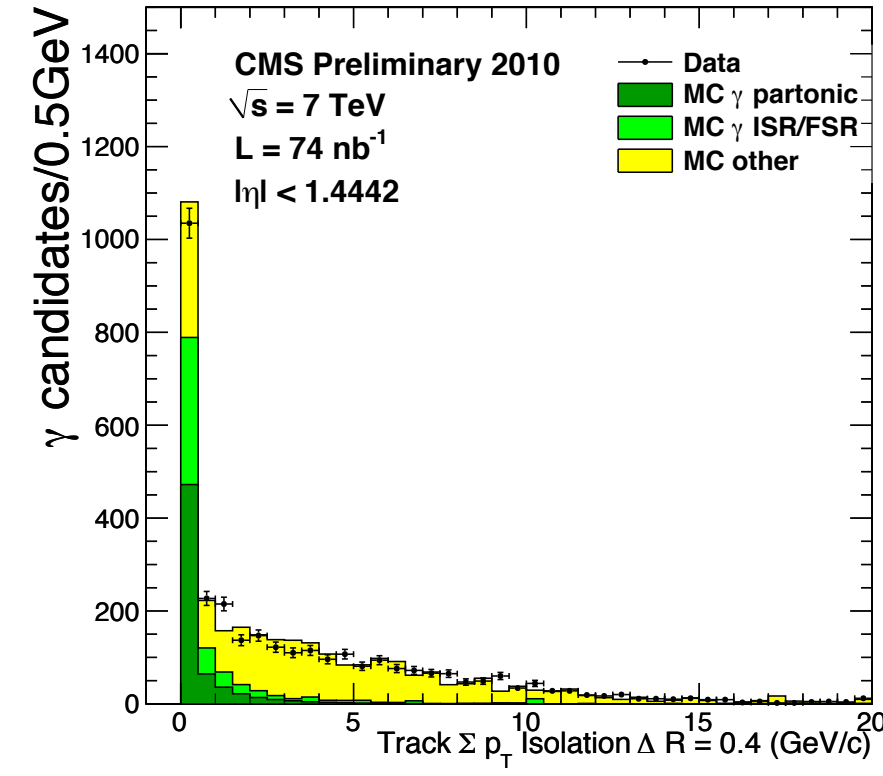
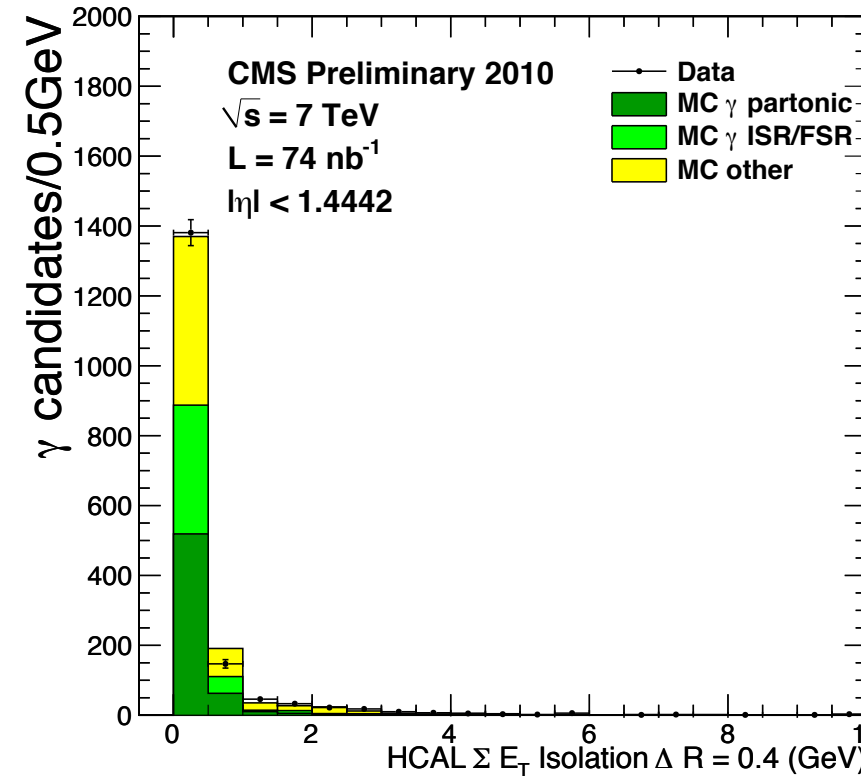
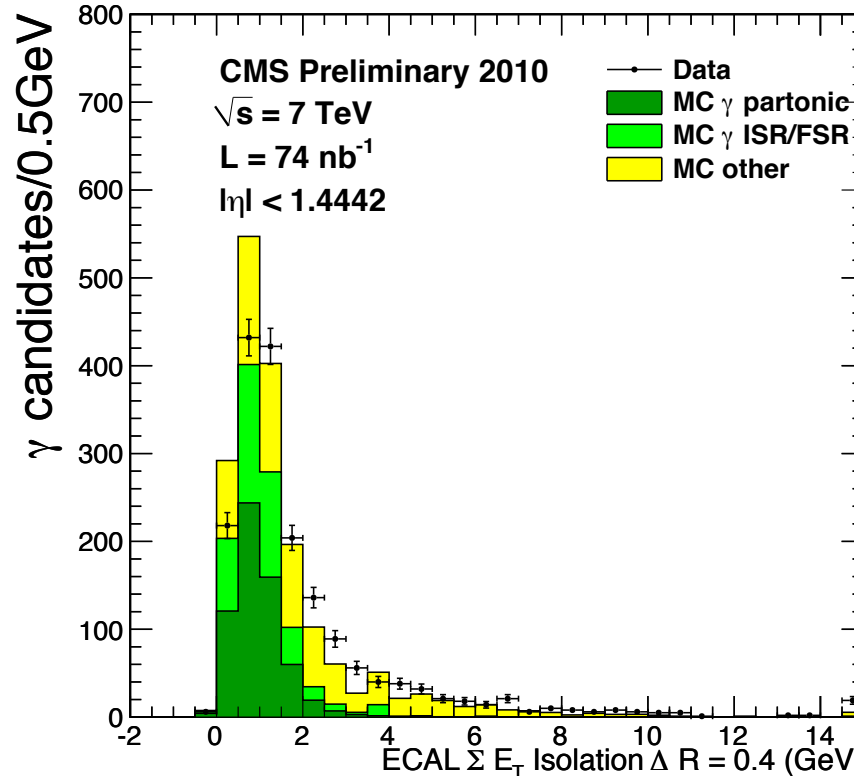
- Form 3×3 matrix of crystals around the photon seed crystal
- Find the 2 highest energy crystals within the matrix
- If the sum of the energies of the 2 highest energy crystals divided by the sum of the energies of all 9 crystals within the matrix exceeds 0.95, reject the photon as ECAL noise



Photon ID variables

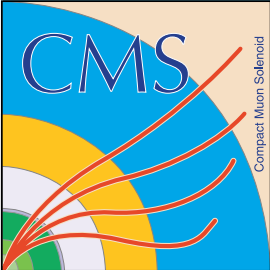


UNIVERSITY
of VIRGINIA

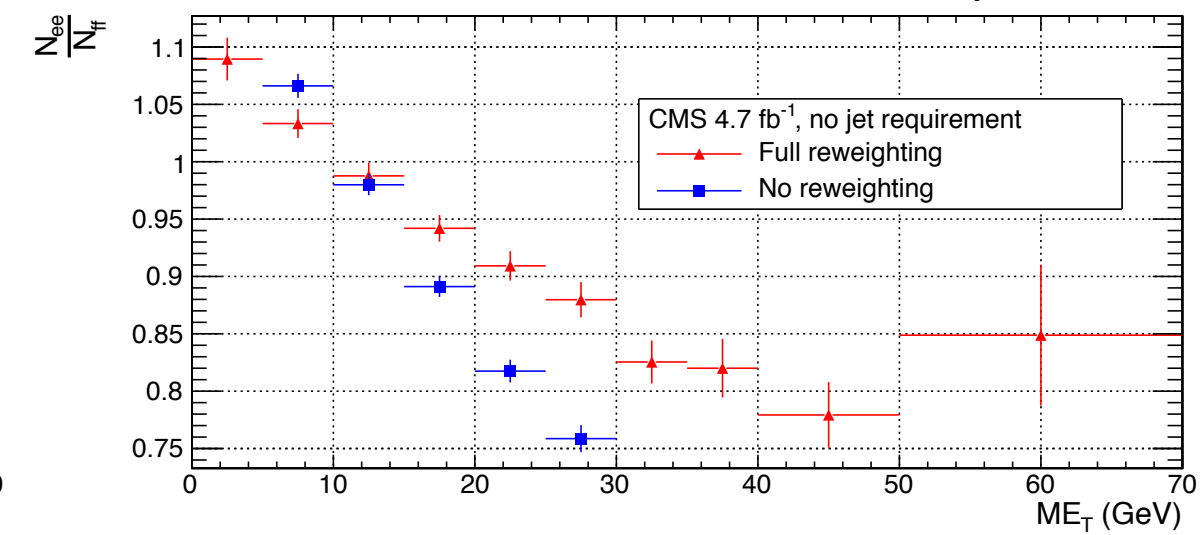
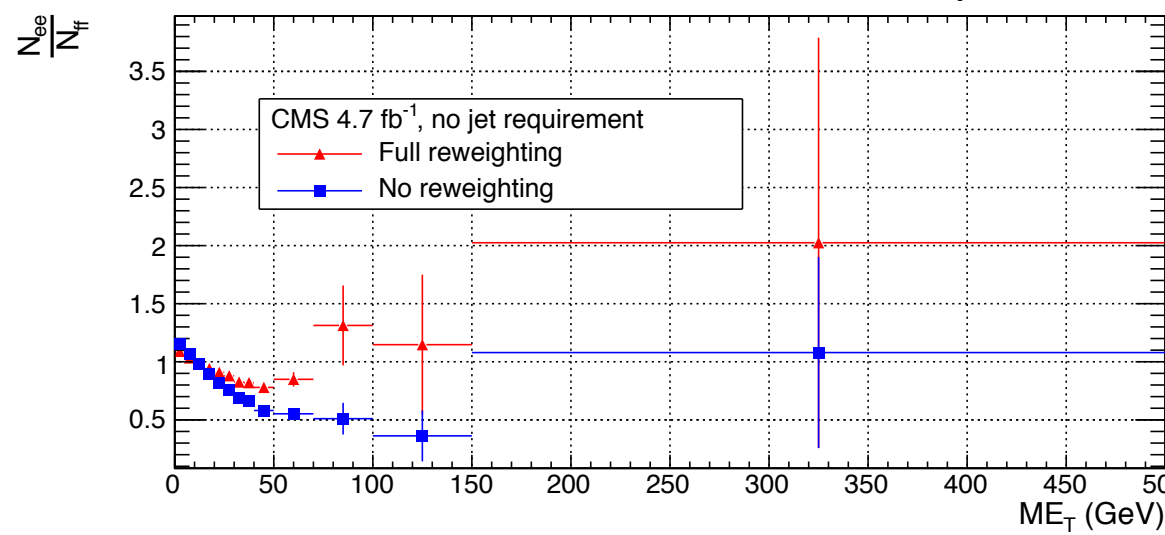
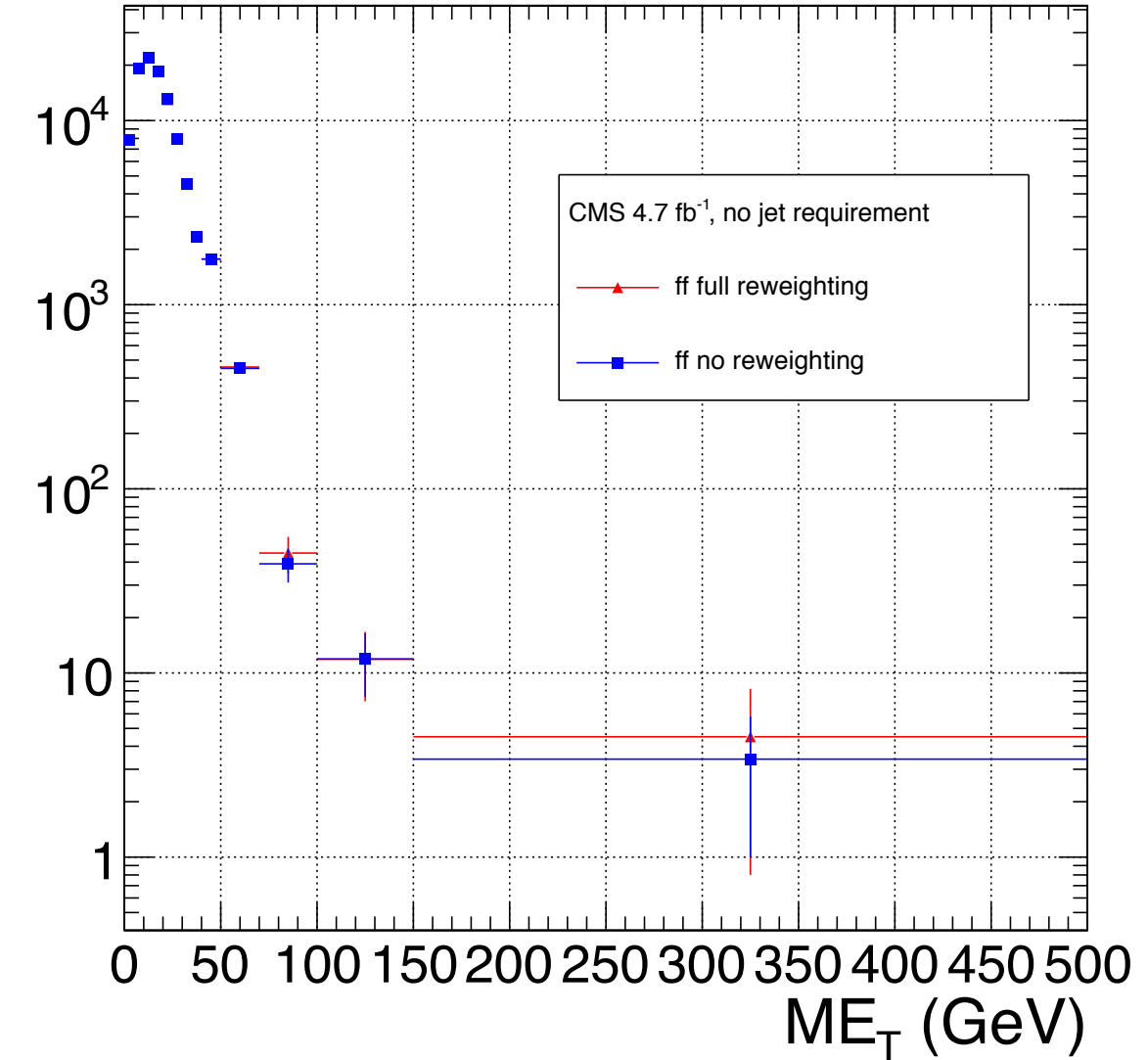
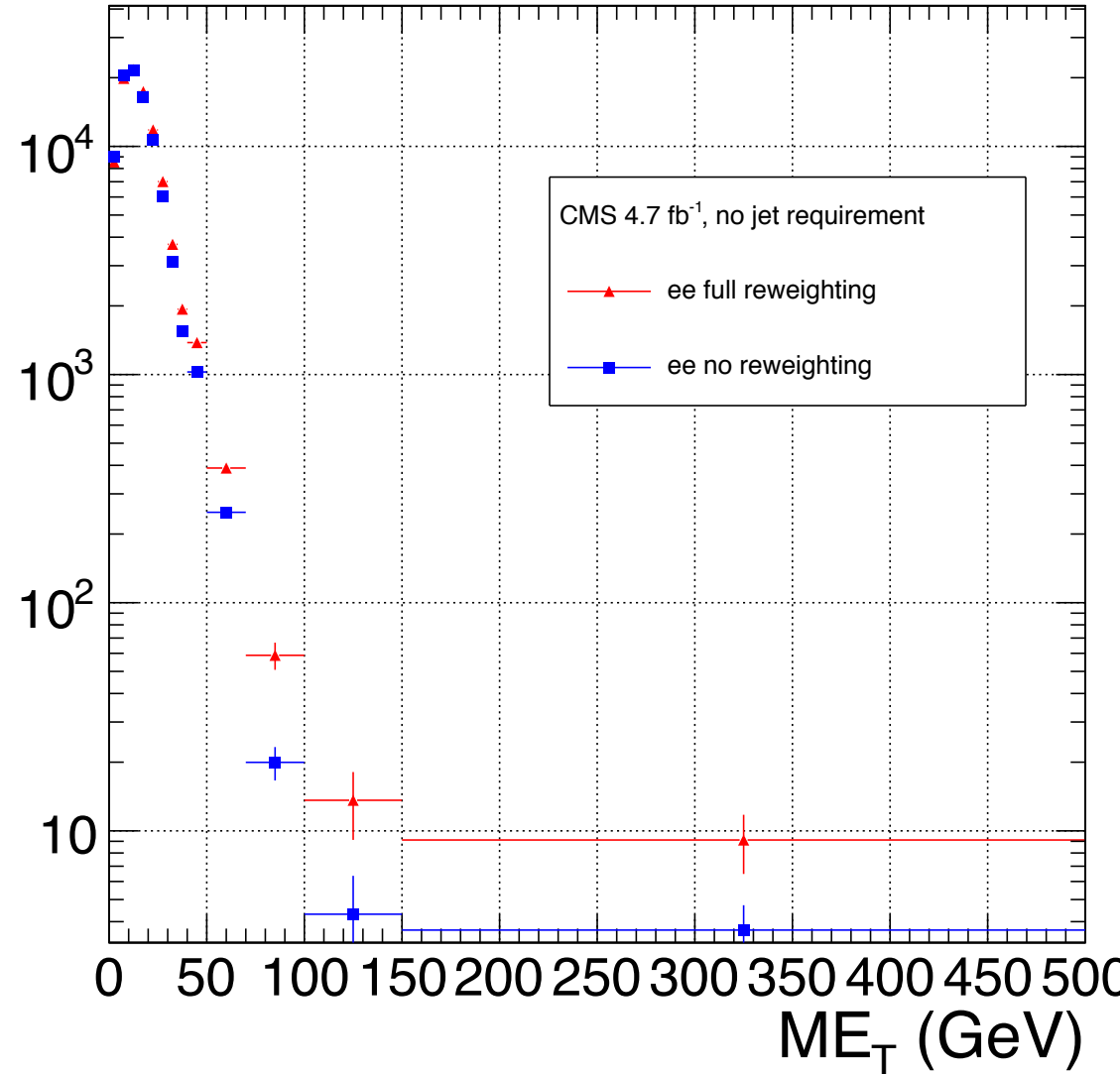


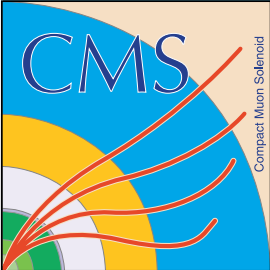
Sample definitions

Variable	Cut			
	$\gamma\gamma$	$e\gamma$	ee	ff
HLT match	IsoVL	IsoVL	IsoVL	IsoVL R9Id
E_T	$> 40/$ $> 25 \text{ GeV}$			
SC $ \eta $	< 1.4442	< 1.4442	< 1.4442	< 1.4442
H/E	< 0.05	< 0.05	< 0.05	< 0.05
$R9$	< 1	< 1	< 1	< 1
Pixel seed	No/No	Yes/No	Yes/Yes	No/No
$I_{\text{comb}}, \sigma_{i\eta i\eta}$	$< 6 \text{ GeV} \&\&$ < 0.011	$< 6 \text{ GeV} \&\&$ < 0.011	$< 6 \text{ GeV} \&\&$ < 0.011	$< 20 \text{ GeV} \&\&$ $(\geq 6 \text{ GeV} \ $ $\geq 0.011)$
JSON	Yes	Yes	Yes	Yes
No. good PVs	≥ 1	≥ 1	≥ 1	≥ 1
ΔR_{EM}	> 0.6	> 0.6	> 0.6	> 0.6
$\Delta\phi_{\text{EM}}$	≥ 0.05	≥ 0.05	≥ 0.05	≥ 0.05



Effect of reweighting



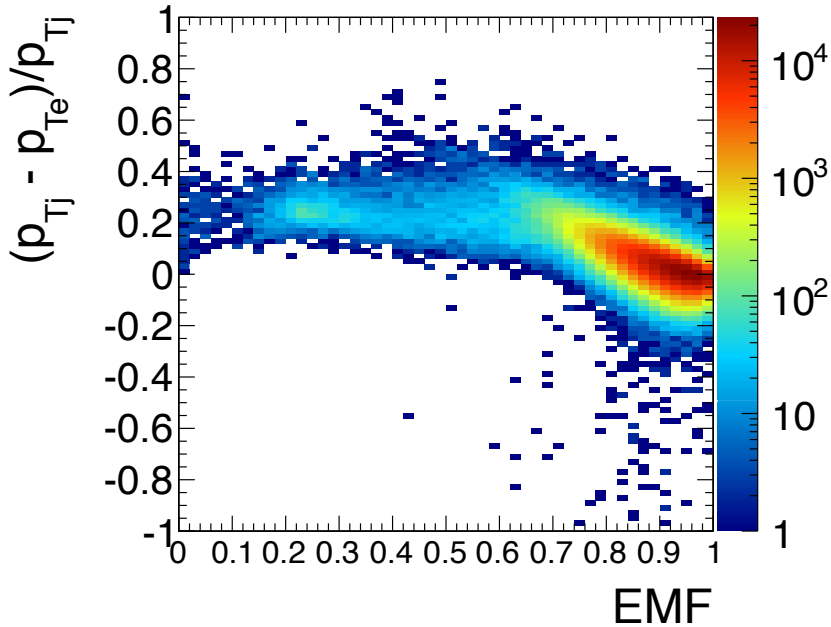


PF vs. ECAL E_T (1)

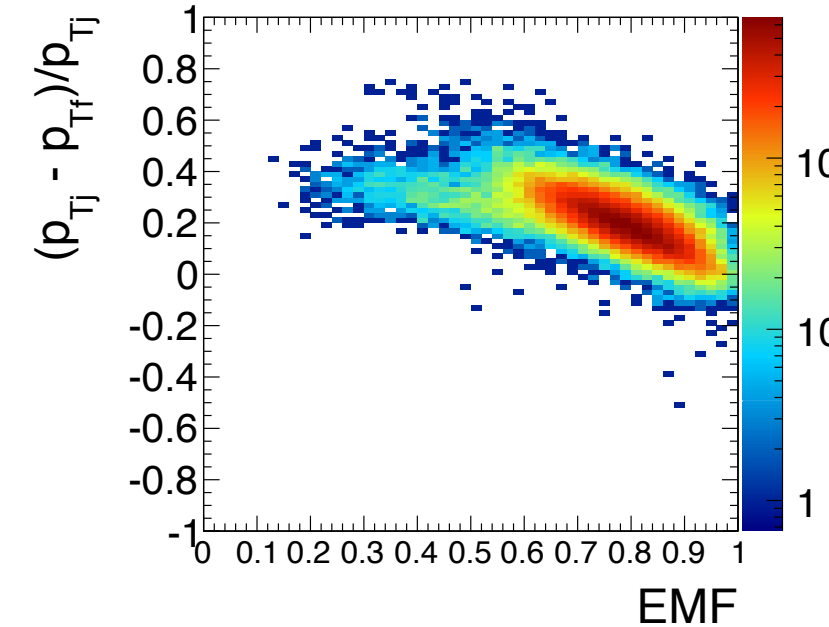


UNIVERSITY
of VIRGINIA

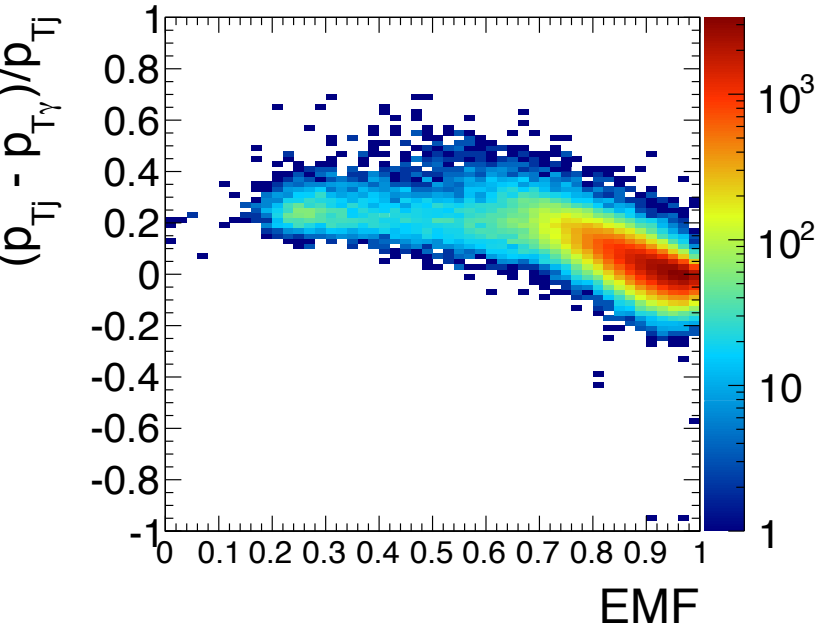
Leading e



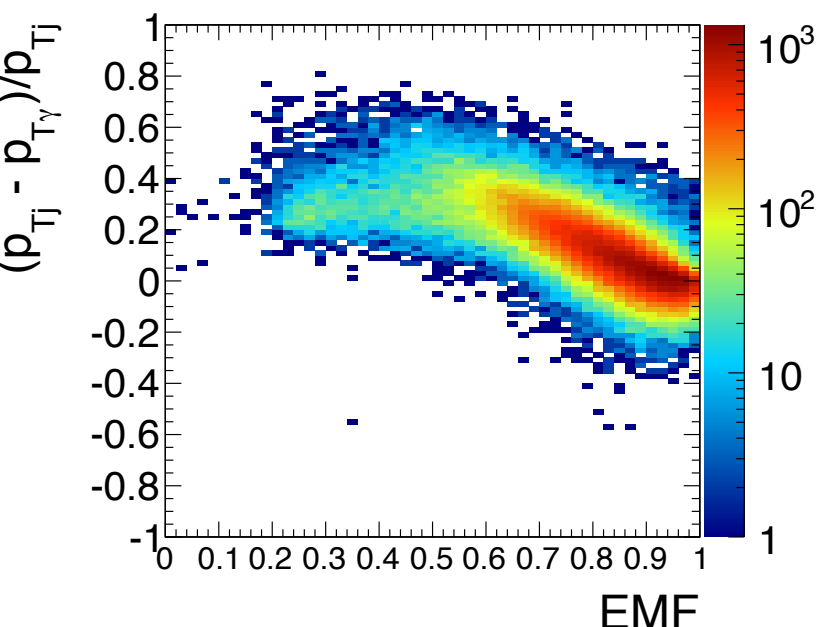
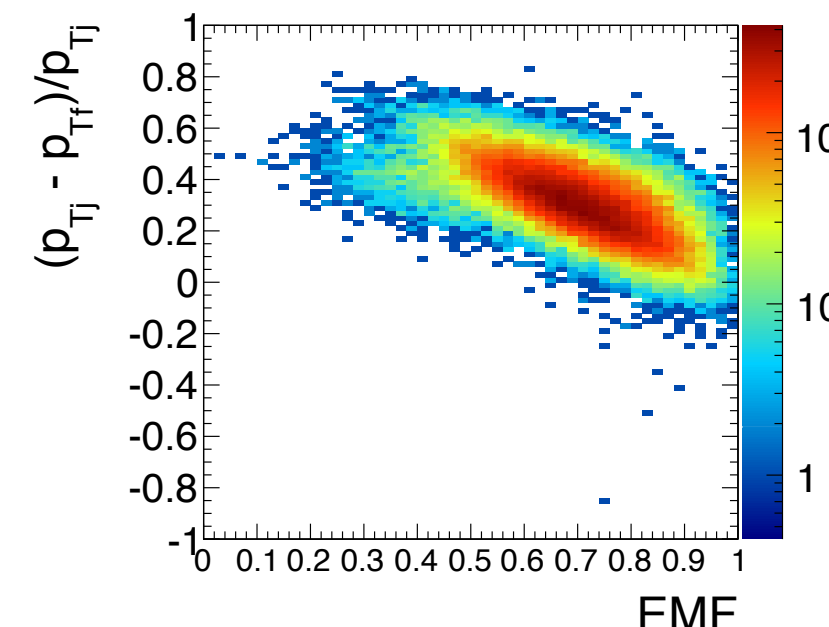
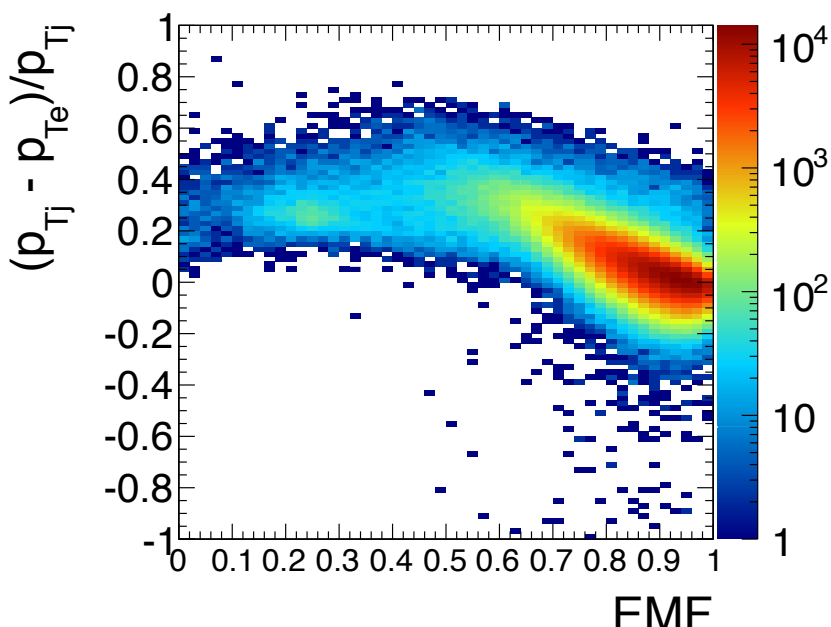
Leading f



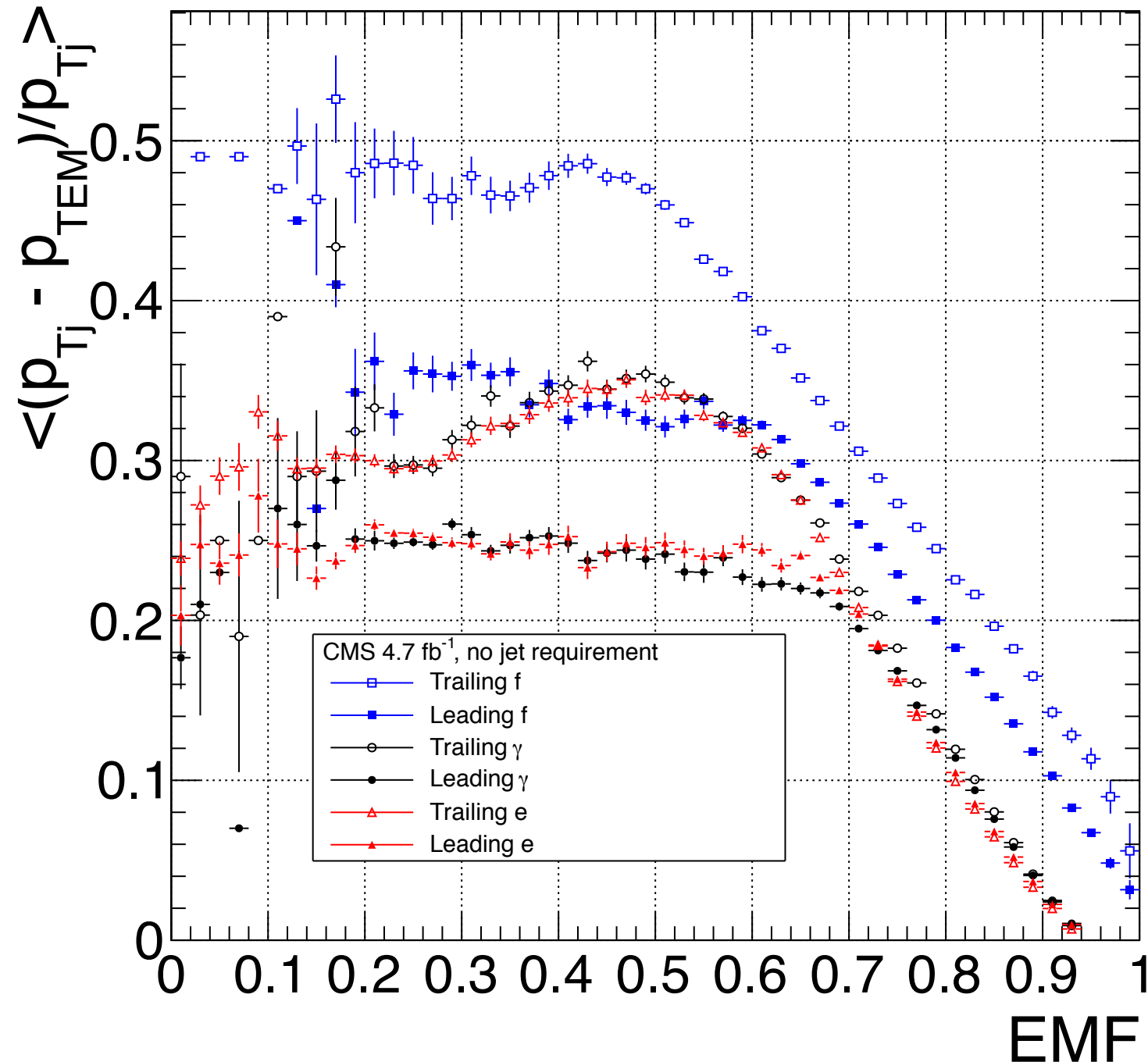
Leading γ



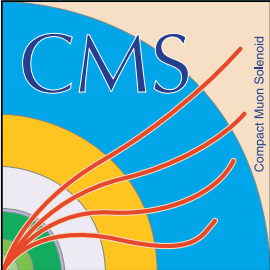
Trailing e



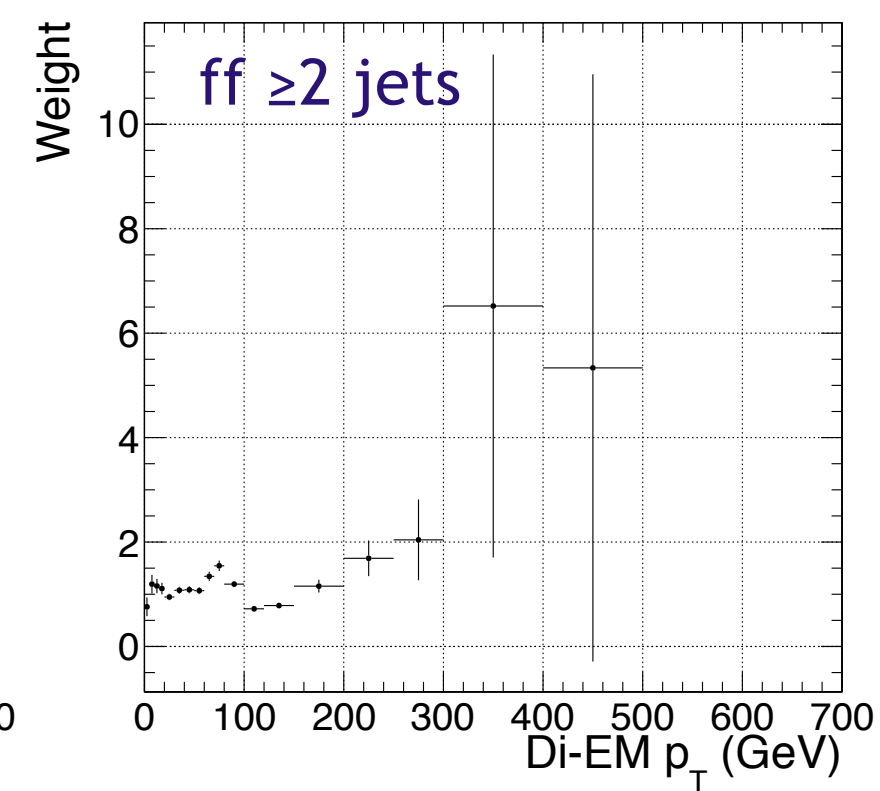
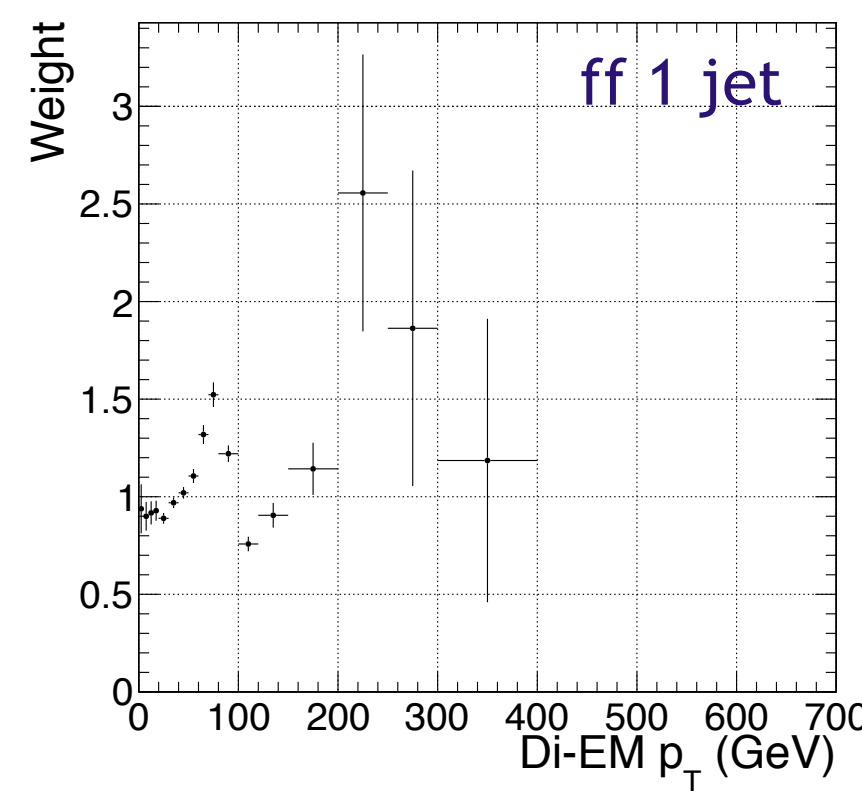
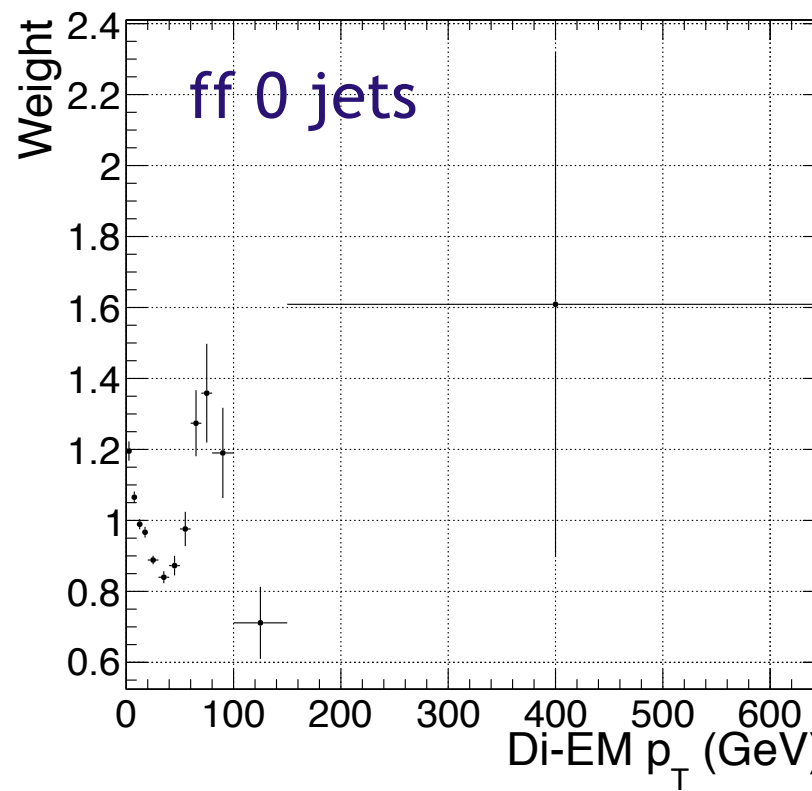
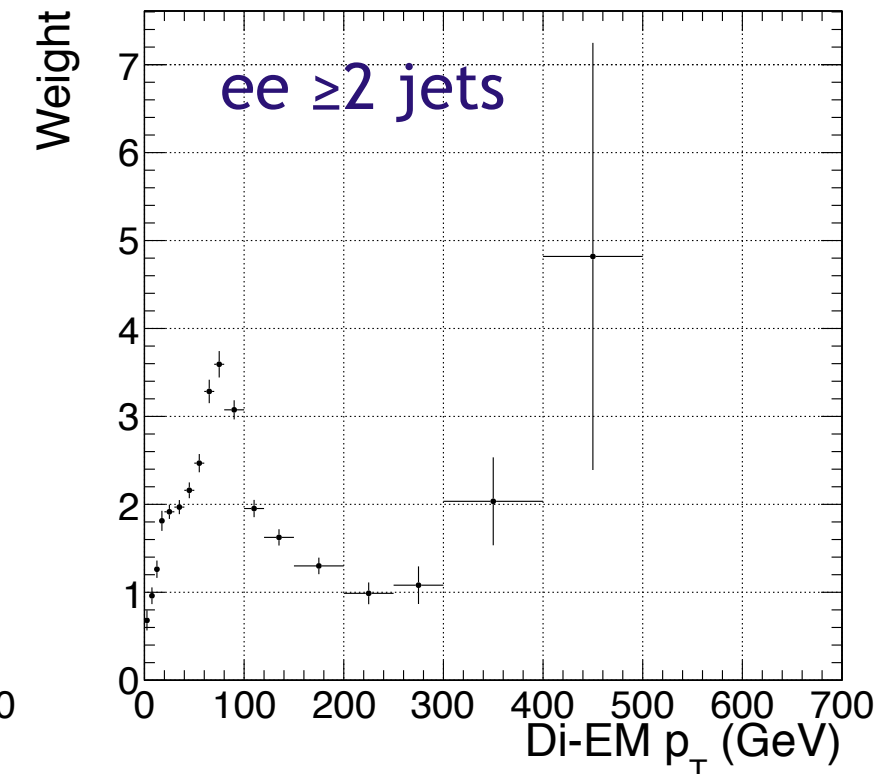
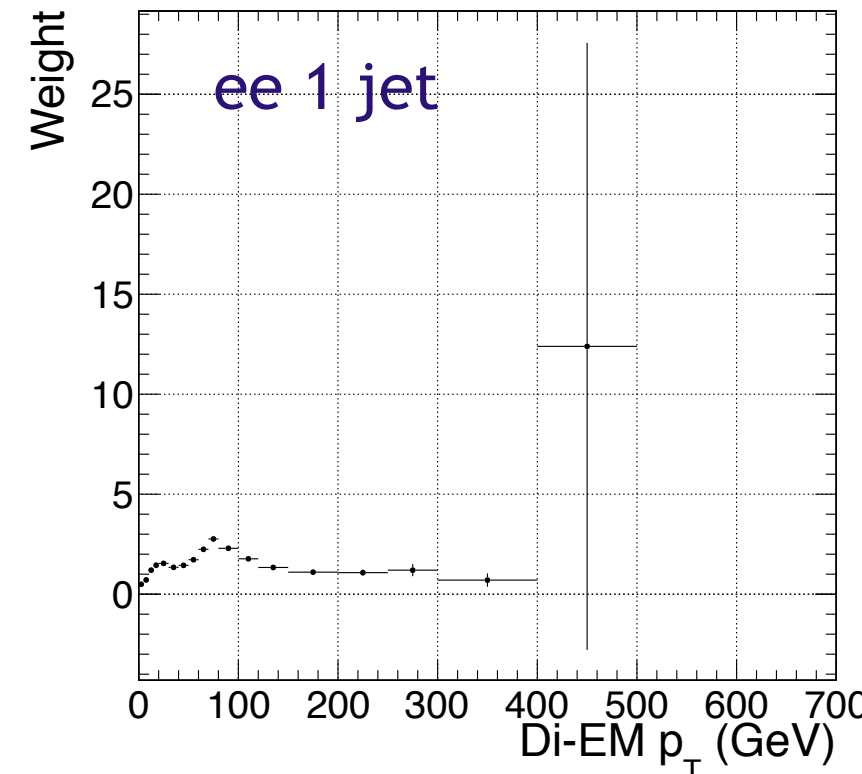
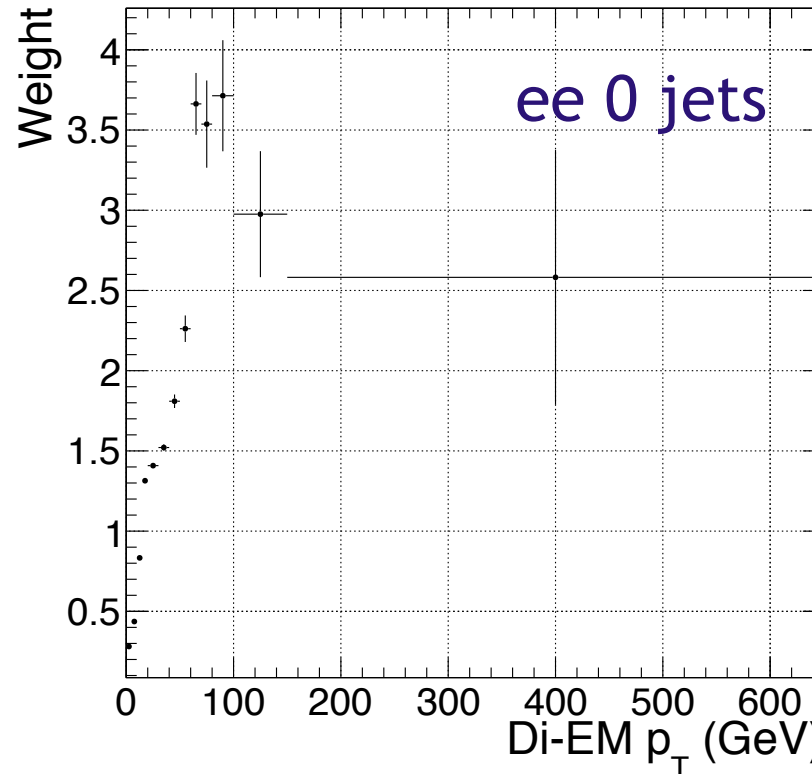
PF vs. ECAL E_T (2)



- Profile histograms of previous slide

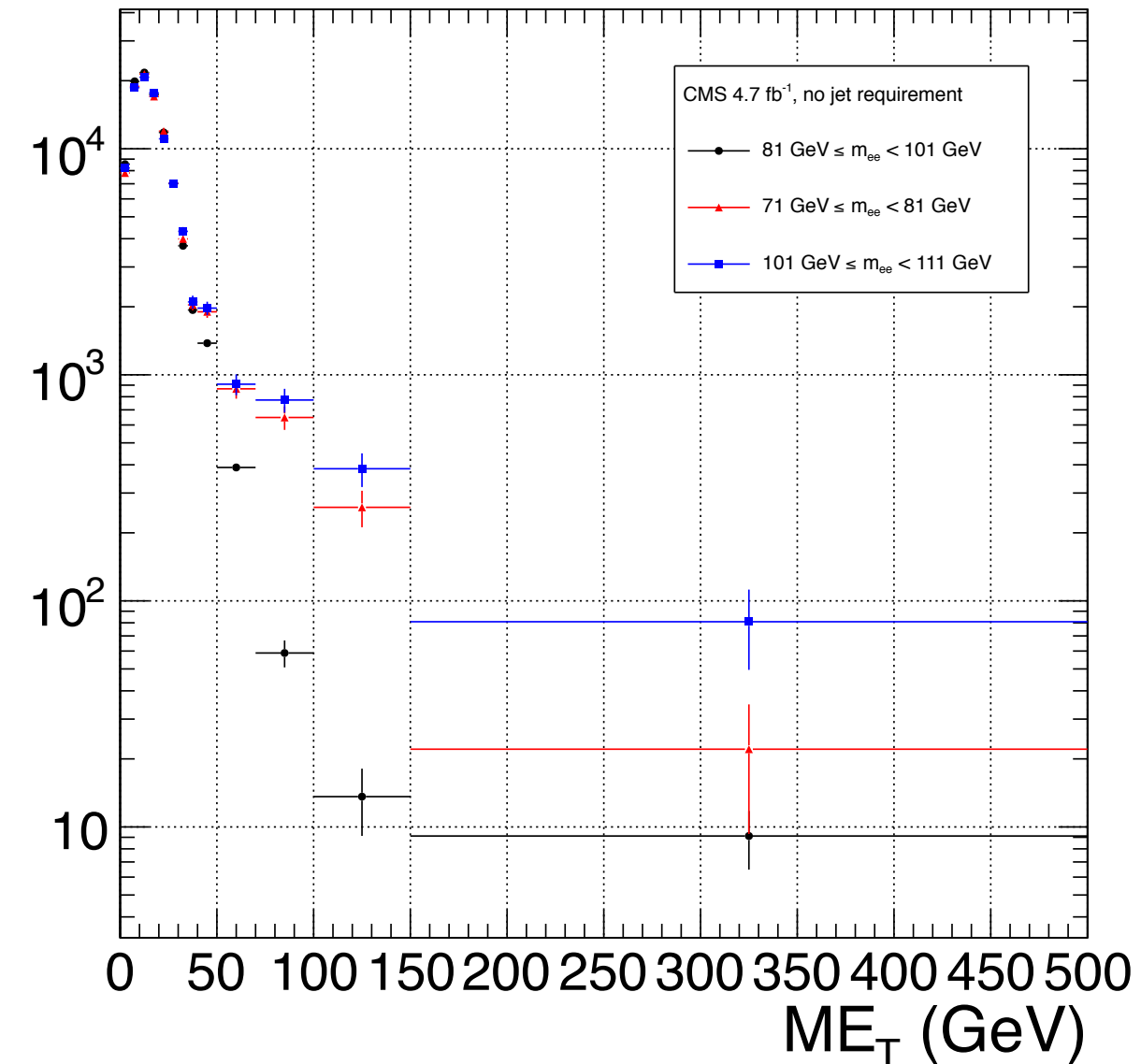


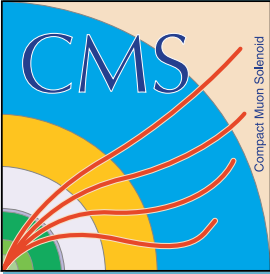
Di-EM p_T weights



Removing ttbar from the ee sample

- ee sample contains a non-negligible high- ME_T background of ttbar events
- $71 \text{ GeV} \leq m_{ee} < 81 \text{ GeV}$ and $101 \text{ GeV} \leq m_{ee} < 111 \text{ GeV}$ sidebands used to estimate the non-Z background in the $81 \text{ GeV} \leq m_{ee} < 101 \text{ GeV}$ ee sample
 - Reweight the low and high sidebands independently, using weights derived from events in those sidebands
 - Subtract the low and high sideband ME_T distributions from the Z signal ME_T distribution
 - Proceed with normalization of the sideband-subtracted ee sample

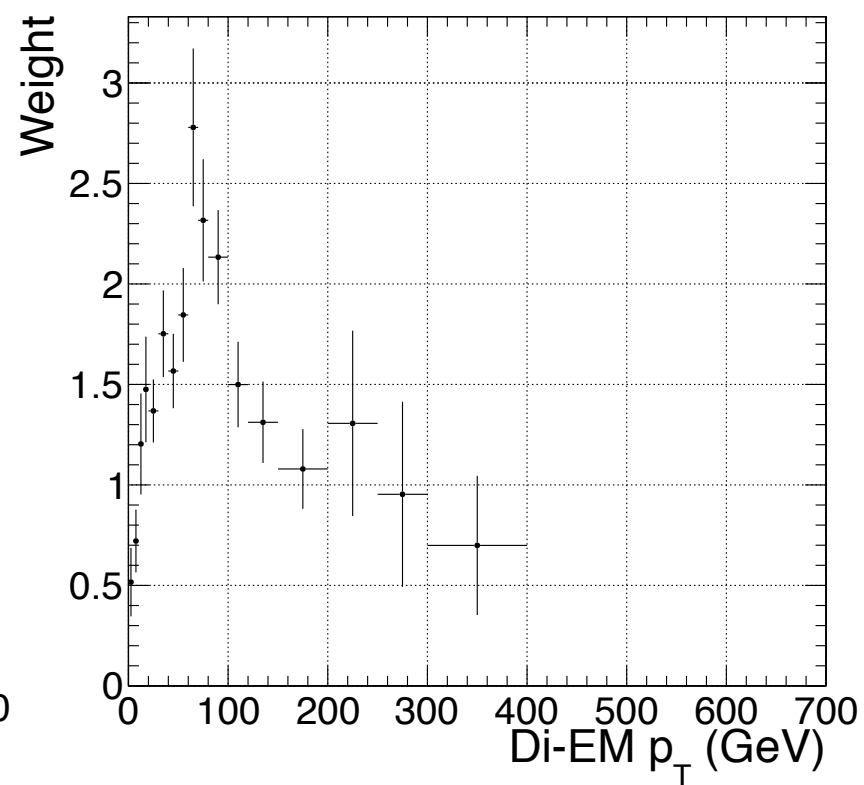
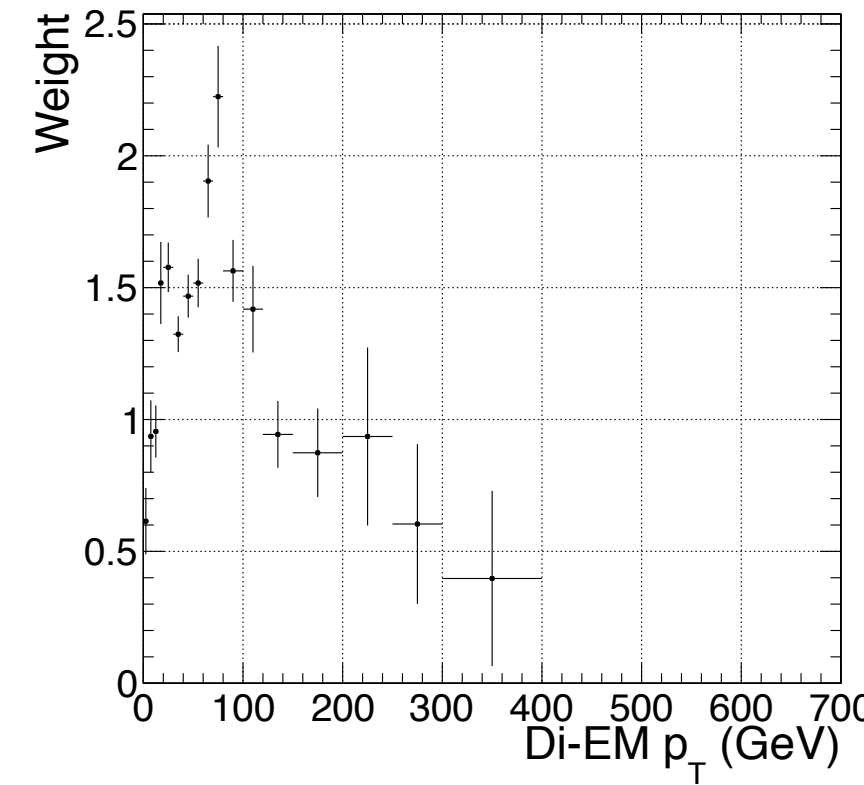
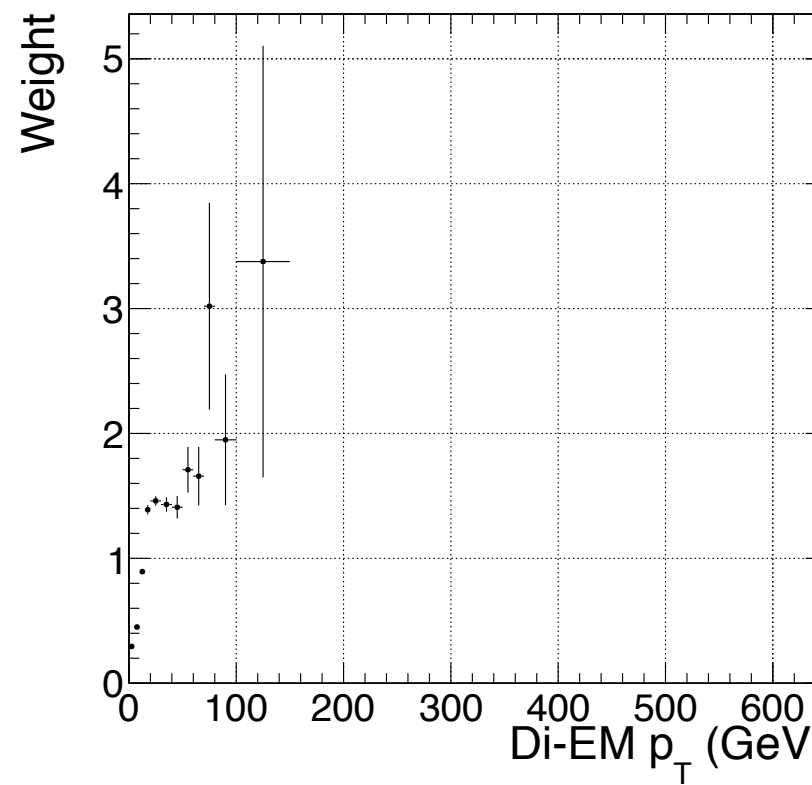
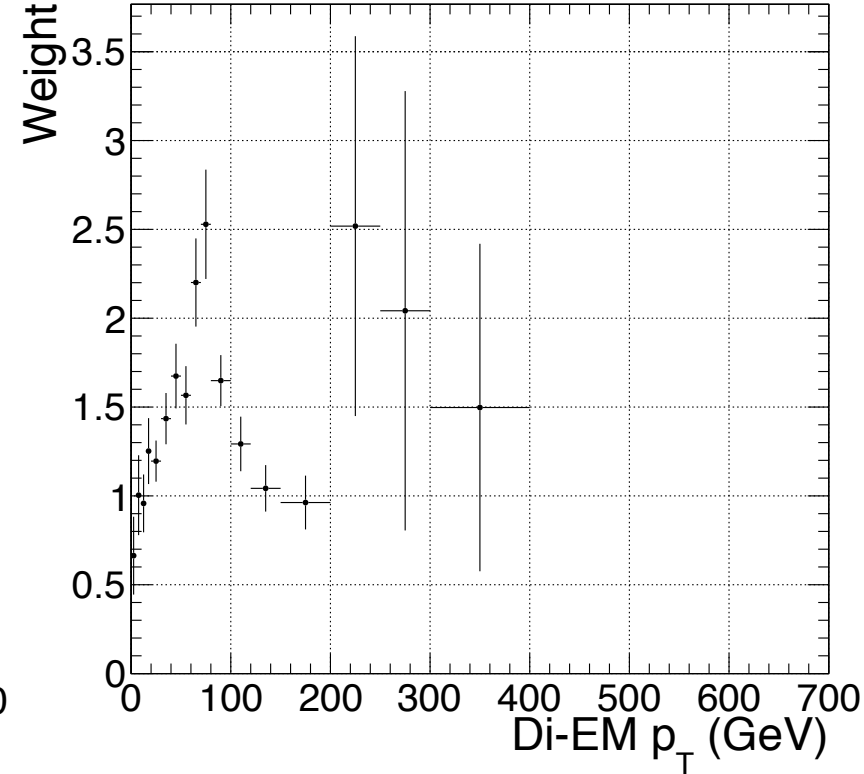
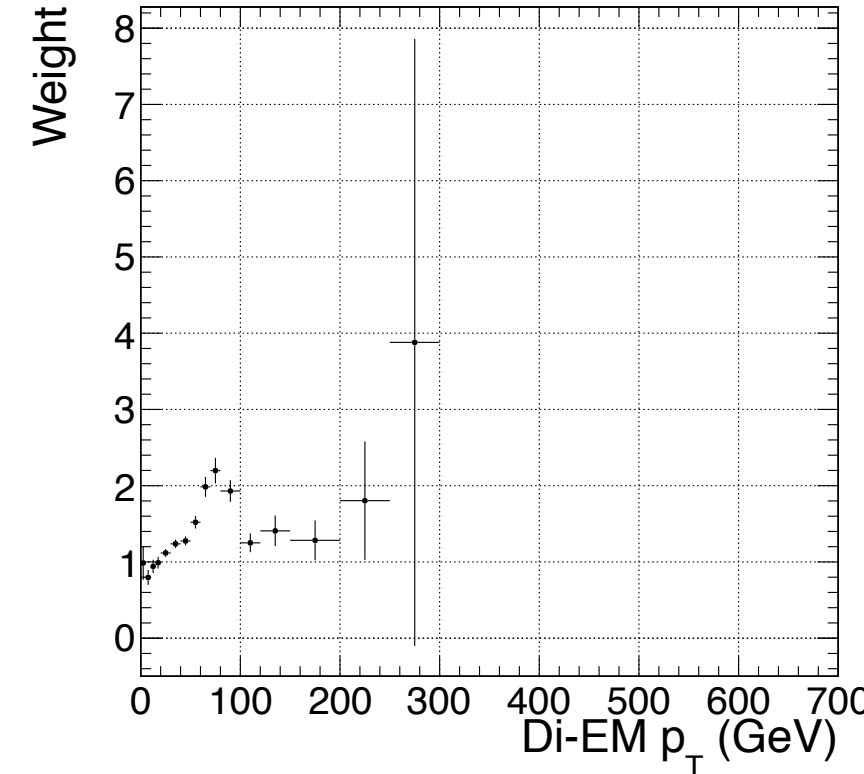
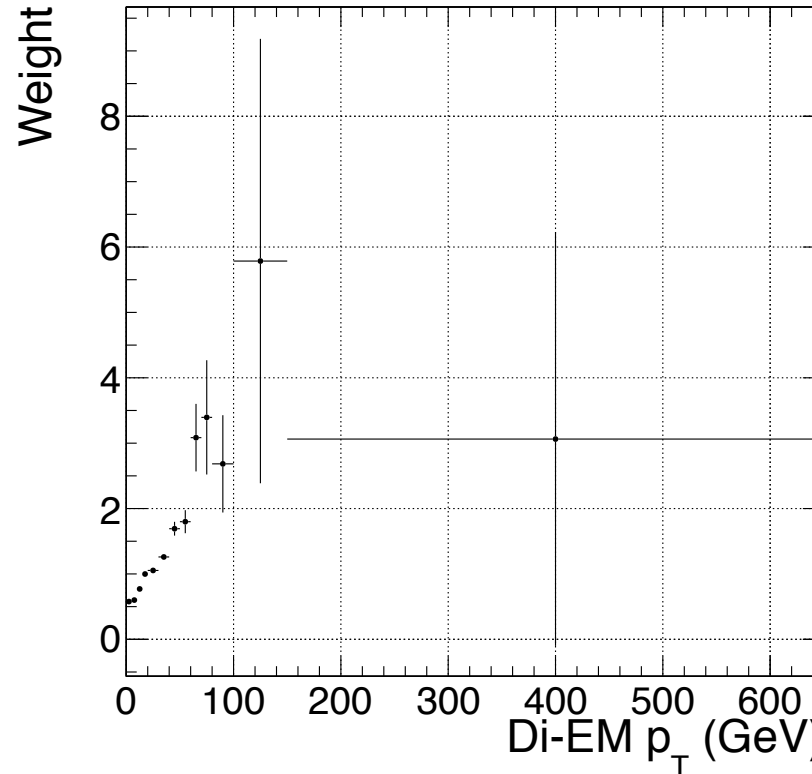


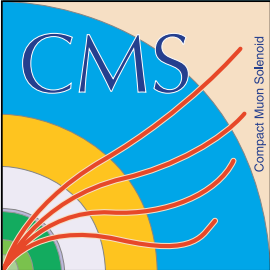


ee sideband weights



UNIVERSITY
of VIRGINIA





$f_{e \rightarrow \gamma}$ calculation



The number of events in the di-electron sample is given by

$$N_{ee} = f_{e \rightarrow e}^2 N_{Z \rightarrow ee}$$

where $f_{e \rightarrow e}$ is the efficiency to correctly identify an electron via pixel match and $N_{Z \rightarrow ee}$ is the true number of Z \rightarrow ee events. The number of events in the e γ sample due to misidentification of 1 Z electron as a photon is given by

$$N_{e\gamma}^Z = 2f_{e \rightarrow e}(1 - f_{e \rightarrow e})N_{Z \rightarrow ee}$$

Solving for $f_{e \rightarrow e}$,

$$f_{e \rightarrow e} = \frac{1}{1 + \frac{1}{2} \frac{N_{e\gamma}^Z}{N_{ee}}}$$

The number of events in the e γ sample due to correctly identifying a W electron is given by

$$N_{e\gamma}^W = f_{e \rightarrow e} N_W$$

where N_W is the number of true W \rightarrow e ν events. The number of $\gamma\gamma$ events from W electron misidentification is given by

$$N_{\gamma\gamma}^{EW} = (1 - f_{e \rightarrow e}) N_W$$

where we have neglected the contribution from Z electron misidentification since it is small (i.e., $f_{e \rightarrow \gamma}$ is small and the Z contribution involves $f_{e \rightarrow \gamma}^2$, since both electrons have to be misidentified). Since

$$f_{e \rightarrow e} = 1 - f_{e \rightarrow \gamma}$$

solving for $N_{\gamma\gamma}^{EW}$

$$N_{\gamma\gamma}^{EW} = \frac{f_{e \rightarrow \gamma}}{1 - f_{e \rightarrow \gamma}} N_{e \rightarrow \gamma}$$

- Signal spectrum generation via SuSpect v2.41
- Signal decays via SDECAY v1.3
- Event generation, parton showering, hadronization, and decay via Pythia 6
- CMS detector simulation (GEANT) and reconstruction
- Gravitino LSP
- NLO production cross sections and renormalization and factorization scale uncertainties calculated with Prospino
- PDF uncertainties calculated using PDF4LHC recommendations